



**MARMARA UNIVERSITY**  
**INSTITUTE FOR GRADUATE STUDIES**  
**IN PURE AND APPLIED SCIENCES**



**INDIRECT METAL COMPLEX PART  
PRODUCTION USING BINDER JETTING  
TECHNOLOGY: A PRELIMINARY  
RESEARCH**

---

**ERTUĞRUL VARLIK**

**MASTER THESIS**

Department of Metallurgical and Materials Engineering

**Thesis Supervisor**

Assoc. Prof. Dr. Serdar AKTAŞ

**ISTANBUL, 2020**

---



**MARMARA UNIVERSITY**  
**INSTITUTE FOR GRADUATE STUDIES**  
**IN PURE AND APPLIED SCIENCES**



**INDIRECT METAL COMPLEX PART  
PRODUCTION USING BINDER JETTING  
TECHNOLOGY: A PRELIMINARY  
RESEARCH**

---

**ERTUĞRUL VARLIK**

**(524717019)**

**MASTER THESIS**

Department of Metallurgical and Materials Engineering

**Thesis Supervisor**

Assoc. Prof. Dr. Serdar AKTAŞ

**ISTANBUL, 2020**

---

## **ACKNOWLEDGMENT**

My supervisor, Dr. Serdar Aktaş, I owe a special thanks to you because of your unstinting support during this Master's Thesis. I could not have done it without your help. Dear Aktaş, I will never forget the time how I became one of your students. Thank you. I also would like to thank dear Research Assistant Burcu Nilgün Çetiner due to the technical support she provides. It was an honor to be a part of your team.

My endless thanks goes to Professor Luca Giorleo. I am grateful that you accepted me as your student and gave me a chance to meet with a topic that I can follow till forever. I always believed that you trusted me even after you were exposed to that design. Grazie mille Professore. Besides, I would like to thank Professor Annalisa Pola and Technician Lorenzo Montesano because of their invaluable help.

Dear Mahmud, you gave me a room and shared your space with me. Thank you thousands of times for being a good friend and above all a good person. Greetings to Pakistan.

Mert Çelik. My fellow, I want to thank you for your precious friendship and valuable ideas that kept me mentally alive. Thanks.

A special thanks goes to Silvia Vailati. You are the person who facilitates my life with your priceless advice in Italy. As I said, you are the one. Thanks a lot.

An informally thanks to all my friends: Orhan, Emna, Abdi, Michele, Eric, Cris, Ekta, Hamza, Anand, Saleh, Joul, and A1cha.

**06/2020**

**Ertuğrul VARLIK**

## Table of Contents

ACKNOWLEDGMENT .....	i
ÖZET .....	iv
ABSTRACT .....	v
SYMBOLS .....	vi
ABBREVIATIONS .....	vii
LIST OF FIGURES .....	x
LIST OF TABLES .....	xv
1. INTRODUCTION .....	1
2. ADDITIVE MANUFACTURING .....	3
2.1. Technologies and Materials .....	3
2.2. Design in Additive Manufacturing .....	8
2.2.1. Step by step design process: digital to physical object .....	9
2.2.2. Design constraints in additive manufacturing .....	11
2.3. A comparison: Additive versus Subtractive Manufacturing .....	13
2.3.1. Similarities .....	13
2.3.2. Dissimilarities .....	13
3. METAL 3D PRINTING IN ADDITIVE MANUFACTURING .....	15
3.1. Metal Additive Manufacturing Techniques .....	15
3.1.1. Powder bed fusion .....	16
3.1.2. Directed energy deposition .....	23
3.1.3. Fused deposition modeling .....	29
3.1.4. Material jetting .....	31
3.1.5. Cold spray additive manufacturing .....	33
3.1.6. Friction-based additive manufacturing technologies .....	35
3.1.7. Ultrasonic additive manufacturing .....	37
3.1.8. Direct ink writing .....	39
3.1.9. Electrochemical additive manufacturing process .....	39
3.1.10. Laser-assisted electrophoretic deposition .....	40
3.1.11. Laser-induced forward transfer .....	41
3.1.12. Focused electron beam induced deposition .....	42
3.2. Relationship Between the Energy Source and Feedstock .....	42
4. THE STATE OF ART - BINDER JETTING TECHNOLOGY FOR CASTING APPLICATIONS .....	44
4.1. Binder Jetting Technology .....	44

4.2. The State of Art: Binder Jetting for Casting Applications .....	48
4.3. The Purpose of the Thesis .....	55
5. EXPERIMENTAL PROCEDURES .....	57
5.1. Design Activities .....	57
5.1.1. Design of the lattice structures .....	57
5.1.2. Design of the gating systems .....	59
5.1.3. Assembling of gating systems and lattice structures into the mold.....	67
5.2. Production Activities .....	71
5.2.1. The Projet CJP 460Plus .....	71
5.2.2. Mold production .....	72
5.2.3. Used powder and binder in printing .....	75
5.2.4. Post processing .....	75
5.3. Mold Cavity Verification .....	76
5.4. Temperature Test.....	76
5.5. Aluminum Casting.....	77
6. RESULTS AND DISCUSSION.....	78
6.1. Mold Cavity Verification .....	78
6.1.1. Demo mold production.....	78
6.1.2. Silicone rubber casting .....	79
6.1.3. Results of the mold cavity verification.....	82
6.2. Temperature Test.....	83
6.2.1. Demo mold production.....	84
6.2.2. Heat treatment.....	85
6.2.3. Silicone rubber casting .....	89
6.2.4. Results of the temperature test.....	91
6.3. Aluminum Casting.....	92
6.3.1. Casting process .....	92
6.3.2. Results of the aluminum casting.....	95
7. CONCLUSIONS .....	109
8. REFERENCES .....	110

## ÖZET

### BAĞLAYICI PÜSKÜRTME TEKNOLOJİSİ KULLANARAK DOLAYLI METAL KOMPLEKS PARÇA ÜRETİMİ: BİR ÖN ARAŞTIRMA

Nispeten yeni bir üretim yöntemi olan Eklemeli İmalat, üretim kolaylığı nedeniyle tasarım alanında yeni olanaklar sunmaktadır. Serbest biçimli imalat, geleneksel üretim teknikleri kullanılarak elde edilmesi çok daha zor olan karmaşık geometriye sahip güçlü, aynı zamanda hafif yapıların oluşturulmasına izin verir. Bağlayıcı Püskürtme, alçı ve bağlayıcı yardımıyla parçaların katman katman üretilmesine olanak sağlayan Eklemeli İmalat Teknolojilerinden birisidir. Metal parçalar, Bağlayıcı Püskürtme kullanılarak doğrudan veya dolaylı olarak üretilir. Bu çalışma, karmaşık kalıplar oluşturmak için tasarım parametrelerinin sınırlarının araştırılmasına odaklanmıştır. Çalışma sırasında, çizgilerin kalınlığı, çizgi sayısı ve çizgiler arasındaki boşluğun bir fonksiyonu olarak farklı kafes yapıları tasarlanmıştır. Bağlayıcı Püskürtme ile üretilen kalıpları döküm ile tamamen doldurmak için üç farklı gidici sistemi tasarlanmıştır. Kimyasal formülü  $AlSi9Cu3Fe1$  olan bir alüminyum alaşımı kalıplara dökülmüştür. Geleneksel döküm yöntemiyle elde edilmek istenen kafes yapılarının tasarım karmaşıklığı ve tasarım özgürlüğü arasındaki ilişki incelenmiştir. Bulgular, kalıp içi tasarımının kalıbın tamamen doldurulması üzerine doğrudan bir etkiye sahip olduğunu göstermiştir. Dökümden önce kalıp içerisinde bulunan gevşek hammaddelerin çıkarılmasındaki başarının, kafes yapılarının tasarım parametrelerine bağlı olduğu gözlemlenmiştir.

## **ABSTRACT**

### **INDIRECT METAL COMPLEX PART PRODUCTION USING BINDER JETTING TECHNOLOGY: A PRELIMINARY RESEARCH**

As a relatively novel production method, Additive Manufacturing offers new possibilities in the design area owing to the ease of production. Freeform fabrication permits the formation of strong, also lightweight structures with complex geometry, which is much more difficult using conventional manufacturing techniques. Binder Jetting is one of the Additive Manufacturing Technologies present the fabrication of parts layer by layer with the help of gypsum and binder. Metal parts can be produced directly or indirectly utilizing Binder Jetting. This study focused on the investigation of the limits of design parameters to generate complex molds. During the study, different lattice structures have been designed as a function of the thickness of lines, the number of lines, and the void between lines. Three different runner systems were designed in order to completely fill the molds produced with Binder Jetting by casting. An aluminum alloy of that has a chemical formula  $AlSi9Cu3Fe1$  was cast into the molds. The relationship between the design complexity and design freedom of the lattice structures desired to be obtained by the conventional casting method has been examined. The findings showed that the in-mold design had a direct effect on the complete filling of the mold. It was observed that the success of removing loose feedstocks in the mold before casting depended on the design parameters of the lattice structures.

## SYMBOLS

$A$ :	Cross-Section of the Liquid ( $\text{mm}^2$ or $\text{m}^2$ )
$d_d$ :	Void Thickness Between Lines (mm)
$d_e$ :	Thickness of Lines (mm)
$f$ :	Friction
$g$ :	Gravity
$h$ :	Altitude (mm)
$n_r$ :	Number of Lines
$p$ :	Pressure
$\rho$ :	Density
$Q$ :	Flow/Flow Rate ( $\text{mm}^3/\text{s}$ or $\text{m}^3/\text{s}$ )
$t$ :	Time (s)
$T$ :	Temperature ( $^{\circ}\text{C}$ )
$v$ :	Velocity

## **ABBREVIATIONS**

AFSD:	Additive Friction Stir Deposition
AJP:	Aerosol Jet Process
AM:	Additive Manufacturing
ASTM:	American Society for Testing and Materials
BJ:	Binder Jetting
CAD:	Computer Aided Design
CEM:	Composite Extrusion Modeling
CMT:	Cold Metal Transfer
CNC:	Computer Numerical Control
CSAM:	Cold Spray Additive Manufacturing
DED:	Directed Energy Deposition
DIJP:	Direct Ink Jet Printing
DIW:	Direct Ink Writing
DMLS:	Direct Metal Laser Sintering
DMD:	Directed Metal Deposition
DOD:	Drop on Demand
EBAM:	Electron Beam Additive Manufacturing
EBM:	Electron Beam Melting
EFAB:	Electrochemical Fabrication
FBAM:	Friction Based Additive Manufacturing
FD <sup>1</sup> :	Fused Deposition
FD <sup>2</sup> :	Friction Deposition
FDB:	Furan Direct Binding
FDM:	Fused Deposition Modeling
FEBID:	Focused Electron Beam Induced Deposition
FF:	Freeform Fabrication
FFF:	Fused Filament Fabrication
FLM:	Fused Layer Modeling
FSAM:	Friction Stir Additive Manufacturing
HIP:	Hot Isostatic Pressing

HMP:	Hot Melt Printing
LAED:	Laser Assisted Electrophoretic Deposition
LDW:	Laser Deposition Welding
LENS:	Laser Engineered Net Shaping
LFW:	Linear Friction Welding
LIFT:	Laser Induced Forward Transfer
LMD:	Laser Metal Deposition
LMP:	Liquid Metal Printing
ME:	Material Extrusion
MIG:	Gas Metal Arc Welding
MJ:	Material Jetting
MJS:	Multiphase Jet Solidification
MPW:	Micro Pen Writing
NC:	Numerical Control
NPJ:	NanoParticle Jetting
OM:	Optical Microscopy
PAW:	Plasma Arc Welding
PCM:	Patternless Casting Manufacturing
RFW:	Rotary Friction Welding
RPD:	Rapid Plasma Deposition
RS:	Reinforcement Structure
SC:	Sand Casting
SL:	Sheet Lamination
SLA:	Stereolithography
SLM:	Selective Laser Melting
SLS:	Selective Laser Sintering
SM:	Subtractive Manufacturing
SPD:	Shaped Metal Deposition
STL:	Standart Triangle Language
TIG:	Gas Tungsten Arc Welding
UAM:	Ultrasonic Additive Manufacturing
UV:	Ultraviolet

WAAM: Wire and Arc Additive Manufacturing

XRD: X-ray Diffraction

2D: Two Dimensional

3DP: Three Dimensional Printing



## LIST OF FIGURES

<b>Figure 2.1.</b> Additive Manufacturing technologies categorized by ASTM F42 Committee. ....	4
<b>Figure 2.2.</b> Basic process steps in AM. ....	9
<b>Figure 2.3.</b> Pattern image in STL format, (b) is the zoom of the sprue-top region. ....	10
<b>Figure 2.4.</b> [18]; Schematic representation of the average design parameters that needed to be considered while designing for all AM methods, (a); explains the fillet ratio that should be in the vertical edges remaining on the internal surface, here R represents radius, D represents the depth at the cavity, (b); expresses the thickness ratio for the metals and plastics, (c); showing that the information about the depth limitation in all spaces of the design. ....	12
<b>Figure 3.1.</b> Schematic illustration of Powder Bed Fusion approach (PBF). ....	16
<b>Figure 3.2.</b> Processing of the regions where selectively required by reflecting the laser source with the help of a mirror. ....	18
<b>Figure 3.3.</b> Schematic representation of the EBM method, where (i), (ii), and (iii) represents a sequential production. ....	22
<b>Figure 3.4.</b> The illustration of the working principle of the DED-3D machine, where (a) represents a machine that is using a laser beam as an energy source and supply material in powder form, the technology called DED-Laser Beam, where (b) represents a machine that is using an electron beam as an energy source and building material in wire form, the technology called DED-Electron Beam. ....	24
<b>Figure 3.5.</b> A schematic representation of powder feed-DED. ....	25
<b>Figure 3.6.</b> Schematic representation of wire feedstock-EBAM technique. ....	28
<b>Figure 3.7.</b> Schematic representation of Material Extrusion. ....	30
<b>Figure 3.8.</b> Depiction of Material Extrusion process: (a) printing process, (b) chemical purification process, (c) sintering process, (d) ready-to-use part [42]. ....	31
<b>Figure 3.9.</b> Schematic representation of the material jetting process. ....	32
<b>Figure 3.10.</b> Schematic illustrations of cold systems: where (a) represents low, (b) represents high cold spray. ....	34
<b>Figure 3.11.</b> Categorized friction-based additive manufacturing techniques [59]. ....	36
<b>Figure 3.12.</b> Schematic view of the Additive Friction Stir Deposition system. ....	37
<b>Figure 3.13.</b> Schematic illustration of UAM [65]. ....	38

<b>Figure 3.14.</b> An Illustration of Direct Ink Writing (DIW).....	39
<b>Figure 3.15.</b> Schematic depiction of (a) [40] EBAM and (b) [80] FluidFM 3DP.....	40
<b>Figure 3.16.</b> Schematic representation of Laser-assisted electrophoretic deposition....	41
<b>Figure 3.17.</b> Depiction of Laser-induced forward transfer. ....	41
<b>Figure 3.18.</b> Schematic view of Focused Electron Beam Induced Deposition (FEBID). .....	42
<b>Figure 3.19.</b> The illustration of metallurgical reactions that occur when the heat source and the feeding material meet [93]. ....	43
<b>Figure 4.1.</b> An illustration of a typical BJ machine and production cycle [8,9].....	45
<b>Figure 4.2.</b> The number of publishment released by Scopus about BJ in the years between 2013 and 2019 [12]. ....	46
<b>Figure 5.1.</b> Schematic representation of the experimental cycle. ....	57
<b>Figure 5.2.</b> Schematic representation of a lattice structure which has dimensions of 5_2.5_3, where (a) shows the actual view of the lattice structure, (b) shows the transparent image of it and, (c) represents the thickness of each bar ( $d_e$ ), void thickness between two bars ( $d_a$ ), and the number of lines ( $n_r$ ) respectively. ....	58
<b>Figure 5.3.</b> The representation of the first gating system was designed to overcome several casting problems; filling, hot-point, and turbulence. Where (a) shows the actual image of the whole system, (b) the transparent illustration of the gating system, where shows the top of sprue, sprue, sprue base, and runner, (c) front view, (d) top view. ....	60
<b>Figure 5.4.</b> Schematic representation of the sprue system where illustrates $h_1$ , $h_2$ , $A_1$ , $A_2$ that are assumed variables. ....	63
<b>Figure 5.5.</b> Dimensions of the sample lattice structure. ....	63
<b>Figure 5.6.</b> The illustration of the second gating solution employing the strategy of side- attack to let molten metal penetration. Where (a) represents the actual view of the gating design, (b) shows the transparent image of it, (c) shows the front view, (d) represents the top view of the system. ....	65
<b>Figure 5.7.</b> The depiction of the third gating system utilizing the strategy of base-attack to fill the Mold in time. Where (a) shows the actual view, (b) represents the transparent of a, (c) shows the front view, (d) illustrates the top view of the system. ....	66
<b>Figure 5.8.</b> An expression, which regions where molten metal starts to fill the lattice structure up. In the first gating system, (a) shows the molten metal entered the part from	

the bottom. In the second gating system, (b) represents the molten metal entered the part from the middle. In the third gating system, (c) illustrates the molten metal entered the part from the left-base side. .... 67

**Figure 5.9.** Schematic illustration of the assembling of the gating systems and components into the mold. (a) represents the third gating system, (b) represents the component, and (c) shows the assembled part of them called ‘positive.’ ..... 68

**Figure 5.10.** Schematic representation of the drawing of the mold-boundaries. .... 69

**Figure 5.11.** Schematic representation of the solid-Boss-Extrude. .... 69

**Figure 5.12.** The depiction of the Combine process. .... 70

**Figure 5.13.** Schematic representation of the mold and its section view. .... 70

**Figure 5.14.** Schematic representation of the Projet CJP 460 Plus. .... 71

**Figure 5.15.** The images of the printed molds. The representation of the geometry of 2.5\_2.5\_3 combined with the gating system 1 is given in Figure 6.16. .... 74

**Figure 5.16.** Schematic view of a demo mold of 5\_2.5\_3. .... 76

**Figure 6.1.** Printed demo molds to check powder-removal behaviors of the lattice structures. .... 79

**Figure 6.2.** An illustration of the silicone rubbers of R PRO 30 A and R PRO 30 B. ... 80

**Figure 6.3.** Representation of the demo molds after silicone rubber casting. Where (a) shows that the excess mixture flow towards the outside, where (b) shows that the exit tunnels strategy was successful. .... 81

**Figure 6.4.** The parts extracted from the demo molds. .... 82

**Figure 6.5.** Schematic representation of the silicone rubber parts. .... 83

**Figure 6.6.** Schematic representation of the sample geometries. .... 84

**Figure 6.7.** Depiction of the first test group of geometries after heat treatment. .... 85

**Figure 6.8.** Depiction of the second test group of geometries after heat treatment. .... 86

**Figure 6.9.** Depiction of the third test group of geometries after heat treatment. .... 87

**Figure 6.10.** A comparison of the temperature test results of each group. .... 88

**Figure 6.11.** The representation of the molds after silicone rubber casting. .... 90

**Figure 6.12.** Depiction of the extracted parts from the molds. .... 91

**Figure 6.13.** The illustration of the cast molds of the geometry 2.5\_1.25\_6 combined with gating systems 2 and 3. .... 93

**Figure 6.14.** The illustration of the cast molds of the geometry 2.5\_2.5\_3 combined with

gating systems 2 and 3.....	93
<b>Figure 6.15.</b> The illustration of the cast molds of the geometry 5_2.5_3 combined with gating systems 2 and 3.....	94
<b>Figure 6.16.</b> The illustration of the casting mold of the geometry 2.5_2.5_3 combined with gating system 1.....	94
<b>Figure 6.17.</b> Schematic representation of the part-removal process of the geometry of 2.5_1.25_6 integrated with the gating system 2.....	95
<b>Figure 6.18.</b> An illustration of the extracted 5_2.5_3 lattice structure integrated with gating system 3.....	96
<b>Figure 6.19.</b> An illustration of the extracted 5_2.5_3 lattice structure integrated with gating system 2.....	96
<b>Figure 6.20.</b> An illustration of the extracted 2.5_1.25_6 lattice structure integrated with gating system 3.....	97
<b>Figure 6.21.</b> A comparison between geometries of 5_2.5_3 and 2.5_1.25_6.....	98
<b>Figure 6.22.</b> An illustration of the extracted 2.5_1.25_6 lattice structure integrated with gating system 2.....	98
<b>Figure 6.23.</b> Comparison of the filling performance of the gating systems.....	99
<b>Figure 6.24.</b> An illustration of the extracted 2.5_2.5_3 lattice structure integrated with gating system 3.....	100
<b>Figure 6.25.</b> An illustration of the extracted 2.5_2.5_3 lattice structure integrated with gating system 2.....	100
<b>Figure 6.26.</b> An illustration of the extracted 2.5_2.5_3 lattice structure integrated with gating system 1.....	101
<b>Figure 6.27.</b> A comparison of the extracted parts integrated with gating system 3. ...	102
<b>Figure 6.28.</b> A comparison of the extracted parts integrated with gating system 2. ...	103
<b>Figure 6.29.</b> Depiction of the new design strategy of sample geometry of 5_2.5_3. Where (a) and (b) shows the actual and transparent view of the lattice structure respectively. Where (c) shows the detail of the new design strategy.....	104
<b>Figure 6.30.</b> Representation of the mold from different aspects. Where (a) shows the actual view of the mold, (b) illustrates the mold cut in half by employing a feature of Solidworks, and (c) shows the front view of the mold as transparent.....	105
<b>Figure 6.31.</b> An illustration of the lattice structure of 5_2.5_3 after casting performed.	

..... 106

**Figure 6.32.** An image of the lattice structure of 5\_2.5\_3..... 106

**Figure 6.33.** A comparison of the 5\_2.5\_3 sample results. .... 107



## LIST OF TABLES

<b>Table 2.1.</b> Categorized materials used in AM methods. ....	8
<b>Table 3.1.</b> Commercial 3D machine manufacturers using SLM / DMLS technologies in their products. The properties are shown on the table are belongs to the 3D machine that is marked by *. These are the best AM machines under their corporate umbrella. ....	19
<b>Table 3.2.</b> Available commercial EBM machine manufacturers. The properties are shown on the table are belongs to the 3D machine that is marked by *. ....	23
<b>Table 3.3.</b> Commercial organizations and their products using Direct Energy Deposition technology. DED-L-P indicates that Direct Energy Deposition-Laser-Powder. ....	26
<b>Table 4.1.</b> Available commercial 3D machine manufacturers are utilizing BJ. ....	46
<b>Table 5.1.</b> The dimensions of all lattice structures. ....	59
<b>Table 5.2.</b> Technical specifications of the ProJet CJP 460Plus[118]. ....	72
<b>Table 5.3.</b> Technical pieces of information about printed molds. ....	73
<b>Table 5.4.</b> Physical and Chemical Properties of Calcium Sulphate Hemihydrate Powder. ....	75
<b>Table 5.5.</b> Heat treatment experiment values. ....	77
<b>Table 5.6.</b> Composition of the Aluminum alloy used in this study. ....	77
<b>Table 6.1.</b> General observations of the temperature tests. ....	89

## 1. INTRODUCTION

Although Sand Casting (SC) has been taking a vital role in foundry community come until today [1] due to its advantages such as; comparatively at below cost, applicable to various part size and geometry [1,2], it is evident that soon it will integrate with the Additive Manufacturing (AM) technology to improve casting quality, reducing the lead time and diminish cost [3]. AM is accepted as a novel way to produce metal parts if we take a look last 30 years. Ever since invented, it has always managed to stay up to date among scientists. AM permits the realization of durable, lightweight structures unreachable by conventional manufacturing techniques, including metal parts [4]. Many AM methods have been developed and divided into seven primary categories. Binder Jetting Technology (BJ), is one of the AM technologies utilizes to create objects layer by layer without any design limits [5], can be accepted as the most accurate AM technique among opportunities to realize molds which can be used in casting applications [3,6].

In contrast to other AM Technologies, there are some admirable properties in BJ;

- Heat source; There is no need to use a heat source to joining of structure materials that are in powder form [5]. It can say that manufacturing is entirely happening without any heat source (cold process).
- Support material; Unlike some other important AM methods, there is no need to use any kind of support material in this technology because of the non-adherent material does this job.
- Easy-post process; On account of there is just one thing needed to be done after printing, the post-process, which consists of removing the dust from the inside of the produced part, is quite easy.
- Cost-effective; Because this technology does not need any support structure and a heat source for forming parts, it is less expensive rather than other AM technologies, which enable the production of metal parts.
- Time-effective; Due to it does not need more steps like sintering, it is faster than many AM methods.
- More-sustainable; BJ is more sustainable technology due to the reusability of non-stick powder, which has the feature of supporting material during production. It is used repeatedly.

Today, although efforts are made to use the support materials effectively and to reduce their effects on the design [4], it is not possible to produce products without support materials by methods that allow direct metal parts production such as Selective Laser Melting (SLM) and Electron Beam Melting (EBM). The obligation to use support materials continues to be an obstacle to the production of complex structures in front of these technologies.

In this master's thesis, we have looked for an answer to the possible design limits to cast aluminum onto a mold produced with BJ Technology. During these processes, the machine using BJ technology used gypsum and liquid binder to create the final part used as a mold. To obtain a successful filling during the casting process, three different gating systems designed by using a Computer Aided Design (CAD) program. In order to understand the relation between the inner complexity of the mold and the powder-removal ability, eight lattice structures were designed through three critical design parameters. After the molds fabricated, the heat treatment process performed at three different temperatures. BJ can fabricate metal parts in two ways as a direct or indirect way. This study is focused on its ability to produce metal parts indirectly.

## **2. ADDITIVE MANUFACTURING**

### **2.1. Technologies and Materials**

AM arose approximately three decades ago as a high-tech manufacturing method that could force all traditional methods to combine with that novelty. Stereolithography (SLA) was the first AM technic to enter the literature. It was generated and patented by Chuck W. Hull, the founder of 3D Systems Corporation in 1984 and 1986 [7]. At those times, even though several people claim that Baker was the first person who patented in a former metal deposition technology with the aid of electric arc [8] yet this idea could not find a place to itself in the literature. Though AM has many synonyms such as Additive Fabrication, Additive Processes, Rapid Manufacturing, Direct Digital Manufacturing, Rapid Prototyping, Layer Manufacturing, and Solid Freeform Fabrication [9] it has only one standard definition which is expressed as "a process of joining materials to make objects from 3D model data, usually layer upon layer, as opposed to subtractive manufacturing (SM) methodologies" according to the American Society for Testing and Materials (ASTM) F42 Committee [10]. The scientists went further because of its whet appetite benefits such as reduced cost and lead times, permits freeform fabrication, and so on.

As shown in Figure 2.1, seven AM methods developed by researchers and categorized by the ASTM subcommittee until today;

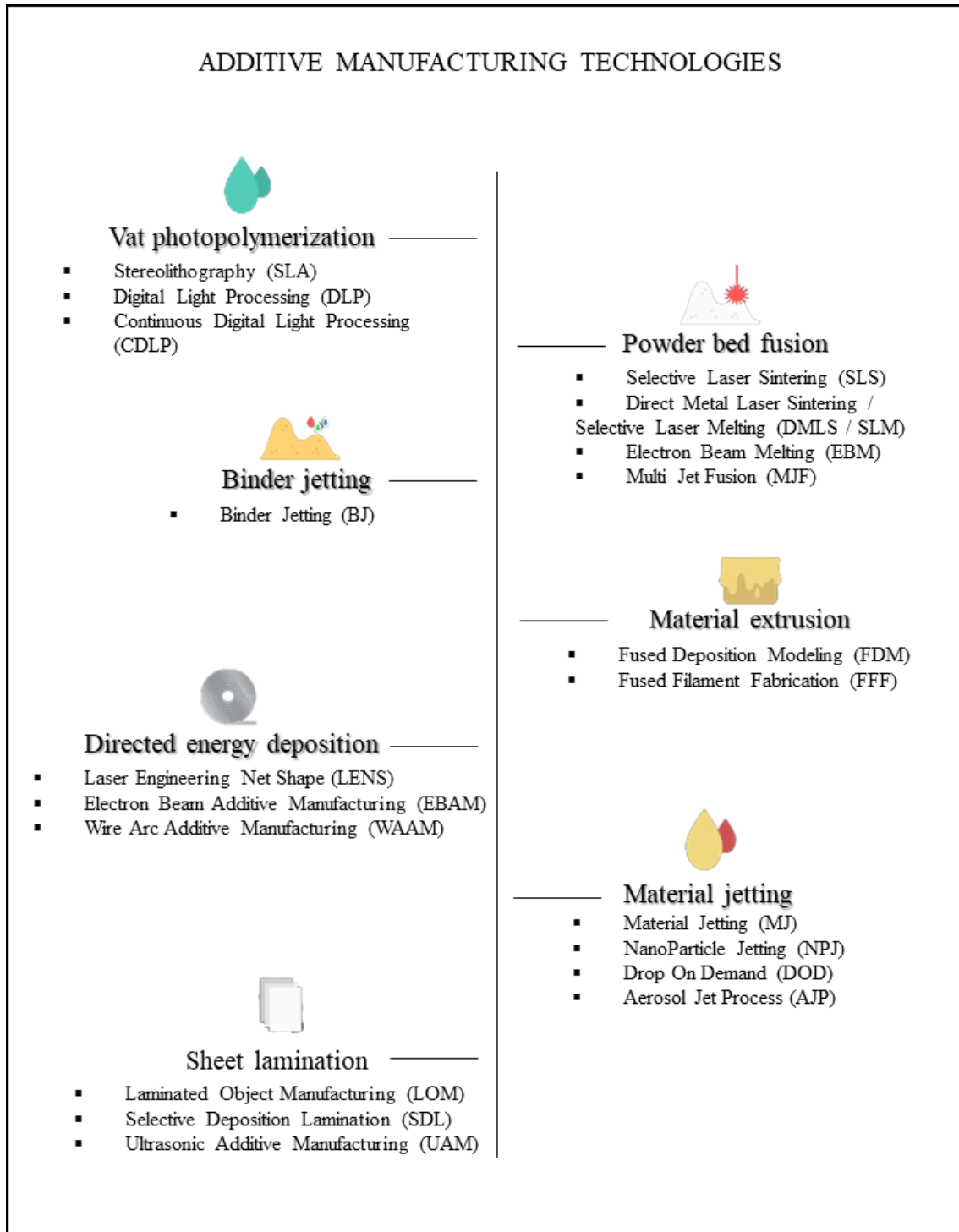


**Figure 2.1.** Additive Manufacturing technologies categorized by ASTM F42 Committee.

- a) Vat Photopolymerization (VP) is a process a heat source layer by layer selectively cures a liquid photopolymer contained inside a container until the part created [11].

Steps of Vat photopolymerization:

- First, the building chamber moves down with the first layer thickness.
- Then, the UV light used hardens the resin layer in layers. The platform continues to move down, and additional layers added on top of each other.
- After the operation is done, the vat is drained with the help of resin, and the object is removed.

b) Powder Bed Fusion (PBF) is quite popular among 3D-Machine Manufacturers owing to its benefits like manufacturing end-use parts. PBF approaches such as SLM and Direct Metal Laser Sintering (DMLS) utilize high-energy beams such as laser or electron to creates desired parts selectively. Like it happens in all AM methods, allow the powder to spread over previous layers to create a new layer. The leveling roller or a blade does this job. A structure like a hopper next to the bed is ready to provide material for new layers [12].

Steps of Powder bed fusion:

- A layer that has nearly 0.1 mm thickness is spread over the build platform.
- Before the leveling roller or a blade brings a new layer towards the built platform, a laser fuses the first layer or first cross-section of the part.
- The process of fusing powders and adding layers is continued repeatedly.
- The loose non-stick powder remains around the piece produced. After the part is created, it is taken around the part in the cleaning process.

c) Binder Jetting, which is generally used for mold manufacturing, an adhesive material is applied on the powdered material with a movable head like ink printers, and the next layer of powder spread over to the top of the previous one, then it is hardened. As the adhesive is the primary holder, generally, more fragile solutions are realized. There are two primary materials used in Binder Jetting technology. The built material is usually in powder form. The binder is a substance in liquid form that provides adhesion between the layers [2, 6, 13–15].

Steps of Binder jetting:

- First of all, the process starts with the powder is spread over onto the building platform using a leveling roller.
- Then the inkjet releases the liquid droplets, which are binder into the first layer where required.

- Once the releasing process of binder done, the platform goes downwards.
- The leveling roller brings another powder layer then is spread over the previous one. Thus, the parts begin to form gradually in the areas where the binder is left.
- Like we mentioned in the introduction section as well, the stick-free building powder acts as a support material. So, there is no need to use any external support structure in this technology.
- The process repeats until the final part obtained.

d) Material Extrusion (ME), Fused Deposition Modeling (FDM) is the only and famous technique of the ME whereabout material is selectively distributed throughout a print-head or hole. It is a commonly used technique used on many inexpensive, domestic, and hobby 3D printers. Polymers and plastics are used in this technology as the primary supply materials [16, 17].

Steps of Material extrusion;

- ME technology utilizes a continuous thermoplastic filament, which is in the polymer family as a material source. The filament is nourished from a spiral throughout a moving printer head, which is pre-heated, often abbreviated as an extruder.
- The metal, which is in molten form, is obtruded from the nozzle of the extruder and first released on a 3D printing platform, which can be heated for extra cohesion. Once the first layer is completed, the extruder and platform are separated, and then the second layer is formed on the last layer laid.
- The operation continues until the final part's forming is done.

e) Directed Energy Deposition (DED) is a process where metal wire or powder is united with energy supply to deposit material onto a build platform or a piece. The methods of this technology can do building huge large parts and are fashionable, owing to the rapid speed of deposition. Because it looks like a welding process, it utilizes to repair and maintain existing parts [18].

Steps of Directed energy deposition:

- The nozzle, which can move in many directions such as 4 or 5 axis rotates around the move-free part that is desired to be produced. This turn is also a necessity of leaving the material on the desired surfaces.
- The built material is provided in wire or powder form. It is commonly fused with the aid of a laser and electron beam, and plasma arc deposition is also used depends on which technique of DED applied.
- This process is applied to a new part or a part that is damaged to repair it. It lasts layer by layer until the final piece created.

f) Material Jetting (MJ), in this method, liquid or melt wax type materials are formed by controlling, spraying, and curing by ink printer-like moving heads. The most significant advantage of this method is that sensitive and bright surfaces can be obtained easily; however, it is a relatively fragile and time-consuming manufacturing method [19, 20].

Steps of Material jetting:

- The supply material is deposited from the nozzle towards the surface where required.
- Then the structural material solidifies, and the first layer takes place.
- The next layers are added to the previous one, following the same path.
- The layers are allowed to cool and harden or are cured by UV light.
- Since the support structure has to be used during fabrication, it is removed after all layers are added.

g) Sheet Lamination (SL) is a way to fabricate pieces involving the principle of superpositioning of several layers of material capable of foil to form an object. Each foil is cut with a knife or laser to fit the desired design [20].

Steps of Sheet lamination:

- The material is placed on the cutting bed and adhered to the previous layer.
- After the desired shape is cut, the next layer is added.
- It can also be cut before adhering to the layer on-demand or as required.

The constant development of layered manufacturing methods provides new opportunities in the production field [21]. Due to its advantages, this technology easily penetrated aerospace, medicine, architecture, casting, and many other industries. However, there are

still some constraints about the cost of raw materials used at those technologies. As shown in Table 2.1 below, there is a material limitation on every specific method. In other words, although there is unlimited freedom of design, there is no unlimited supply of materials that can be used in this technology.

**Table 2.1.** Categorized materials used in AM methods [9-11].

Binder Jetting	Aluminum alloys, Co-Cr alloys, Nickel alloys, Stainless steel, Ti-6Al-4V, Tool steel
Directed Energy Deposition	Aluminum alloys, Co-Cr alloys, Nickel alloys, Stainless steel, Ti-6Al-4V, Tool steel
Material Extrusion	Polycarbonate, ABS, HIPS, PC/ABC Blend, Polyetherimide, Polylactic acid, Advanced Plastics (PEEK, PEI), Ceramics
Material Jetting	Thermosets (Acrylics, Acrylates, Epoxies), Stainless steel, Wax
Powder Bed Fusion	Polyamide (Nylon), Polystyrene, Polypropylene, Polyester, PEEK, Aluminum alloys, Co-Cr alloys, Gold, Nickel alloys, Silver, Stainless steel, Titanium, Ti-6Al-4V, Tool steel
Sheet Lamination	Paper, Plastic, Stainless steel, Aluminum alloys, Ti-6Al-4V
Vat Polymerization	Acrylics, Acrylates, Epoxies

## 2.2. Design in Additive Manufacturing

Its ability to manufacture without being dependent on the complexity levels of the parts can be considered the most important of its amazing features. An essential difference between AM and SM is that it is mainly the ability to produce low volume pieces with high design complexity [9]. In AM, the progress in production is happening layer by layer. Because of its production style, it enables the formation of parts where can not be produced by conventional SM techniques [22]. AM is used in many fields such as manufacturing applications, medical/dental implant construction, conceptual modeling, direct casting mold and part production, metal and prototype part production, architectural applications, space/automotive industry, rapid mold manufacturing, educational equipment [9,13]. The main reason it can adapt to many areas in a short time is the design freedom feature.



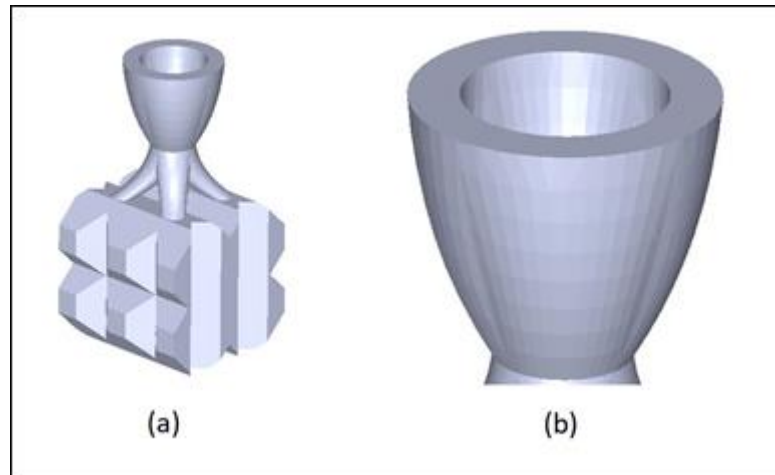


**Figure 2.3.** Pattern image in STL format, (b) is the zoom of the sprue-top region.

As it is illustrated in Figure 2.3 above, the triangles use to identify the surfaces of an object. These triangles do not exist in designs that have not been converted to STL format. After an STL file created, the file is transferred into a program called a slicer. That program takes the STL file and transforms it into G-code, numerical control (NC) programming language [26]. It is now ready to print.

- c) FILE Transfer; the file transformed to STL is then transferred to the machine with the aid of particular machine software. The file transfer step is the last station to check the design of the file before the printing process.
- d) MACHINE Setup; 3D printing machines differ from those used in traditional methods due to their high technology. It usually consists of many small and complex parts. For this reason, machine maintenance and calibration should be kept up-to-date to produce error-free parts. At this stage, it is checked whether the feedstock is sufficient in the machine, if not, loading is done by an operator. Raw materials used in AM are generally not long-lasting and require careful use. Some AM techniques allow repeated use of feedstock that acts as a support building material. Attention should be paid to this situation due to the decrease in material quality owing to continuous use. In this step, some critical production parameters like timing, thickness are reviewed.
- e) MANUFACTURING Process; generally, AM machines do not need to be checked with the help of an operator after printing begins. The machine works automatically. Since the feedstock and binder level in the machine is checked

before printing starts, errors can be observed only due to software, connection, and mechanical machine problems.

- f) POST Processes; the support structure used is removed from the produced parts at this step. Depending on the AM technique applied, the difficulty of the operations to be performed after production varies. In some AM methods such as SLM or EBM necessitate using a support structure to constant for overhanging pieces and reduce the residual stresses [4]. The operator has to remove the support structure from the part carefully. On the other hand, in some AM methods like BJ, there is no need to use any external structure because the loose powder does it. Besides, cleaning with high-pressure air, polishing, painting are the other applications in this step.

### **2.2.2. Design constraints in additive manufacturing**

Design freedom can be accepted as the most crucial feature of AM technology. Owing to its unique capabilities to perform such as shape, hierarchical, material, and functional complexity [27], it responds to the demands of the entire manufacturing industries that are using design in their applications. However, AM methods have dissimilar design limitations as well as unusual features. The fact that an idea can be designed in 3D without any design restrictions does not mean that this design can be produced in 3D. All AM methods have their limitations. Due to these limitations, some design parameters to be considered during design are listed below;

- a. Overhangs; design should be carried out using angles smaller than 45° without using as many protrusions as possible.

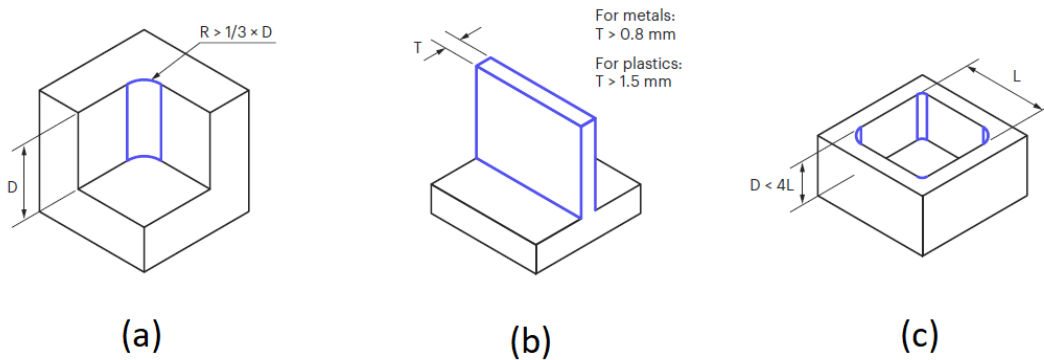


**Figure 2.4.** Schematic representation of the average design parameters that needed to be considered while designing for all AM methods, (a); explains the fillet ratio that should be in the vertical edges remaining on the internal surface, here  $R$  represents radius,  $D$  represents the depth at the cavity, (b); expresses the thickness ratio for the metals and plastics, (c); showing that the information about the depth limitation in all spaces of the design [28].

- b. Wall thickness; the wall thickness is vital for all AM techniques. For example, when considering a mold produced in the BJ technique, when molten metal is poured into it, it should have a wall thickness that can withstand the first effect of this metal. Otherwise, the mold cannot show the desired performance during hot casting. Besides, producing thin-walled parts results in fragility in the structure. For these reasons, at the design stage, a minimum of 0.8 mm wall thickness should be added to the parts desired to be produced, to avoid manufacturing defects.
- c. Warping; while modeling a part of a new idea in 3D, there is a thing that is important not to be overlooked. These are the situations where changes may occur in shape, change of state, and appearance of the part during the printing process. Because the behavior of a material under hot and cold is different. For instance, when the Titanic ship hit the iceberg, the bottom layer of the ship was torn like paper. Since the material covering the bottom layer of the ship at that temperature was almost zero in energy absorption, it could not absorb the energy released by the impact. What they missed was to rely on data from impact tests at room temperature. In summary, the heat source (laser) used by some AM techniques during production, and the environments in which the produced parts are kept after production are essential. Oval corners and large flat surfaces should be added to the part to avoid warping in part.

- d. Level of detail: unnecessary details should be avoided in the design of the part to be produced, and the production method to be chosen should be carefully considered. This choice has a direct impact on the duration and cost of production. The designer should be realized that the production method should be determined according to the level of detail to be used in the models.

### **2.3. A comparison: Additive versus Subtractive Manufacturing**

The production of non-damaged, properly shaped products at low cost has always been a challenge for the manufacturing industry. As a result of many years of work, two different approaches have emerged in order to produce these products at an acceptable price and performance. In the first, the material is added layer by layer to create a three-dimensional piece, whereas, in the other, the material is removed as layer by layer from the piece to obtain the desired three-dimensional product. The human being is not foreign to the concept of AM and SM. A building can be constructed, whereas putting the bricks on top of each other is an example of AM. An example of SM, if we need a tapered pile in nature, we can cut a piece of wood layer by layer with the help of a knife to make it sharp. So, it can be said that humankind has already been using these technologies with primitive methods for years.

#### **2.3.1. Similarities**

- ❖ As with traditional methods used in the industry, the primary purpose of these two technologies is to manufacture parts with excellent surface quality economically.
- ❖ Both technologies are widely used in manufacturing industries.
- ❖ They can produce pieces faster than conventional production methods.

#### **2.3.2. Dissimilarities**

- ❖ As it is mentioned in the introduction sentences of this part, in the AM process, while the building material is added over each other as layer by layer, in SM the building material is extracted from the part as layer by layer. Briefly, the production concepts of them are different.

- ❖ While the AM method is generally suitable for materials that have a low melting point, the SM method can be applied to all solid materials without such constraints.
- ❖ In AM while the process is happening with almost zero waste of materials, yet in SM there is always waste of materials such as scraps or chips.
- ❖ Although there is a limited capability of design in SM, there are no design restrictions in AM. Freeform fabrication (FF) is one of the most significant novelties that entered our life with AM.
- ❖ Even though entirely hollow parts can be produced with AM, it is only possible with SM as long as joining is permitted.
- ❖ While SM techniques are capable of processing a wide variety of materials, this amount is quite low in AM.

### **3. METAL 3D PRINTING IN ADDITIVE MANUFACTURING**

The art of processing metals has become the most prominent driving force behind the civilization of humankind for thousands of years. This adventure continued with the alloying of metals such as iron, copper, bronze, and aluminum, starting with the processing of pure metals such as gold in nature. Extraction and processing of metals have progressed in parallel with technology. With the arrival of new ages such as discovering and computer, new technologies emerged over conventional techniques. The AM is one of them and has proved to be a revolution in technology in a short time thanks to its features such as design freedom and production speed. Whereas conventional production methods still broadly accepting among manufacturing industries, it is apparent that it can not find a place among the developing technologies such as AM methods. Nevertheless, it can not be said that the industry is entirely integrated with this novelty as well. Currently, the issue of trust, especially in critical point applications of 3D produced metal parts, is still discussed among experts. Although this method is still critically approached by researchers, it has made tremendously significant progress, especially in the direct production of metal parts in the last ten years. This chapter presents direct AM metal production techniques and comprehensive reviews.

#### **3.1. Metal Additive Manufacturing Techniques**

AM has become a highly-demand fabrication method in recent years to produce metal parts. It is necessary to look at its surprised features such as minimum human effort, short production cycle, and profound design freedom to understand how it stands out as a popular technique among others in this competitive industry environment. According to the latest reports [19,20], the number of metal 3D Machine Manufacturers, the market size of 3D printed metal parts, and the amount of investment has been dramatically increased over the last five years. This increase will undoubtedly remain the driving force behind the constant development of metal AM techniques. It is a fact that innovative technologies such as PBF, DED, BJ, ME, MJ, which have entered our lives with the term additive production, have brought in many new concepts such as their technologies as well. However, it cannot be said that these new concepts are met by all the AM technologies that have entered our lives. For instance, technologies like PBF-DED, beam-based techniques, are energy-inefficient, and operation costs are high owing to its high

technology. Moreover, because of the nonequilibrium metallurgical effects that might occur during material deposition, internal stresses, cracks, or point defects may occur in the parts. Unlike beam-based manufacturing technologies, many industrially broadly-accepted non-beam-based methods can be used for real fusion between structural materials such as powder or wire. These methods can reach the desired final product properties such as surface quality and economy, which cannot be achieved with beam-based techniques. The popularity of these non-beam based techniques has increased rapidly in recent years due to the advantages they add to the industry. The number of scientific publications in the last five years supports this idea [31]. In summary, it should not be overlooked that each technique has important advantages and disadvantages to others. It is significant to note that this chapter will be focused on the technologies that are popular among 3D-Machine manufacturers, yet it will also talk about all existed 3D metal production methodologies. BJ technology will not be in this chapter. In the following chapter, it will be analyzed in detail.

### 3.1.1. Powder bed fusion

PBF is a technology that is broadly-accepted among 3D metal machine manufacturers. It is using a high amount of power source to fuse powders selectively. There are two primary energy sources that PFB uses to melt or sinter powders represents in Figure 3.1.

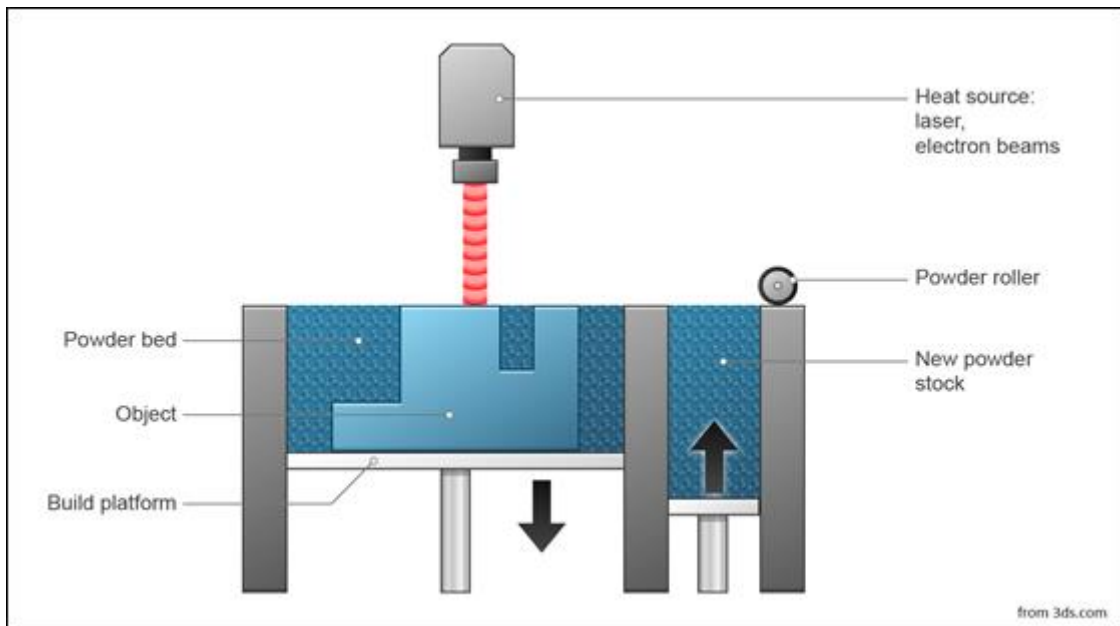


**Figure 3.1.** Schematic illustration of Powder Bed Fusion approach (PBF).

PBF approach consists of four sub-techniques. Three of them, while Direct Metal Laser

Sintering, Selective Laser Melting, and Selective Laser Sintering (SLS) use a laser source which has high-intensity, Electron Beam Melting utilizes an electron beam source. However, only three of these techniques are applicable to produce metal parts. SLS only allows for fabricating rigid plastic parts. For that reason, we will just look at those techniques that enable metal pieces production.

### **3.1.1.1. Selective laser melting and direct metal laser sintering**

SLM and DMLS, both of these techniques have very similar principles to SLS in manufacturing the desired parts, yet SLM and DMLS, the most crucial feature that distinguishes these techniques from SLS, are that they are used only in the production of metal parts. SLM operates on the principle of applying heat power until the metal powder used melts ultimately. The metal powder is expected to be in an entirely melt form. However, DMLS applies heat until the temperature that will allow the metal powders to fuse chemically. While the DMLS technique only is used with alloys such as titanium, nickel, SLM has no such restriction. In other words, SLM allows for the use of single-component metals such as pure aluminum. Events such as melting, flow due to melting, and rapid solidification that may distort the lattice structure may occur because of the interaction of powder and beam source during production. No matter how these techniques are fit for the metal part production, because of those events, it should not be forgotten that the residual stresses, distortion or warping may occur in the metal pieces to be manufactured. However, it is possible to diminish such production errors by using support structures. This approach works with the principle where it represents in Figure 3.2.

A beam source that is a laser in SLM /DMLS is reflected onto the platform selectively through a movable mirror through the lenses.

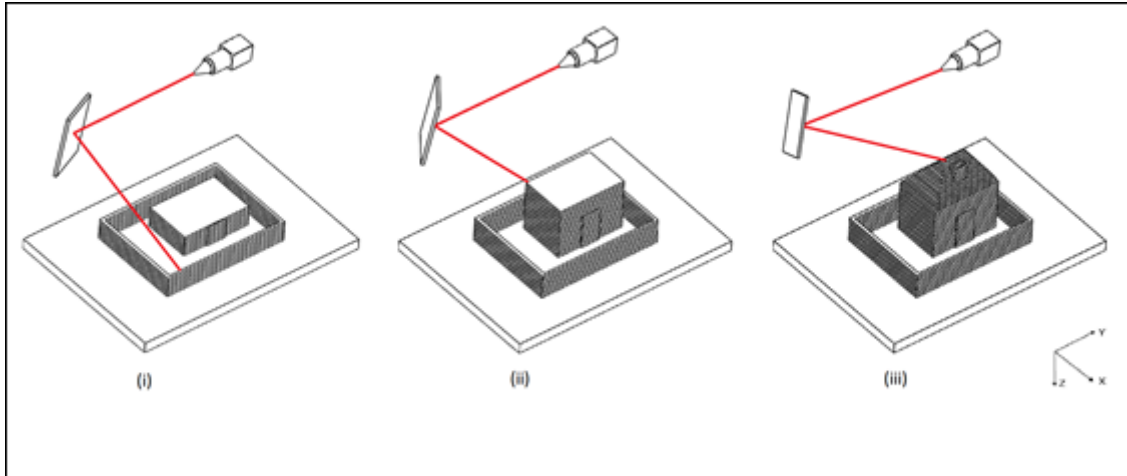


**Figure 3.2.** Processing of the regions where selectively required by reflecting the laser source with the help of a mirror.

Nevertheless, what is that mean selectively exactly? It means that it is the process of directing the beam source in planar according to the design configuration of the moving mirror in the system. In other words, that is a process of reflecting the beam source only to the regions where required. As with other AM techniques, production takes place in 3D (XYZ). However, melting or sintering occurs only along the X and Y planes. After the curing process of the powder layer is finished, the platform moves downwards as much as the pre-determined layer thickness. This direction is the Z-direction, and no melting or sintering process takes place along this direction. The dust layer that will form the next layer is laid on the platform with a knife-like mechanism. This process continues until the desired piece is obtained. The piece is exposed to a high temperature due to the beam source used during the production. To avoid oxidation problems that may occur owing to this temperature, the process is continued by giving inert gas to the environment [20, 32, 33].

Nowadays, many 3D Machine manufacturers use SLM/DMLS technologies in their machines. A list of manufacturers using technologies of SLM / DMLS is given in Table 3.1.

**Table 3.1.** Commercial 3D machine manufacturers using SLM / DMLS technologies in their products. The properties are shown on the table are belongs to the 3D machine that is marked by \*. These are the best AM machines under their corporate umbrella.

Commercial 3D Machine Manufacturers						
Companies	Products	Technology (SLM / DMLS)	Beam Source Configuration	Layer Thickness ( $\mu\text{m}$ )	Built Volume (XYZ, mm)	Used Materials
EOS[34]	EOS M 100, EOS M 290, EOS M 300-4, EOS M 400, EOS M 400-4*	SLM/DM LS	Yb-fiber laser; 4 x 400 W	90 (max)	400 x 400 x 400	Aluminum, Cobalt-Chrome, Precious metals, Tool steel, Stainless steel, Titanium
3D Systems [35]	DMP Factory 500 Solution*, DMP Flex 350, DMP Factory 350, DMP Flex 100, ProX DMP 300, ProX DMP 200	SLM/DM LS	3 x 500 W / Fiber laser	2-200	500 x 500 x 500	Aluminum, Cobalt-Chrome, Stainless steel, Titanium, Maraging steels, Nickel-Super alloys
SLM Solutions [36]	SLM 125, SLM 280, SLM 500, SLM 800*	SLM/DM LS	Quad (4x 400W or 4x 700W) IPG fiber laser	20-90	500 x 280 x 875	Aluminum alloys, Titanium alloys, Nickel alloys, Tool, and Stainless steel, Cobalt alloys, Copper alloys, Titanium
RENISHAW	RenAM	SLM/DM	Quad 4 x	20-100	245 x	Titanium

[37]	500Q*, RenAM 500S, RenAM 500E, RenAM 500M, AM 400, AM 250	LS	500 W – ytterbium fiber lasers			245 x 335	alloy, Aluminium, AlSi10Mg alloy, Cobalt- Chromium , Stainless steel, Nickel alloys
CONCEPT LASER [38]	M2 Series 5, Mlab, Mlab R, Mlab 200R, M line Factory, X Line 2000R*	DMLS	2 x 1000 W (cw) fiber lasers	30-150		800 x 400 x 500	Aluminum (AlSi10Mg), Titanium (Ti6AL4V Grade 23), Nickel 718
Additive Industries [39]	MetalFAB 1*	SLM	Yb Fiber Lasers 500W	20-100		420 x 420 x 400	Titanium (Ti6Al4V) , Aluminium (AlSi10Mg), ScalmAlloy©, Stainless Steel (316L), Inconel (IN718), Tool Steel (1.2709)
SISMA[40]	MYSINT 100, MYSINT 100 PM, MYSINT 100 PM/RM, MYSINT 100 RM, MYSINT 100 RM PRO,	SLM	2x Fiber Laser 200 W	20-40		100 (Diameter) x 100 (Height)	null

	MYSINT 100 DUAL LASER, MYSINT 100 RM DUAL LASER*, EVEMET 200, MYSINT 300							
ReaLizer	SLM 50, SLM 100, SLM 125, SLM 250, SLM 300, SLM 300i*	SLM	Fiber Laser 400- 1000 W	20-100	300 300 300	x x	Metal (undescr ib ed)	
DMG MORI[41]	LASERTE CH 12 SLM, LASERTE CH 30 DUAL SLM*	SLM	Fiber Laser 600 W - 1 kW	20-100	300 300 300	x x	null	
TRUMPF [42]	TruPrint 1000, TruPrint 2000, TruPrint 3000, TruPrint 5000*	SLM	TRUMPF fiber multilaser 3 x 500 W	30-150	300 (Diamet er) 400 (Height)	x	Stainless steels, tool steels, Aluminum alloys, Nickel- Based alloys, Titanium alloys	

Surprisingly, a 3D System is the only company that can offer solutions below 20 microns layer thickness and over 150 microns with its own production DMP Factory 500 Solution. Even though lowering the layer thickness increases lead time and residual stresses, It should not be overlooked that it is also a meaningful way to manufacture high-strength parts. Apart from those manufacturers as listed in Table 3.1, there are many other successful sellers such as CREATOR from Coherent Company, which is a German product, FS301M from FARSOON company from China.

### 3.1.1.2. Electron beam melting

EBM provides an opportunity to build parts faster while using more low-energy than other PBF methods such as SLS, SLM, or DMLS. On the other hand, active part production capability results in lower surface roughness and insufficient layer thickness. However, a study reported that [43] it has been observed that the temperature that occurs while the fusion takes place between the powders is evenly distributed. For this reason, EBM enables the fabrication of high strength parts. As the name suggests, EBM utilizes high-energy electron beams to fuse metal powders selectively. When it compares with a laser beam, it is stated that it is a more powerful beam source. In this way, it can reach a thicker surface thickness with each scan. Its fast production ability comes from the electron source it uses. Stresses that distort parts are seen in EBM technology rarely. Each layer must be sintered to eliminate unwanted electrostatic charges and particle repulsions before electron beam scattering. As we mentioned above, this is due to the pre-heating process that reduced residual stress during production. For this reason, it is not necessary to use support structures mostly, as in SLM and DMLS. Besides, just like in the SLM and DMLS duo, production takes place under vacuum. Moreover, there is no broad range of materials that can be used for manufacturing. It works only with conductive materials[20].

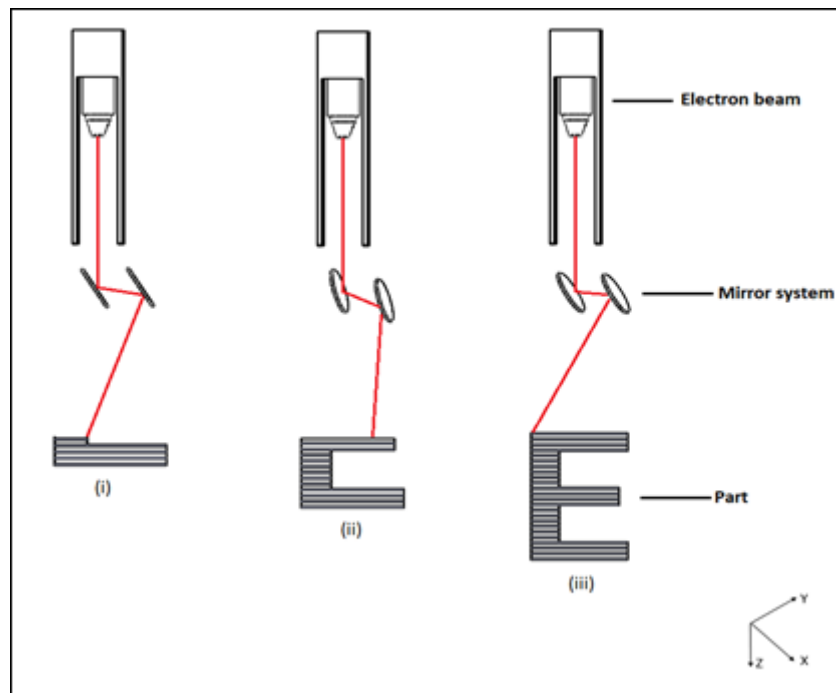


**Figure 3.3.** Schematic representation of the EBM method, where (i), (ii), and (iii) represents a sequential production.

As shown in Figure 3.3, the electron beam source is located at the top of the EBM machine. The released electron beams are transmitted to the specified point with the help of a structure called the mirror system. The remaining procedures are similar to SLM. After the melting process is completed selectively, the new powder layer is brought to the building chamber. These processes continue until the part is entirely manufactured.

**Table 3.2.** Available commercial EBM machine manufacturers. The properties are shown on the table are belongs to the 3D machine that is marked by \*.

Commercial 3D Machine Manufacturers					
Companies	Products	Technology (EBM)	Power level (range)	Built Volume (XYZ, mm)	Used Materials
Sciaky[44]	EBAM 300*, EBAM 200, EBAM 150, EBAM 110, EBAM 40	EBM	42 kW- 60 kV	5791 1219 1219	x x Titanium, Titanium alloys, Tantalum, Tungsten, Inconel 718, Niobium, Stainless steel (300 series), 2319- 4043 Aluminum, 4340 Steel, Zircalloy, 70-30 Copper Nickel, 70-30 Nickel Copper
Arcam[45]	Arcam EBM Spectra L*, Arcam EBM Spectra H, Arcam EBM A2X, Arcam EBM Q10plus, Arcam EBM Q20plus	EBM	Null- 4.5 kW	350 (Diameter) x 430 (Height)	Ti6Al4V Grade 5, P-Material, Ti6Al4V Grade 23, P-Material

### 3.1.2. Directed energy deposition

DED is another widely-used AM method among 3D machine manufacturers. It has a broad range of names such as Laser Engineered Net Shaping (LENS), Directed Metal Deposition (DMD), Laser Deposition Welding (LDW), and 3D Laser Cladding. The

reason for this is that standardization has not been carried out entirely for naming. DED that is the name of this part, is the only well-accepted standardized name by ASTM. This naming sophistication was created unintentionally by manufacturers using this technology in their 3D printers. However, even though the process varies in some ways, it is similar. In general, there are four kinds of energy sources and two kinds of feedstocks in this method. A laser beam, electron beam, plasma, and electric arc are used as energy supplies. Feedstocks are generally in powder or wire form. These technical features vary from manufacturer to manufacturer according to the technology used in their machines [33, 46].

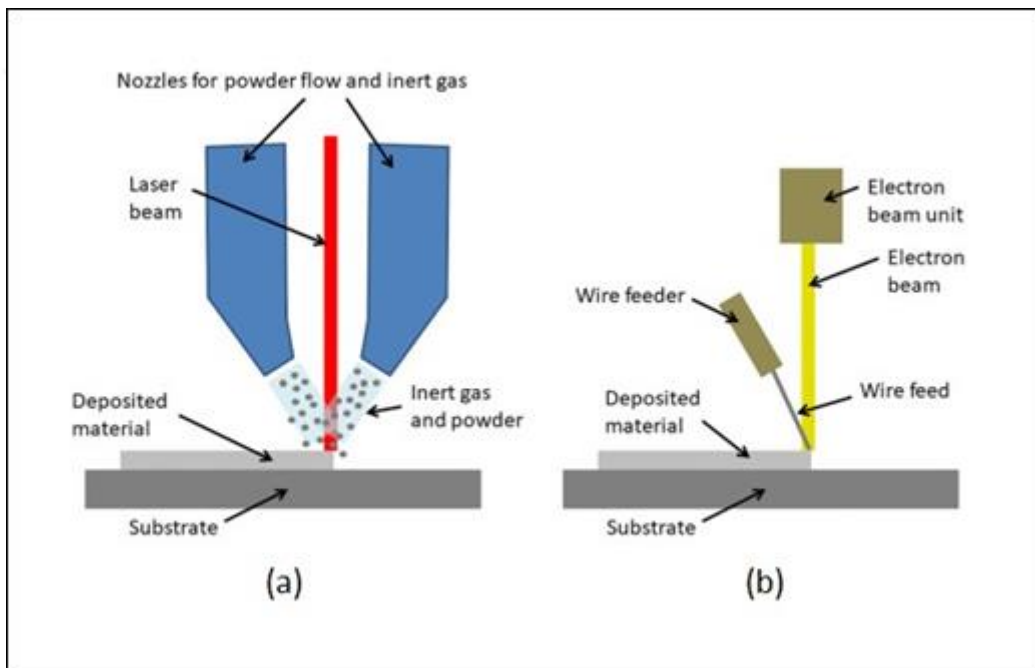


**Figure 3.4.** An illustration of the working principle of the DED-3D machine, where (a) represents a machine that is using a laser beam as an energy source and supply material in powder form, the technology called DED-Laser Beam, where (b) represents a machine that is using an electron beam as an energy source and building material in wire form, the technology called DED-Electron Beam [47].

As shown in Figure 3.4, as generally, a 3D-DED machine is composed of a nozzle that is attached to the arm, which can move in many directions, a build chamber where oxidation is prevented by giving an inert gas, and an energy source. With the help of deposition that occurs at the point where the feedstock and heat source meet, the desired parts are produced layer by layer. The DED approach gathers several different technologies under

a single roof. These are Laser Metal Deposition (LMD), Laser Engineered Net Shaping (LENS), Directed Metal Deposition (DMD), Electron Beam Additive Manufacturing (EBAM), and Wire Arc Additive Manufacturing (WAAM). However, we will only examine LENS, EBAM, and WAAM techniques under this section.

### 3.1.2.1. Laser engineered net shaping

It is a first developed technique on behalf of the DED approach by Sandia National Laboratories nearly 25 years ago. Behind the development of this technique, the current knowledge in the field of laser coating and Computer Numerical Control (CNC) motion technology has a significant impact. In this method, the feedstock can be in Powder or wire form, and the laser beam is used as an energy source [48].

As given in Figure 3.5, the feedstock feeds into the road where the laser source released.

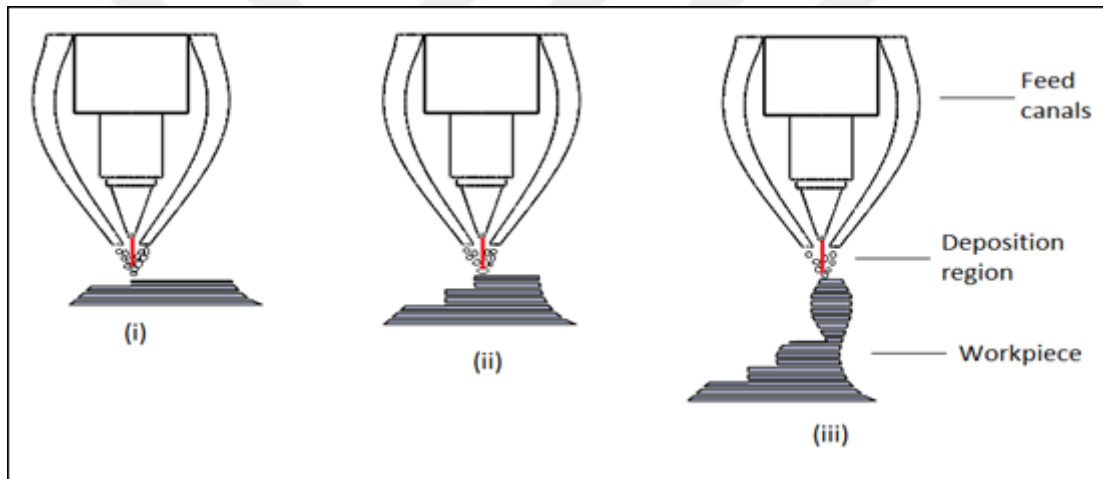


**Figure 3.5.** A schematic representation of powder feed-DED.

Metal in powder or wire form creates a melt-like region under the influence of laser beams. The metallic powders are regularly sprayed towards this area. Any spraying interruption that may occur during the process can cause significant defects in the structure. The first layer is fabricated with the aid of nozzle movement as selectively. The part is obtained by repeating these processes. This technique is widely used to produce parts from scratch, as well as to repair existing damaged parts. In general, powder-fed techniques are applied to obtain a substantial thickness of layers. However, as a result, lower resolution parts are obtained compared to powder bed technologies. In wire fed methods, the process is generally the same. However, since there is no standardization

yet, it can be said that it is still a technique applied under the name of welding processes. Although both feeding methods, wire, and powder are industrially broadly-accepted, powder feeding technology is more widely used by 3D machine manufacturers. A comprehensive screening of machine manufacturers using this technology is given in Table 3.3.

**Table 3.3.** Commercial organizations and their products using DED technology. DED-L-P indicates that DED-Laser-Powder.

Commercial 3D Machine Manufacturers						
Companies	Products	Technology (Powder-P, Wire-W, DED-L-P, DED-L-W)	Beam Source Configuration or Power level (range)	Built Volume (XY Z, mm)	Used Materials	
Sciaky[44]	EBAM 300*, EBAM 200, EBAM 150, EBAM 110, EBAM 40	DED-L-P DED-L-W	42 kW - 60 kW	5791 x 1219 x 1219	Titanium, Titanium alloys, Tungsten, Inconel 718, Niobium, Stainless steel (300 series), 2319-4043 Aluminum, 4340 Steel, Zircalloy, 70-30 Copper Nickel, 70-30 Nickel Copper	
BeAM[49]	MODU LO 250, MODU LO 400, MAGIC 800*	DED-L-P	500W to 2kW fiber laser	1200 x 800 x 800	Titanium alloys, Inconel 718, Stainless steels	
TRUMPF[50]	TruLaser Cell 3000, TruLaser Cell 7040*	DED-L-P	2000W 6000W TruFlow	- 4000 x 2000 x 1000	Null	
Optomec	CS 150, CS 600, CS 800, CS 1500, MTS 500,	DED-L-P	high power 3 kW fiber laser	860 x 600 x 610	Stainless and tool steels, Nickel-based alloys, Cobalt, Tungsten, Non-reactive metals	

	MTS 860*, LPE					
FORMAL LOY	FORM ALLOY X, FORM ALLOY L*	DED-L-P	Blue (450nm) up to 8 kW	500 x 500 x 500	Nickel-based, based, Titanium-based, Cobalt-based, Copper- based	Iron-
DMG MORI[41]	LASER TECH 65 3D hybrid, LASER TECH 125 3D hybrid, LASER TECH 65 3D, LASER TECH 4300 3D hybrid*	DED-L-P	Fiber-coupled diode laser 3,000 W	660 x 398 x 1520	Null	
InssTek	MX- Lab, MX- 600, MX- 1000*, MX- Grande, MPC	DED-L-P	Ytterbium Fiber laser Max 2000W	800 x 1000 x 650	Titanium, Stainless steel, Hastelloy, Cobalt	Steel, Nickel, Copper,

### 3.1.2.2. Electron beam additive manufacturing

The Electron Beam Additive Manufacturing is another essential 3D-metal part production technique. NASA invented it in order to print well-functional parts to use in space applications. Unlike the energy source used in the LENS technique, in this technique, electron beams constitute the primary energy source. With the use of electron beams, pieces that have excellent surface quality can be fabricated because of the low deposition rates [51, 52]. In EBAM, the metal source is fed as wire, in contrast to the powder form. However, the printing process is quite similar. Just as it happens in LENS, the end part of the wire used in the feeding process is melted, then it is selectively injected into the

desired areas.

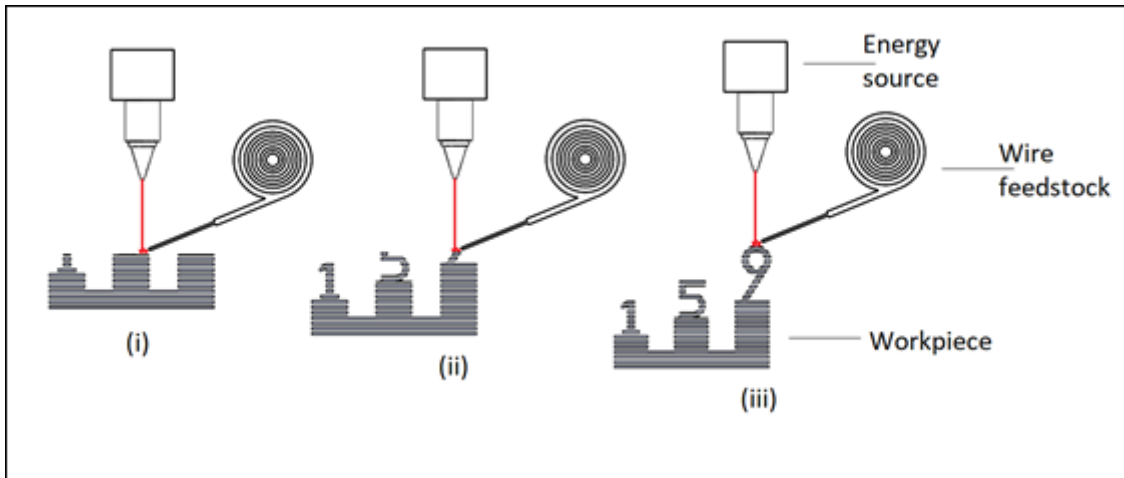


**Figure 3.6.** Schematic representation of wire feedstock-EBAM technique.

During the layer-by-layer creation of the material, conditions such as the distance between the focused electron beams and the piece produced, wire feed speed, and scanning speed are controlled by the sensors. Support structures, which is one of the obstacles that AM technology tries to overcome, also needs to be used in this technique to enable the production of some parts. Generally, the surface quality of the parts produced with this technique is low. In other words, the level of roughness is high. In order to increase the surface quality of the products, some other finishing processes like heat treatment, machining have to be applied to the parts. Industrially, only two companies use this such combination like electron beam as energy source and wire feed as feedstocks. These are Sciaky and EvoBEAM.

### 3.1.2.3. Wire and arc additive manufacturing

WAAM presents extraordinary advantages such as cost-saving, high level of deposition rate, and manufacturing ability to produce large-size pieces. Unlike the powder-bed methods, which are frequently used in beam-based methods, the feedstock is fed as a wire in WAAM. Also known as Shaped Metal Deposition (SMD) or Rapid Plasma Deposition (RPD), WAAM uses an electric arc to fuse layers. Whereas it has the capability to produce large-scale parts, it suffers from a low level of complexity. There is a broad range of metals and alloys used in WAAM. The limits of production capacity can be determined as 2500 cm<sup>3</sup> per hour in volume and 5-6 kg in weight [53]. Generally, the mechanical properties of the printed parts produce better results than other AM methods[53]. The

WAAM can utilize one of a broad group of systems such as gas metal arc welding known as MIG, gas tungsten arc welding known as TIG, or plasma arc welding (PAW). Each system has its own advantages and disadvantages. For example, The deposition rate in MIG is nearly three times higher than TIG and PAW systems. Nonetheless, it is a welding technology which is not stable because of over-high dense arc formation and spatters. As a result, TIG and PAW both are more convenient welding technologies for WAAM due to these technologies have fewer defects when compare with MIG. There are also further developed technologies that initially belong to those welding technologies. TopTIG, which is a TIG approach, uses a particular wire feeding system during production. Cold Metal Transfer (CMT) is another approach that is using a MIG system. Although it enables the production of huge parts, low resolution is a significant disadvantage compared to powder bed feeding techniques. Some researchers from Cranfield University reported that the world's biggest 3D printer can produce metal parts using WAAM technology [54]. Kuka, Fanuc, Lincoln, and Big metal additive are the companies that are generating solutions using WAAM.

### **3.1.3. Fused deposition modeling**

It is a 3D printing technique in which various structural materials such as thermoplastics, hard plastics, ceramics, or concrete are produced in layers selectively by the extrusion method. Although commercially known as Fused Deposition Modeling technology, it also has other names like Fused Layer Modeling (FLM) and Fused Filament Fabrication(FFF) [55]. The modeling of fused deposition was explored by S. Scott Crump, who the founder of Stratasys company. About ten years after this technology invented, it commercialized by his company. This technology uses a filament made of thermoplastic as the primary building material. However, metal parts are produced using a filament made by a mixture of thermoplastic materials and metal particles. Support material is also needed to fabricate the desired parts in this approach.

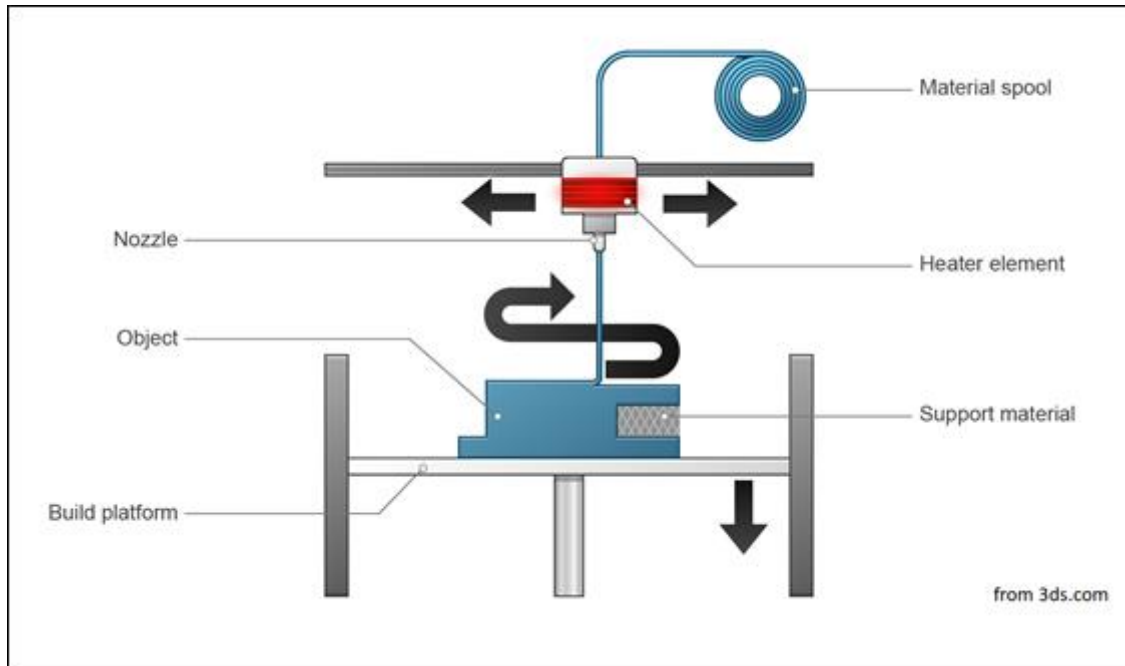


**Figure 3.7.** Schematic representation of Material Extrusion.

As shown in Figure 3.7, this filament is pushed towards the heater head. Then, the filament, which turns into a physically molten structure, flows out of the head to form the first layer. The idea of using FDM technology to print 3D metal parts offers excellent benefits. It is a significant advantage not to use expensive light sources such as electron and laser, which increase the operating costs. Another significant advantage over other direct metal production methods is that thermoplastics and metals can be used in the same structure [56]. This feature is impossible to achieve with beam-based techniques. Nonetheless, it should be expressed that it has some disadvantages too. Since this method uses an extrusion process that does not require high temperatures, it is generally limited to low temperature and low strength alloys. Moreover, the inert gas is not supplied to the place where ME happened, unlike beam-based technologies. Therefore, it is likely that the parts will undergo oxidation. One study has revealed that, although a tin bismuth (Sn60Bi40 and Bi58Sn42) alloy has been successfully produced, the parts have insufficient properties such as conductivity [56]. Nowadays, 3D technologies using extrusion in production are gathered around three different approaches. These are plungers, screw-based, and filament-based [57]. Whereas two of those approaches that are plungers and screw-based are proper to print metal parts, filament-based is not an appropriate approach because of the low mechanical properties it provides. Many studies have been carried out to produce metal parts directly with this method. As a result of these

studies, different ME approaches have emerged. The Multiphase Jet Solidification approach (MJS) presented by Greulich et al. [58]. An FDM 3000 system for electronic circuitry applications developed by Mireles et al. [56]. A screw-based approach as Composite Extrusion Modeling (CEM) is published by Lieberwirth et al. [59]. So to speak, ME technology is experiencing a period of mastery in the name of commercialization as a result of these studies. It has become prevalent not only in the industrial environment but also among people who produce hobby parts.

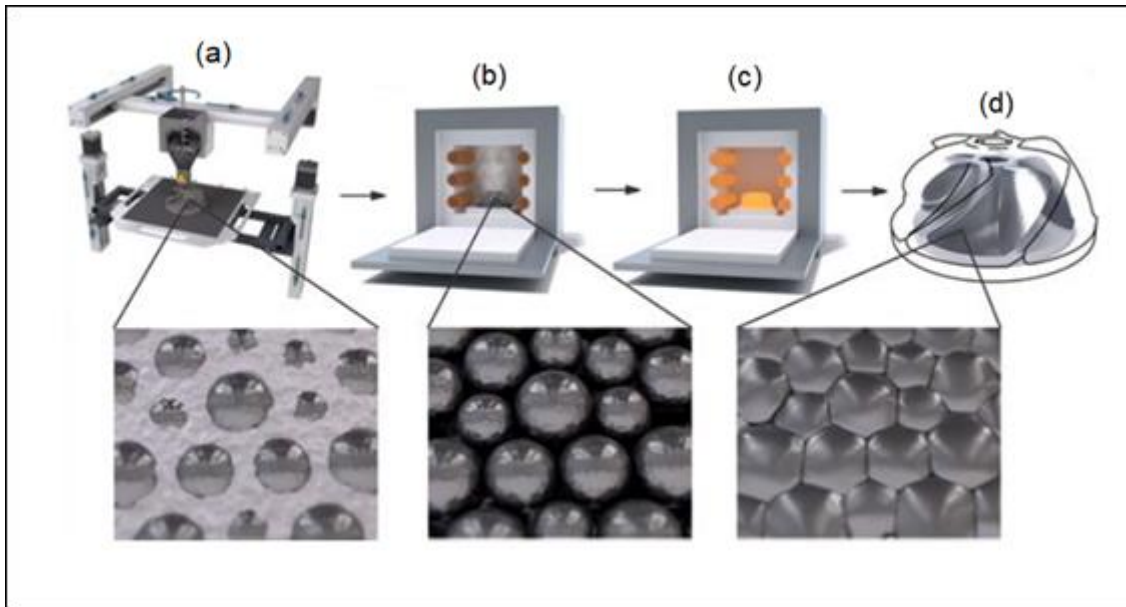


**Figure 3.8.** Depiction of Material Extrusion process: (a) printing process, (b) chemical purification process, (c) sintering process, (d) ready-to-use part [59].

Even though there are various academic researches mentioned above and company efforts like Markforged on metal parts production, there is no commercialized 3D printer that enables fabricating directly metal pieces yet [60].

### 3.1.4. Material jetting

MJ technology presents unique prototype features such as surface quality, which has almost zero roughness and high stability. Naturally, it works like a two-dimensional (2D) inkjet printer as in BJ technology. The difference is that the metal-based filament is dispensed from the nozzle to the platform as selectively. In another saying, it does not use any bed feed system. The material in liquid form solidifies under UV light, allowing the piece to be produced layer by layer. Some studies reported that the solidification might occur with one of those vitrification, crystallization, or evaporation of the binders from

the structure [44,45]. MJ is comprised of approaches like Drop on Demand (DOD), NanoParticle Jetting (NPJ), Aerosol Jet Process (AJP), and Liquid Metal Printing (LMP). Until recently, material jetting technology was used only to produce hard plastic and polymer-structured parts [63]. However, as with the material extrusion technology, stiff efforts have been carried out by companies in order to fabricate direct-metal parts. Finally, XJet presented a new technology, namely NanoParticle Jetting that can print metal parts.

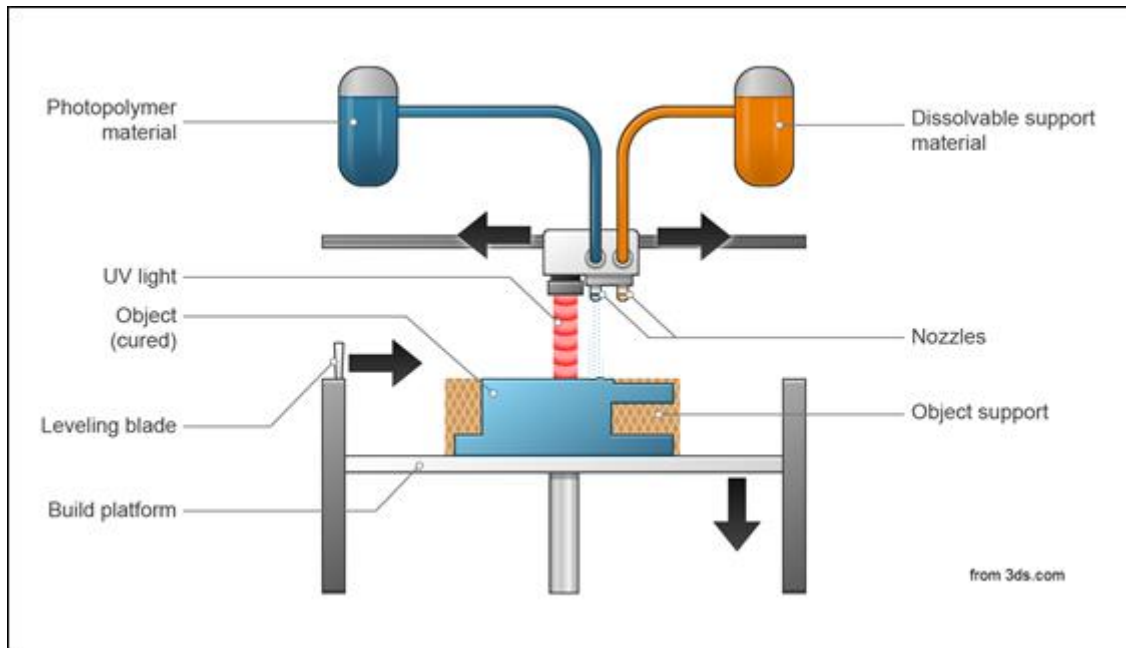


**Figure 3.9.** Schematic representation of the material jetting process.

The NPJ uses a liquid material made of metal nanoparticles. As well as metal part production, ceramic parts can be produced by NPJ. As can be seen from Figure 3.9, the support materials are essential to use in this approach. The latest studies focused more on the development of new jetting systems because of its remarkable properties, such as high surface finish. A previous study reported that the diameter of liquid droplets limited up to 2 times larger than the nozzle [64]. Later on, the development of a new system called pneumatic DOD and impact-driven ejection, made possible printing of new droplets, which have as smaller up to %60 than the nozzle [65]. Furthermore, in order to enhance the properties of liquid metal droplets, studies have been carried out on an inkjet printing system that has a pneumatic system consisting of a star-shaped nozzle [49,50]. An approach that is comprised of an electromagnetic nozzle system has been developed in order to release liquid metal droplets by Zhiwei Luo et al. [68].

### **3.1.5. Cold spray additive manufacturing**

Even though the Cold Spray Additive Manufacturing (CSAM) has been developed as a coating technology in the late 1970s, nowadays, it is a landmark technique that is using as a solid-state material deposition process [69]. During the process, super-pressurized gases such as nitrogen, helium are utilized as an impulsive impact in order to push the feedstock. Generally, the feedstocks are composed of metals or matrix-type metal composites. The powder is bombarded onto the substrate at a velocity between 300-1200 m/s to achieve the desired layer growth. For a successful deposition, the powder must exceed the critical impact velocity [70]. The powder diameter can vary between 1-50  $\mu\text{m}$  [57]. The reason behind a successful deposition process is the acceleration of the feedstock due to the pressure impact. This acceleration transforms into kinetic energy, enabling the partial metallurgical bonding required during the collision [21,22]. Raw material remains in solid form throughout the entire process. The process presents unique benefits because there are no melting and solidification processes that may cause adverse impacts such as residual stress, cracks, oxidation, hot-point errors. In CSAM, the deposition process takes place, comprised of two successive stages. First, the powder particles formed on the first layer are jetted to the surface of the substance. After the mechanical interlocking between the substance surface and the powders, the second stage starts. The second stage consists of the depositing of feedstock particles layer by layer that is a classical AM way. Generally, there is a direct proportion between the desired surface quality and the velocity of the droplets. The feedstock particle size is another critical threshold. The critical velocity threshold value that the particles must exceed depends on the material type, particle temperature, and particle size.

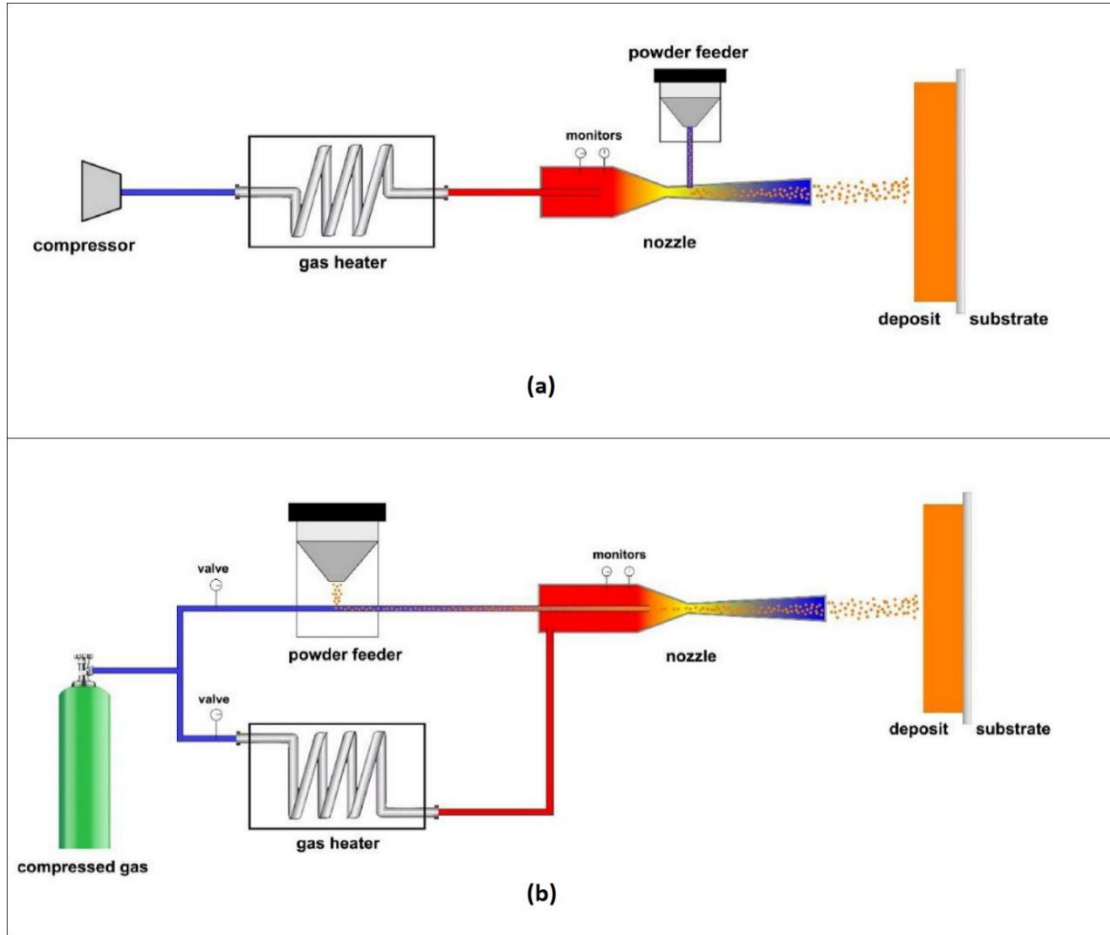


**Figure 3.10.** Schematic illustrations of cold systems: where (a) represents low, (b) represents high cold spray [73].

As can be seen from Figure 3.10, CSAM is divided into two approaches: air source is used in the low-pressure CSAM method, and the pressure is below 1 atm. In the high-pressure CSAM technique, gases such as helium, nitrogen are used and the pressure is above 1 atm. In low-pressure CSAM (a), the compressed air is heated by the heater, and it advances towards the nozzle to be sprayed. One of the most essential differences in low pressure and high-pressure CSAM systems is the location of the powder feeder. Another critical difference is that portable air compressors can easily be used in low-pressure systems instead of pressurized gas. In high-pressure CSAM (b), The pressurized-gas is released and sets off towards the powder and heater tunnels. Once the gas is heated in the heater channel, it moves towards the place where it will mix with the droplets coming from the powder channel. Powder and heated gas from channels combine in a chamber to allow a high-pressure mixture before entering the nozzle. Then the application is made.

CSAM technology, because of its benefits, has been penetrated to additive manufacturing family to fabricate metal pieces and the parts that are damaged. It can produce metal pieces faster, unlike fused-based technologies such as SLM, DMLS, or EBM. Note that, it is still a challenge to fabricate metals like copper and aluminum using beam-based technologies. Several studies have been investigated on printing applications of aluminum and copper of CSAM. A study reported that copper and its alloys were printed as 3D using pressurized-helium gas [74]. Stainless steels are high strength alloys. Because of these features, it is challenging to print in 3D. The mechanical and microstructural properties of printed 304L were investigated by Codded et al. [75]. Titanium is difficult to fabricate with CSAM because of its harmful properties such as high porosity and affinity. Wong et al. have examined particle morphology and size distribution of Ti and Ti-6Al-4V [76]. Owing to it has been newly adopted to the AM technology, there are not many commercial machine applications yet. Titomic company operates using the technology called as Titomic Kinetic Fusion in their commercial machine.

### **3.1.6. Friction-based additive manufacturing technologies**

The production of solid-state materials employing friction is a straightforward process. To understand its nature gives a chance to make the whole story up simply. In order for a material to be shaped in the desired form, two different surfaces must be subjected to strong friction or rotational motion [77]. Surface friction causes the temperature on the interfaces to increase and the material to soften. As shown in Figure 3.11 below, various Friction-Based Additive Manufacturing (FBAM) technologies have been developed come until today, such as Rotary Friction Welding (RFW), Friction Deposition (FD), Linear Friction Welding (LFW), Friction Stir Additive Manufacturing (FSAM), and Additive Friction Stir Deposition (AFSD). Under this heading, only AFSD will examine.

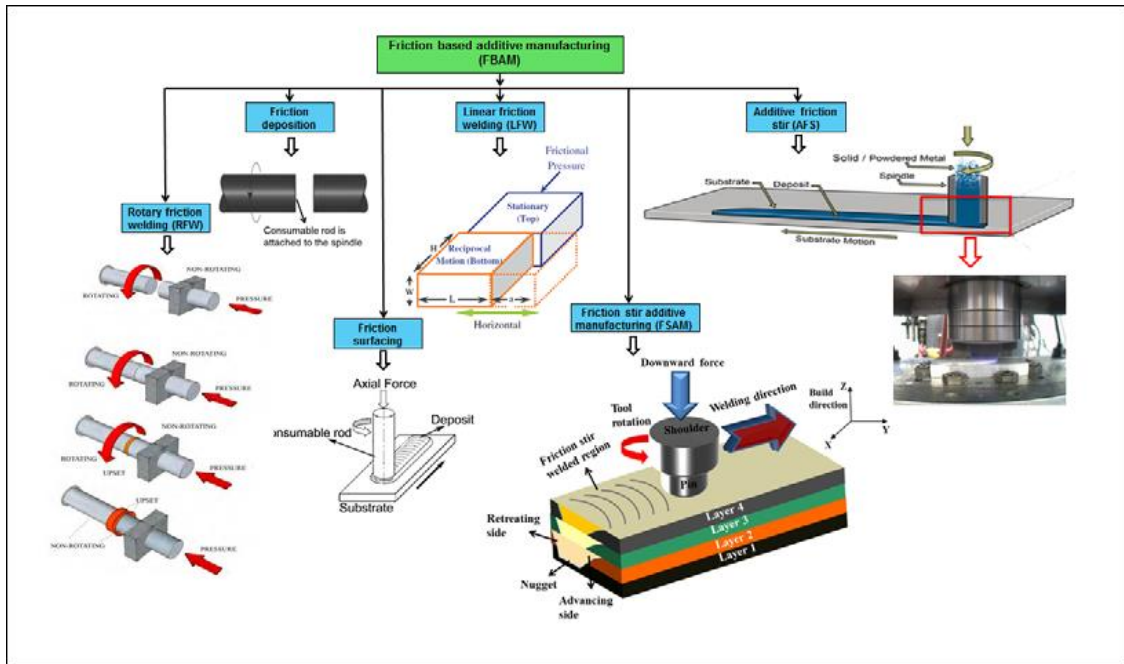


**Figure 3.11.** Categorized friction-based additive manufacturing techniques [78].

### 3.1.6.1. Additive friction stir deposition

Necessarily, the 3D printing of metals is based on powder metallurgy and welding technologies. AFSD is a solid-state deposition technique like CSAM that takes its norms from innovations of welding. It was invented by a MELD manufacturing company and utilized heat and friction to combine layers. Even if it utilizes heat source, the deposition occurs under the melting temperature. The maximum temperature that can be reached during the AFSD process varies between 60% and 90% of the melting temperature [79]. With the use of this technology results in parts that have relatively low mechanical properties, which means that heat treatment requires.

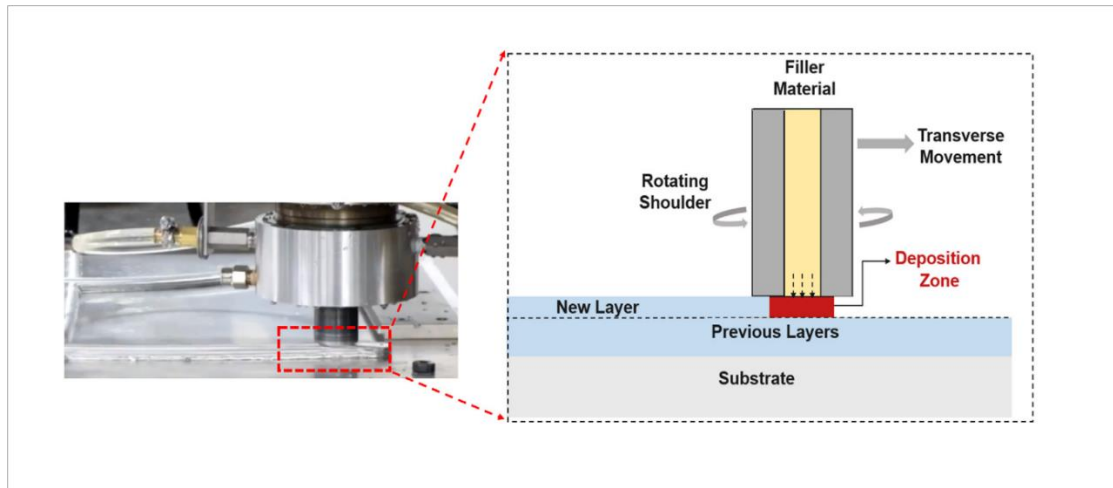


**Figure 3.12.** Schematic view of the Additive Friction Stir Deposition system [77].

As can be seen from Figure 3.12, the AFSD system utilizes a hollow cylindrical structure as a feeding channel. The building material is deposited from this channel in the form of a rod or powder [80]. The friction required by the rotational movement of the cylindrical hollow structure is obtained. The temperature needed for deposition is provided by this movement [81]. The process mainly suffers from local melting that may occur because of the over-rotation frequency. Therefore, the processing algorithm and parameters should be chosen well to prevent unwanted end-piece errors [74]. The AFSD presents some outstanding benefits, such as utilizing non-weldable alloys, which inaccessible with beam-based AM methods. In addition to various materials like Nb/Cu, Ta/Cu, significant alloys such as Al-Mo, Al-W, and Al-SiC have been successfully produced with this technology [80].

### 3.1.7. Ultrasonic additive manufacturing

Sheet lamination (SL), also known as Laminated Object Manufacturing (LOM), is an additive manufacturing technique using metallic sheets as feed material. It utilizes ultrasonic waves as an energy source for joining metal sheets cut [82]. The plastic deformation and shear that occurs between the surfaces due to these vibrational movements prevent unwanted rust-like specks of dust and oxide formation on the surfaces. Ultrasonic Additive Manufacturing (UAM) can be accepted as the only SL approach patented by D. White [83]. It works with the principle of diffusion between layers by applying mechanical pressure and ultrasonic wave to metal plates that are cut precisely. Laser application is used for fine cutting of layers. Precise cut metal layers are

added on top of each other without using any heat source, and the part is produced with the principle of layer by layer. The layers are selectively cut before mechanically bonded, and post-processing operations such as polishing are performed after fabricating done.

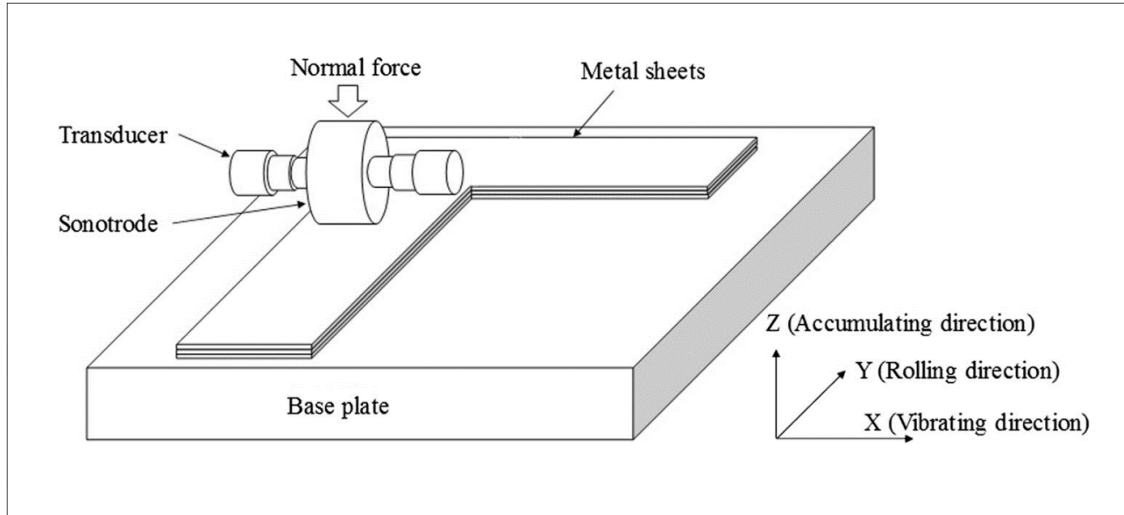


**Figure 3.13.** Schematic illustration of UAM [84].

Metals, alloys, and metal-like materials are coherent materials for production under heavy mechanical loads and ultrasonic vibrations [85]. The most common defect seen in the parts produced by the ultrasonic vibration technique is the micro gaps formed between the layers. This is because of incorrect positions in the metal stack and a high level of welding energy. Even though the materials that are using in UAM processes have superior mechanical properties such as wear-resistance and tensile strength, increased dislocations in the direction of deposition due to plastic deformation and friction causes low strength. Sridharan et al. reported that the physical properties of UAM-printed Al606 vary according to the orientation hardening inside the part [86]. The HIP is a method that can increase the mechanical properties in the places where orientation hardening occurs [68,69]. Utilizing the high level of energy shows that the elastic properties are increased in the structure [89]. Even if utilizing a high level of energy such as 9kW rather than 1.5kW to achieve a part that has excellent mechanical properties, a study reported that the part still suffers from the orientation hardening occurred in structure [86]. UAM can produce carbon fibers, polymer-coated optical fibers, metal-coated optical fibers, or NiTi-shaped alloy fibers by embedding them between layers of aluminum. Novel research has been reported that a metal-reinforced composite and ultrasonic AM come together in order to fabricate an over-functional structure to use in the aerospace field [90].

### 3.1.8. Direct ink writing

Direct Ink Writing (DIW) is a deposition technology with the ability to produce micro-sized parts along with a comprehensive material infrastructure. Although there has been a variety of researches on it [91], further studies about metal production are belongs to Lewis et al. [92]. It is an extrusion-based AM technology, and a nano-scale nozzle jets the feedstocks in liquid form. A schematic image is given in Figure 3.14.

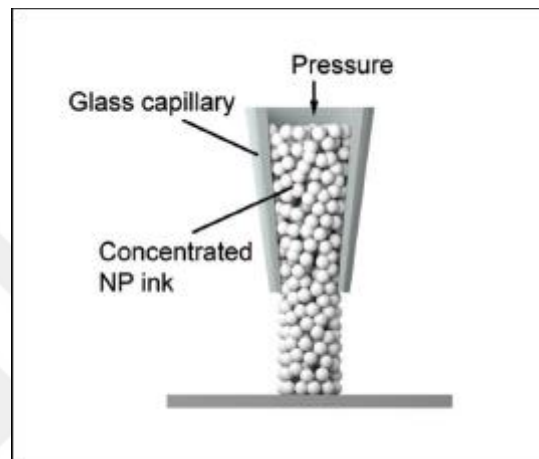


**Figure 3.14.** An Illustration of Direct Ink Writing (DIW) [93].

The viscoelasticity of the ink that is employing during production must be set up studiously in advance to obtain defect-free parts. Many sub-techniques have emerged as a result of progress in technology; 3D Printing (3DP) [94], Direct Ink-Jet Printing (DIJP) [95], Hot-Melt Printing (HMP) [96], robocasting [14], Fused Deposition (FD) [97], and Micro Pen Writing (MPW) [98].

### 3.1.9. Electrochemical additive manufacturing process

Electrochemical fabrication (EFAB) and FluidFM 3DP, as illustrated in Figure 3.18, are electrochemical-based additive manufacturing methods employing electrochemical deposition and subtractive planarization until the final part is obtained [15,19]. EFAB is a process comprising three steps for each layer; first, the process starts with the electroplating of support structure towards the surface of the substrate (will be removed from the structure later). Then, it continues with electroplating of the primary build material onto the sacrificial support structure. Last, it ends with planarization. This process continues until the whole piece is obtained. It was commercialized by

Microfabrica, located in the USA [99].

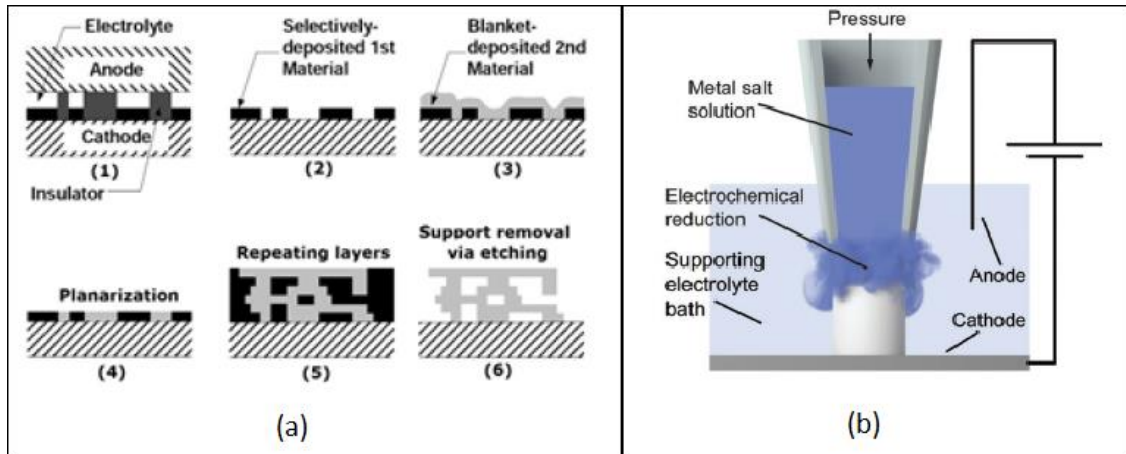


**Figure 3.15.** Schematic depiction of (a) [57] EBAM and (b) [93] FluidFM 3DP.

FluidFM 3DP is another electrochemical-based method carried out with metal ions that are selectively jetted by a micro nozzle immersed in an electrolyte solution. It is a newly-developed technique by the research team of Cytosurge AG company [100].

### 3.1.10. Laser-assisted electrophoretic deposition

Laser-Assisted Electrophoretic Deposition (LAED) is a technique using electrophoresis based on the principle that the charged particles are directed/moved by an electrical force in a liquid colloidal solution. An explanatory study consisting of two primary methods to deposit metal nanoparticles selectively was demonstrated by Iwata et al. [101]. In the first approach, whereas a glass-like capillary is utilized to deposition of metallic nanoparticles, in the second, laser trapping using. LAED is mostly focused on produce microdevices that are using in electronic and medical industries. Many studies are available on this manufacturing method [6–9].

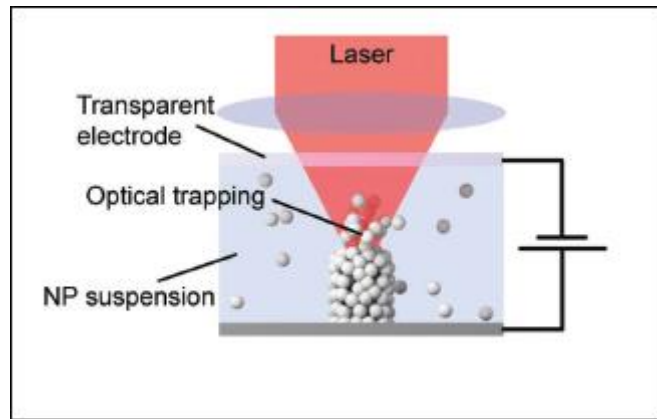


**Figure 3.16.** Schematic representation of Laser-assisted electrophoretic deposition [93].

### 3.1.11. Laser-induced forward transfer

Laser-Induced Forward Transfer (LIFT) was initially developed for producing patterning-like metal structures in two-dimensional [106]. However, as it has the potential to produce 3D metal parts, some studies have been made on its development in this direction [11–13]. As it is illustrated in Figure 3.17, a laser beam that is sent towards a glass-like structure (transporter) is absorbed by way of a thin layer (victim) covered with metal. Once the laser beams are sent by the head selectively, on the regions where beams reached, local melting, which is a metallurgical process, takes place [110]. The pressure that occurs between the glass structure and the thin metal film causes metal droplets to deposit towards the substrate surface located below and then solidification. The rate of accumulation and solidification directly affects the microstructure.

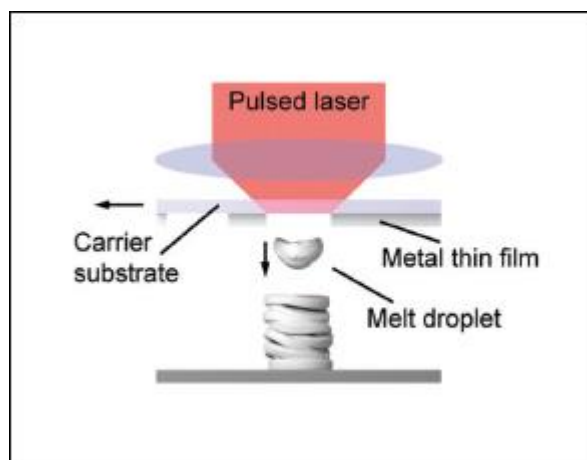


**Figure 3.17.** Depiction of Laser-induced forward transfer [93].

### 3.1.12. Focused electron beam induced deposition

Focused Electron Beam Induced Deposition (FEBID) is a technique that is using electron beams for the deposition of metals. The process starts as a result of a collision of an electron beam and adsorbed forerunner molecules. Then, the molecules are separated onto metallic and organic particles by interactions such. The deposition process is carried out with these metal particles that can not resist gravity. Particles that counteract gravity, in other words, volatile, are adsorbed again. It is possible to deposit in a larger area with enlarging the laser focus. FEBID presents a low-speed metal deposition rate but prevents defects and pollution produced by electron beams [93].

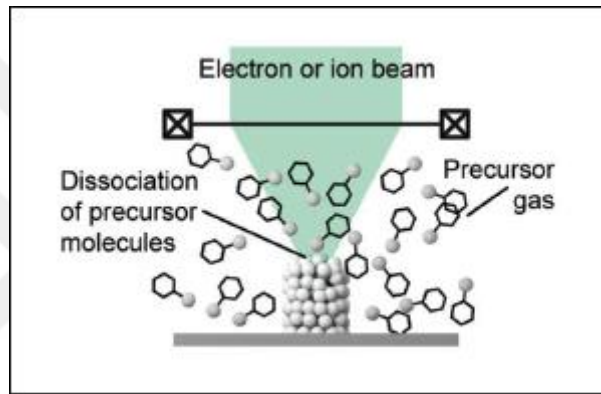


**Figure 3.18.** Schematic view of Focused Electron Beam Induced Deposition (FEBID) [93].

### 3.2. Relationship Between the Energy Source and Feedstock

During the production of metal parts through AM technologies, some chemical reactions occur because of metal's nature. This is a process consisting of known metallurgical events that occur not only in high-tech applications of metals such as AM but also in conventional low-tech applications like SC. For example, oxidation that takes place due to the oxygen affination causes the onset of corrosion on the surface regions of metals. This reaction is independent of the corrosion rate but has an undesirable result, such as rusting. Another example, defects in the microstructure due to nonequilibrium solidification reduce the strength of the part and offer an undesirable mechanical feature. In most cases, oxygen, hydrogen, nitrogen, and moisture can be seen as the enemy of metals because of their negative impacts on the final structure. Continuously delivering inert gas to the environment or providing a vacuum ambiance where fabrication of metals

takes place, reduces the likelihood of a possible reaction. These chemical reactions vary from metal to metal, and the technique to be chosen for a successful production process is as important as the metal or alloy to be chosen.

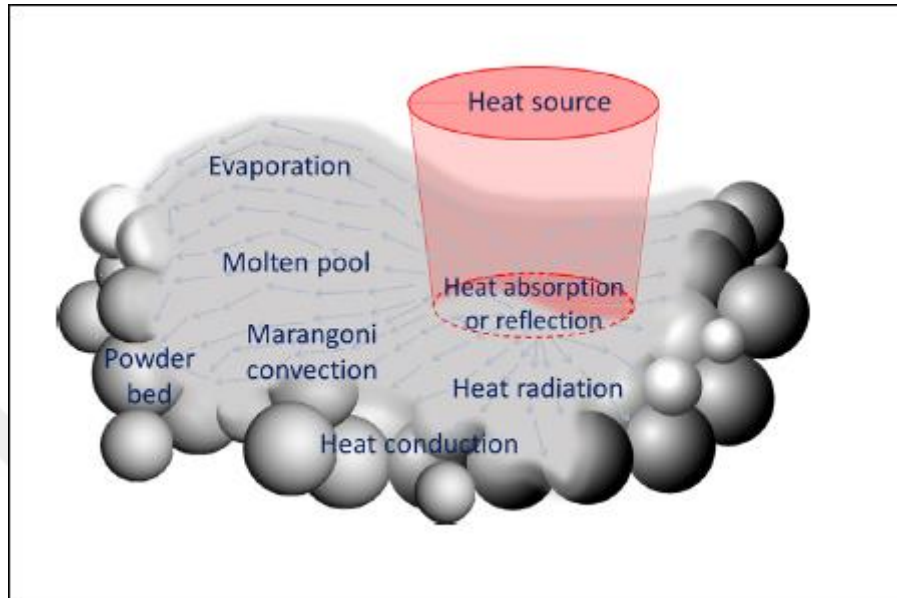


**Figure 3.19.** The illustration of metallurgical reactions that occur when the heat source and the feeding material meet [46].

The applied heat source reacts differently according to the feeding systems in AM. In other words, a laser energy source does not interact in the same way as a metal structure material used in a powder feed, powder bed, or wire feed systems. AM technology with a powder bed system, possible metallurgical events that may arise when encountering an energy source is given by Figure 3.19. The approach of additive manufacturing means that producing takes place as layer by layer. It is not only quite significant to understand the interactions between metals and energy sources, but also the relationship among layers.

## **4. THE STATE OF ART - BINDER JETTING TECHNOLOGY FOR CASTING APPLICATIONS**

### **4.1. Binder Jetting Technology**

Binder Jetting (BJ), also known initially as Three-Dimensional Printing (3DP) technology, is one of the powder bed based AM approaches utilizing liquid adhesive called binder to providing the bonding to each other of powder layers. It was developed and patented by Emanuel M. Sachs et al. at Massachusetts Institute of Technology, the USA in the late 1980s [111]. BJ has an outstanding capability to fabricate parts using a broad array of materials, such as metals [112], ceramics [113], polymers [114], foundry sand [115], shape-memory alloys [116], composites, and drugs [117]. It is based on a powder bed system in which the production cycle comprises several steps, including printing, curing, powder removal, sintering, and finishing. Before the printing process starts, some pre-arrangement is performed to check if there is a mechanical problem that could affect it. Then, with a roller-like structure, the powder that will form the first layer is brought into the building chamber. The process continues with the selectively dispensed of liquid binder droplets to the regions that are predetermined based on the sliced-data. After the liquid binder is released, a new powder layer is spread over onto the previous one. Thus, two layers are connected. The printing process ends by converting the digital data of the part on the machine interface into a physical object. Often, the printed part is called a green body.

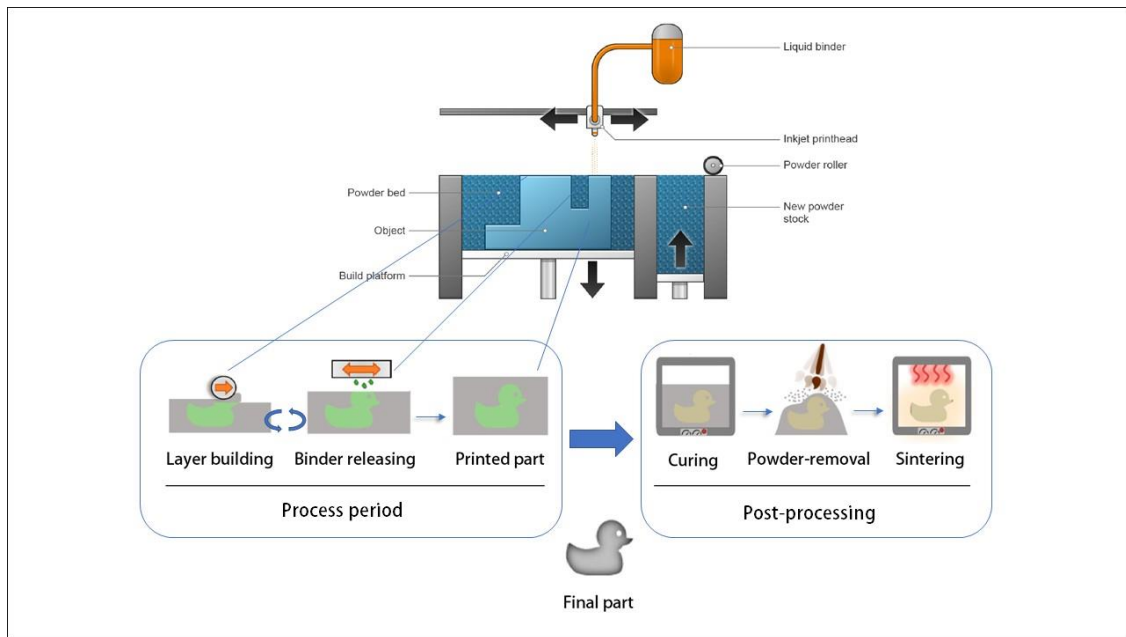


**Figure 4.1.** An illustration of a typical BJ machine and production cycle [8,9].

The green body does not have the desired mechanical properties compared to other powder bed methods such as SLM or EBM. As shown in Figure 4.1, a series of operations called post-processing is essential to enhance mechanical properties following production. The green body is sintered in a heating furnace to carry out the atomic diffusion between powders. During the sintering process, the binders are evaporated by the impact of temperature and leave some gaps behind them, which is in an undesired way. Although sintering enhancing the density of the part to a certain extent, the printed part still suffers from loosely packed powders. In order to achieve the intended densification in the green part, some other approaches could be applied, such as Hot Isostatic Pressing (HIP) or infiltration.

As previously mentioned, a broad range of metallic materials such as stainless steel, biodegradable alloys, titanium, superalloys, magnetic materials, WC-CO tool steels, copper has been expertly printed by BJ, still being challenging for other AM technologies. For example, the production of copper is proper to be produced with BJ rather than other PBF approaches, as there is no melting pool, because of its high level of thermal conductivity and reflectivity [9–11]. Since there is no need to use support structure and a high energy source during printing, BJ presents unique fabrication features such as low residual stresses and shrinkage. The underlying reason for this is because the loose powder acts like a support structure.

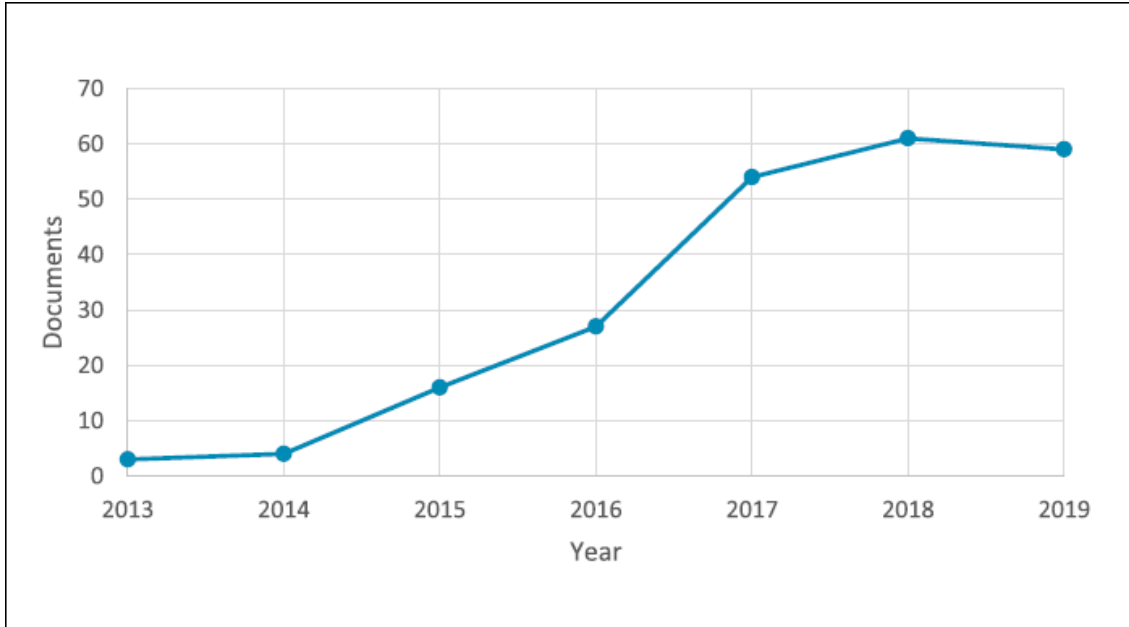


**Figure 4.2.** The number of publication released by Scopus about BJ in the years between 2013 and 2019 [22].

Due to the outstanding features offered by BJ, it attracted the attention of researchers and commercial companies, and as a result, there was a noticeable increase in the number of publications, as stated in Figure 4.2. According to a published reported by Fahimeh et al., four significant issues have a direct impact on BJ printed parts [5]. These are briefly, level of detail in part, features of employing binder and feedstock, properties of the machine utilized, and process parameters. On the other hand, it is crucial to note that some binders utilized show toxic properties, which could be damaged people [121].

BJ, which indirectly allows the production of parts, is faster and cheaper than direct metal production techniques such as SLM and EBM. With the use of BJ technology, highly-demands structures could be produced, such as lightweight-high compatible parts or manufacturing end-use parts unreachable with conventional methods. An example, While the cost of the piece produced with the conventional method, is \$ 400-500 and wear out in 200-300 hours, the cost of the piece produced with the ExOne BJ is \$ 75-150, and no measurable wear has been observed in more than 600 hours. However, it has been using by manufacturers to produce core and molds for conventional sand casting for a long time. As listed in Table 4.1, many successful commercial 3DP companies have focused on direct metal production with BJ.

**Table 4.1.** Available commercial 3D machine manufacturers are utilizing BJ.

---

Commercial 3D Machine Manufacturers

---

Companies	Products	Technology (BJ)	Print Resolution (dpi) or Thickness of layer (mm)	Built Volume (XYZ,mm)
Voxeljet	VX200, VX200 HSS, VX500, VX1000, VX1000 HSS, VX2000, VX4000*	BJ	up to 300 dpi	4000 x 2000 x 1000
ExOne	S-Max Pro*, S-Print, S-Max, Innovent+, X1 25Pro, M-Flex, X1 160PRO	BJ	0.26-0.38 mm	1800 x 1000 x 700
Hp	Jet Fusion 5200 Series*, Jet Fusion 4200, Jet Fusion 500/300 Series, Metal Jet	BJ	0.08 mm - 1200 dpi	380 x 284 x 380
Desktop Metal	Studio System, Shop System, Production System*	BJ	1200 dpi	490 x 380 x 260
3D SYSTEMS	Projet CJP 880Pro*, Projet CJP 660Pro, Projet CJP 460Plus, Projet CJP 360, Projet CJP 260Plus	BJ	0.1 mm - up to 600 dpi	508 x 381 x 229
ComeTrue	T10, M10*	BJ	0.04 mm - 1200 x 556 dpi	200 x 160 x 150
XYZ PRINTING	PartPro350 Xbc	BJ	0.1 mm	222 x 350 x 200
CONCR3DE	HIPPO 3DPRINTER*, ARMADILLO WHITE, ARMADILLO BLACK	BJ	400 dpi	650 x 1400 x 800

---

## 4.2. The State of Art: Binder Jetting for Casting Applications

With the utilization of BJ can produce parts in two ways. First, a part can obtain with the approach of direct metal production as it is performing in SLM, EBM, or DMLS. The difference between them is the energy source that is used during fabrication. Second, mold can be printed by a 3D machine then gravity casting is performed into the produced mold.

Under this section, a comprehensive literature review and current state of the art of BJ presented about the place of BJ in casting applications. This literature review has been carried out based on the data taken from ScienceDirect, Google Scholar, and Springer databases.

In this publication, the authors have been mainly researched the future of the 3D printed sand molds and its place within the heavy sectors. Also, It has been stated that the development of this technology will substitute the old sand mold producing techniques. The benefits of direct metal 3d printing and its importance for the investment casters, the properties such as adoption incentives, adoption barriers, trends of the 3D printed metal parts, and wax/plastic pattern production through sand casting have been examined and discussed by Robert C. Voigt et al. They have been declared that the problems of 3D printed parts such as cost, final quality, and the complex net-shape still unresolved [3].

The authors have aimed to obtain data such as temperature, pressure, moisture, evaporation, the motion of the molds and internal cores, and the magnetic field during casting by inserting thermocouples sensors on different points of the mold they produce employing BJ technology. In this study, where the Internet of Things strategy is applied, eight different types of thermocouples were used. All data were taken with the use of wireless and wired technology from thermocouples. The simulation and interpretation of the data were carried out with MAGMASOFT software. The 3D Printer used for sand mold production was S MAX, which is an ExOne product. After the aluminum casting took place, it was stated that data flow from the sensors continued for approximately two minutes. With AM technology, from thermocouples placed in designated locations after the part has been produced, the data obtained have been shown to support the pre-casting simulations. As a result, the authors conducted a study demonstrating the integration of electronic sensors and additive manufacturing technology with casting [122].

The properties of the 3D printed molds, such as gas permeability, strength, heat absorption characteristics, and its importance and connections for the industry has been prepared as a review study comprised of under three main titles by authors. These; 1- mold properties and their effect on the cast metal, 2-design capability and accuracy, and 3-material systems and the issues in the 3D printing technology. First, In the mold properties and their effects on the cast metal section, it has been reported by authors that there are many types of sand, binder, and activator. It is mentioned that organic binders can produce toxic gases during casting. Also, furan, which is a binder, poses a health risk such as carcinogens. It has also been stated that the properties of sand molds are affected by characteristics of the sand, concentration and the type of binder and activator, printing speed (powder recoating speed), job-box coordinate, and build orientation of the printed pieces. Decreasing of layer thickness and increasing the binder saturation improves tensile strength but reduces the surface quality. This research has also been focused on the effect of curing time and temperature on mechanical properties such as permeability and strength of the sand molds. They have been researched that the variables such as curing and temperature effect on compressive strength and permeability of the printed molds. The temperature range was 150 c to 250, and the curing time was between 4-8 h. It is found that permeability was increased due to the volatility of the components. The authors have been stated that apart from the properties of the mold, it is also essential to study the effects of the mold on the produced castings. In the design capability and accuracy section, the 3D Printer chose by the authors was Voxeljet VX200. They have been focused on researching these topics, splitting the mold for quick assembly, incorporating positioning pads, mold cast dependence on the part volume, and drilling vents to help with the release of gases. In order to get more compared results, they have chosen the ExOne machine, which is using furan as a binder. The Voxaljet VX200 is using binder called as Spectrum 510. They observed better permeability and mechanical properties from the specimens produced by the ExOne 3D Printer. In the last part, the authors mainly criticized the cost of feedstocks [15].

The authors have been investigated the printing of a sand mold employing an inorganic binder that is unusual and the relation of quality-relevant process parameters. In the production where typical quartz sand is chosen as feedstock, in organic and inorganic mold production, resin or curing and dry sodium silicate with water were used as binders,

respectively. The VX-500 from Voxeljet used as a 3D printer. The process parameters of testing of molding sand and binder properties were performed according to standardization that belongs to The Association of German Engineers database, specifically VDI-Richtlinie 3404 and VDG-Merkblatt P38, P72. The results were criticized according to the thermal process analysis and quality features. It is found that fluid migration within the box has a significant influence on final part strength. The increase in fluid migration increases in strength in the structure [123].

This study focused on producing a 3D printed mold with BJ that has been aimed to use in the casting of metal joints in architecture. The authors stated that the metal joints have a significant impact on space frame constructions, such as the design of the joint regions and the strength of the joints. A couple of systems were realized by MAS Postgraduate students to examine the method's limits. To achieve desired goals such as ease of assembly and disassembly, lightweight structure, compatible design for casting, and less post-processing, four joint systems were investigated, then casting performed into the 3D printed sand molds. In this study, where the parametric mold design approach is used, instead of designing a separate gating system for all parts, a central gating system, an innovative approach, has been designed. The results showed that joints could be used in architectural applications because of its fair enough mechanical properties. It is also reported that the process still suffers from over-post processing efforts [124].

The article presents a comprehensive review of existing 3D mold fabrication techniques and a new approach based on line forming. The authors have aimed to increase the production speed with this newly developed technique. According to the literature, there are three different 3D sand mold manufacturing approaches; SLS, BJ, and Patternless Casting Manufacturing (PCM). It has been claiming because these techniques have a scanning mode based on point-line-area-layer-solid instead of line-area-layer-solid possesses a relatively low build speed. As opposed to those techniques, the results state that technology employing line forming approach found to be faster because of its technology. It is also mentioned that line forming technology is more compatible where large-scale mold production needed [125].

In this article, the authors compared the conventional sand mold production approach with 3D sand mold production in terms of weight savings, surface quality, design

freedom, and coating. For the conventional method, the no-bake sand casting approach was used. The grain size of the sand used in the conventional method was chosen between 200-220  $\mu\text{m}$ . Sulfonic acid was used as the catalyst and furan as the binder. In the 3D method, Furan Direct Binding (FDB), a Voxeljet production, was used as a binder. The 3D Printer used is VX 500, which is also a Voxeljet product. The results revealed that the molds produced by conventional methods on the waste of sands, designability, and coatability showed lower performance. It is also stated that the molds produced in 3D show high mechanical properties due to the physical combination of the powders that occur during production [13].

The authors aimed to manufacture Ceramic-Reinforced Metal-Matrix-Composite then investigate the mechanical properties. Basically, the production cycle followed these steps; selection and preparation of the main components of the reinforced ceramic structure, the printing of ceramic parts that will use as reinforcement, the preparing of the sand mold with conventional methods, inserting the reinforcement structures into the mold, casting performing with selected alloy, cleaning, and post-processing, performing mechanical tests. Rather than employing a single component such as alumina to produce ceramic-based reinforcement structure, cordierite ( $2\text{MgO} \cdot 2\text{Al}_2\text{O}_3 \cdot 5\text{SiO}_2$ ) that is composed of silica ( $\text{SiO}_2$ ), magnesia ( $\text{MgO}$ ), and alumina ( $\text{Al}_2\text{O}_3$ ) composition with better thermal shock resistance was used. The reinforcement structure (RS) was designed as a cellular repeating octet truss pattern. The reinforcement structures were printed by R2, an ExOne product utilizing a glycol-based binder, then sintering in an electrical furnace. X-ray diffraction (XRD) and Optical Microscopy (OM) tests performed to obtain properties of sintered ceramic RS. Zamak-3 ( $\text{Zn-4Al-0.4Mg}$ ) is one of the Zinc alloys selected to perform casting into the conventionally prepared mold. The reason behind this selection is its outstanding fluidity property. The printed RS parts were placed in the middle of the sand mold, then casting of Zamak-3 performed. Because of the high fluidity property of Zamak-3 alloy, high infiltration was observed into the cellular structured RS. Three-point bend tests were performed by employing an Instron 5984 one by one on each structure of Cordierite (RS), Zinc (Zamak-3), and metal-matrix composite. The results showed that the mechanical properties of the composite metal matrix structure have revealed in lower contrary to expectations. Besides, the mechanical test results of the RS were lower than the data obtained from the literature. In general, the mechanical

properties and strength of both the ceramic reinforcement structure and the ceramic reinforced metal matrix composite structure were obtained lower than expected. It has thought that the mixture of raw materials that are magnesia, alumina, and silica to print ceramic reinforcement was not balanced and homogeneous. Besides, the sintering process caused high porosity in structure resulted in low mechanical properties [126].

The authors have carried out a series of studies on whether conventional cast sand, which does not have a specific standard, can be used in a 3D printer. It is mentioned that the operation costs of old metal production techniques and how it is hard to replace AM technology with old production techniques. M-Flex Sand Printer, which is an ExOne product, was chosen in order to produce parts. For printing, 3,5 kg of sand was used. P-toluene sulphonic acid was used as an activator; it enables a mixture of quartz sand. Binder was furfuryl alcohol. It is reported that during the creation of parts, a chemical reaction between activator and binder took place. In order to avoid this reaction, a temperature test was performed by authors during 12h at 80 C<sup>0</sup> in a large oven. Four different types of sands were used for the fabrication of the 3D printed sand molds. They used a formula to determine the optimum number of samples.  $X=2^n$  where x is the number of samples, and where n is the number of variables. Those four variables are sands, which means that x=16. So, they were assumed that 16-1=15 samples that can be generated. They have been tried to identify the optimum binder saturation level to avoid brittle or stiff mold structure. The results showed that conventional foundry sand could be used within a 3D printer. However, it still has some constraints such as flowability because of the binder saturation level and employed chemical reaction between activator and binder to cause unwanted polymeric inclusions [2].

A comparison was investigated by authors between two molds in terms of fabrication time, solidification rate, dimensional deviation, surface finish, surface porosity, and defects. The sand molds were produced by BJ and conventionally, respectively. A commercial aluminum alloy (Al-9Si3Cu3ZnFe) was selected to perform casting for both. Any Casting software simulated the simulation of casting and design accuracy. The patterns of conventionally prepared sand mold were printed by the FDM Technique. Those patterns were printed, taking into account the whole gating system components. The sand used in conventional mold making was petrobond commercial silica sand (quartz) mixed with pale oil paraffin. After produced positive, conventional sand mold

preparation steps were followed in order to perform casting. The second sand mold was obtained by employing ProJet CJP 660Pro that has BJ technology. VisiJet PXL (hemihydrate calcium sulfate) and PXL (2-pyrrolidone) were used as feedstock and binder, respectively. The mold wall thickness was set to 10 mm to withstand the initial effect of molten aluminum. A K-type thermocouple has inserted into the mold in order to measure the solidification rate. The results revealed that lower heat dissipation was observed in the casting of the sand mold. This is because the wall thickness in the sand mold is higher than the mold produced by BJ. Dimensional defects were measured by a Breuckmann Smart SCAN3D-HE that is a light scanner. The dimensional analysis reports proved that the BJ produced sand molds have the ability to produce more accurate parts. Mitutoyo SurfTest SJ-500 profilometer was employed to measure surface roughness. It turned out to have acceptable surface roughness in molds produced in two ways. However, the conventionally casted part shows a better surface quality. It is stated that he is due to a feature offered by FDM produced patterns. When the produced parts are evaluated in terms of surface porosity, it was revealed that the surface porosity of the part poured in 3D was higher than conventional sand casting. The reason for this is that the gas permeability of the sand produced in 3D is lower than that of quartz sand, or it is caused by the gases formed during production. As a result of those comparisons, it has been observed that 3D and traditionally produced parts have similar properties [127].

In this study, a novel approach employing BJ technology has been presented by authors. This novel approach promises that producing a multi-material mold utilizing some powders such as silica, aluminum, alumina, and steel. Generally, this study questioning the relationship between hot spot problem and design freedom, announced that authors developed a new BJ 3D printer using an inorganic binder. Basically, this study follows the production cycle; Materials with different thermal properties are selected (in powder forms such as silica, aluminum, alumina, and steel), the nozzle selectively jets the desired powder to the desired regions during production (e.g., commonly, every 3D Printer uses just one powder as feedstock during fabrication, in this consideration, the newly developed 3D Printer used four different types of materials in powder form as mentioned above), this process is continued layer by layer until the desired part is produced (typical process cycle in every 3D printing approach). In the developed 3D Printer, there are some unusual properties such as 6-axis robotic arm equipped with many HP C6602 nozzles. It

is basically a redesigned version of Stäubli TX2 90 robotic arm. Some numerical simulations and iterations have been performed to prove whether the machine can spray materials at the right time to the desired regions. The results showed that it has. The arm composed of the binder jetting tool, a doctor blade and the sand hopper can print parts up to 96 resolution as dpi. Another critical innovation presented in this study is the use of sodium silicate, which is an inorganic binder rather than organic binders such as furan. Linseis THB 100 machine that is employing the principle of a self-heated wire was used in order to measure thermal conductivity activities. The results showed that the alumina powder is not a proper powder in 3D applications because of its volatile property. It is also mentioned that the aluminum powder did not show excellent performance as a conductor in the sprue base of the gating system as rather than expected. The authors mentioned that this is because of the used binder or process. As a result, it could be mentioned that by reviewing and analyzing the thermal conductivity results, the multiple 3D printing technology can reduce hot spots defects by controlling and changing the thermal conductivity [128].

The mechanical properties of BJ-3D printed sand molds have been investigated by Jinwoo Lee et al. In this study, the authors aimed to produce a sand-polymer composite mold with a lightweight structure whereas reducing the production time and waste of feedstock. In this experiment, a VoxelJet VSX1000 used as a 3D printer. 3-matic was used as a topology optimization software. The authors also followed the instructions of Korean standards as well as the American Foundry Society. The results showed that there are two significant interrelated factors needed to take into account during the design process of ceramic-based composites; strength and powder-removal. It is mentioned that an increase in the dimension of inner holes to make ease of powder-removal has revealed lower strength in the structure [129].

In this article, the authors have been researched conventional principles of casting hydrodynamics and are advanced by validated novel numerical models for novel sprue designs to improve melt flow control. In other words, numerical models for two complex sprue profiles, which called Parabolic Sprue Casting and Conic-Helix Sprue Casting, are designed and have been established their effects on casting performance. In order to obtain the results of the overall casting defects, presence of globular oxide inclusions, flexural strength, which can be formed during or after casting process, they used these

techniques; SEM, EDS, Computed Tomography Scans, Three-Point Flexural Testing, Computational Flow Simulation. The material to be used in casting was chosen as 17-4 stainless steel, which is a martensitic structure contain 3wt% Cu. They also performed with grey cast iron and aluminum alloy. According to the literature, interfacial fluid modeling by tracking free surfaces can be employed using Eulerian techniques through marker method and Volume of fluid VOF methods, or by using Lagrangian methods such as smoothed particle hydrodynamics. As a result, it is stated that there is a maximum sprue length to control turbulence. If this limit is over, it is not possible to control turbulence during casting. Reducing melt flow turbulence resulted in reducing mold wall erosion in Conical-Helix Sprue design. Both optimized Parabolic and Conical-Helix designs reduce surface turbulence below critical velocity that is 0.5 m/s. According to the CT scan results, casting defect volume can be reduced by 99.5% using Conical-Helix Sprue design [130].

### **4.3. The Purpose of the Thesis**

According to the literature, the current state of the art of BJ technology for casting applications was generally focused on the casting capabilities of BJ-manufactured molds and its properties such as gas permeability, strength, heat absorption capacity, binder evaporation, and moisture. However, the common design approach in the casted parts, in general, has caused a lack of information on the casting of complex-shaped parts. Besides, only a few studies are available on innovative sprue-gating systems that could be used in casting applications in addition to a lack of information about the production of complex-shaped parts. Ordinary sprue-gating system and part design studies in the literature have also led to a lack of knowledge about the relationship between design complexity and powder-removal capability. There is directly no study on this relationship in the literature.

In this master's thesis, we conducted a study on the ability to produce complex shaped parts missing in the literature by making casting through molds produced with BJ. We tried to reveal the design complexity and limits through the lattice structures that have not been previously studied on casting applications in the literature.

In order to achieve that goal, we designed eight lattice structures. Three critical parameters took into account while the lattice structures were generating. Three different gating systems were designed to perform a successful casting. In casting applications, we

used a popular aluminum alloy, which has an essential place in the industry.

Briefly, with this preliminary research we have carried out, we have brought the design freedom that was theoretically said to the field. In the future, we hope that there will be light on the works based on the production of complex parts.



## 5. EXPERIMENTAL PROCEDURES

The thesis study consists of four main titles, as illustrated in Figure 5.1. The study started with the design procedure of the components and gating systems. Then the pieces designed with the Solidworks were assembled. By transferring the digitally designed works to the physical environment, the last operations to be done before the temperature test were carried out, such as powder-removal. After heat treatment, molds were prepared for aluminum casting. Afterward, the results obtained by breaking the casted molds were evaluated.

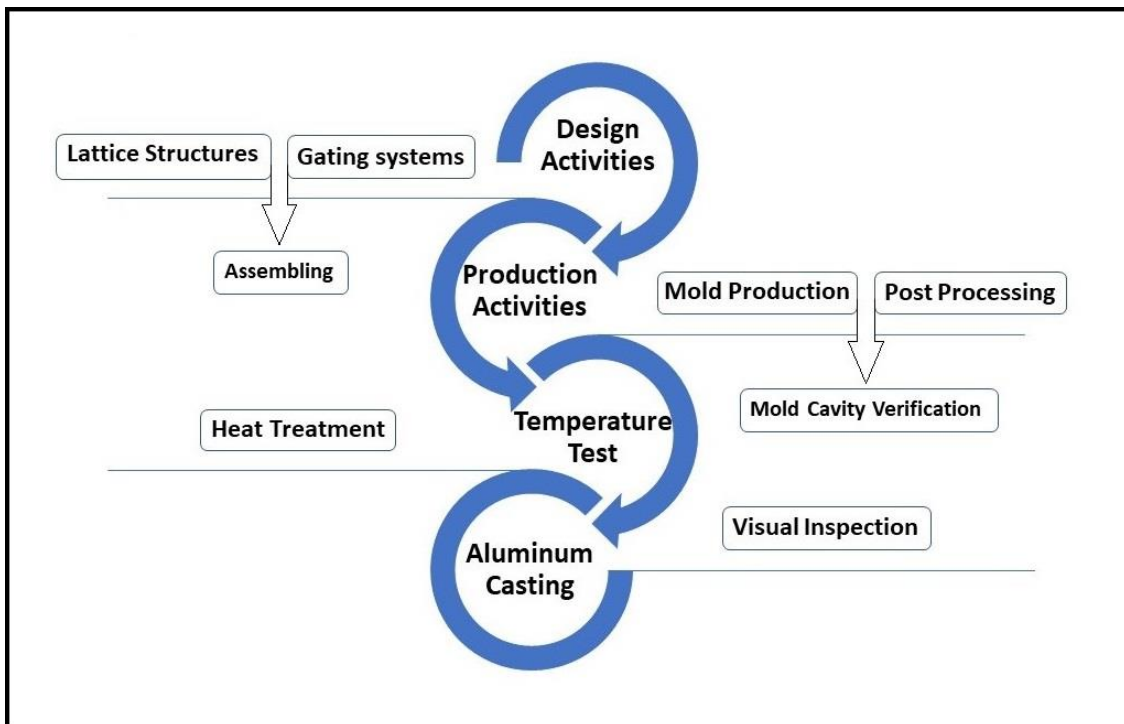


**Figure 5.1.** Schematic representation of the experimental cycle.

### 5.1. Design Activities

In this study, Solidworks version 2018 employed to design the unit cell structure and its mold sequentially before transformed the file format from 'SLDPRT' to 'STL'. 3DPrint and 3DSprint programs provided by the Manufacturer were utilized for the managing of printing details.

#### 5.1.1. Design of the lattice structures

It can be said that Lattice structures are formed by a combination of a specific material and space, which can be divided into two classifications; a)stochastic (foam) structures,

b) periodic structures [131]. If there is no layout among layers of the structure as generated, then it has a stochastic structure [132]. Basically, the design is inherent in periodic structures. Eight lattice structures were generated to measure the possible limit constraints of the part that has a periodic structure. Whereas the lattice structures were designing, three different parameters took into account as thickness ( $d_e$ ), the number of lines ( $n_r$ ), and void thickness ( $d_d$ ), where can be seen in Figure 5.2.

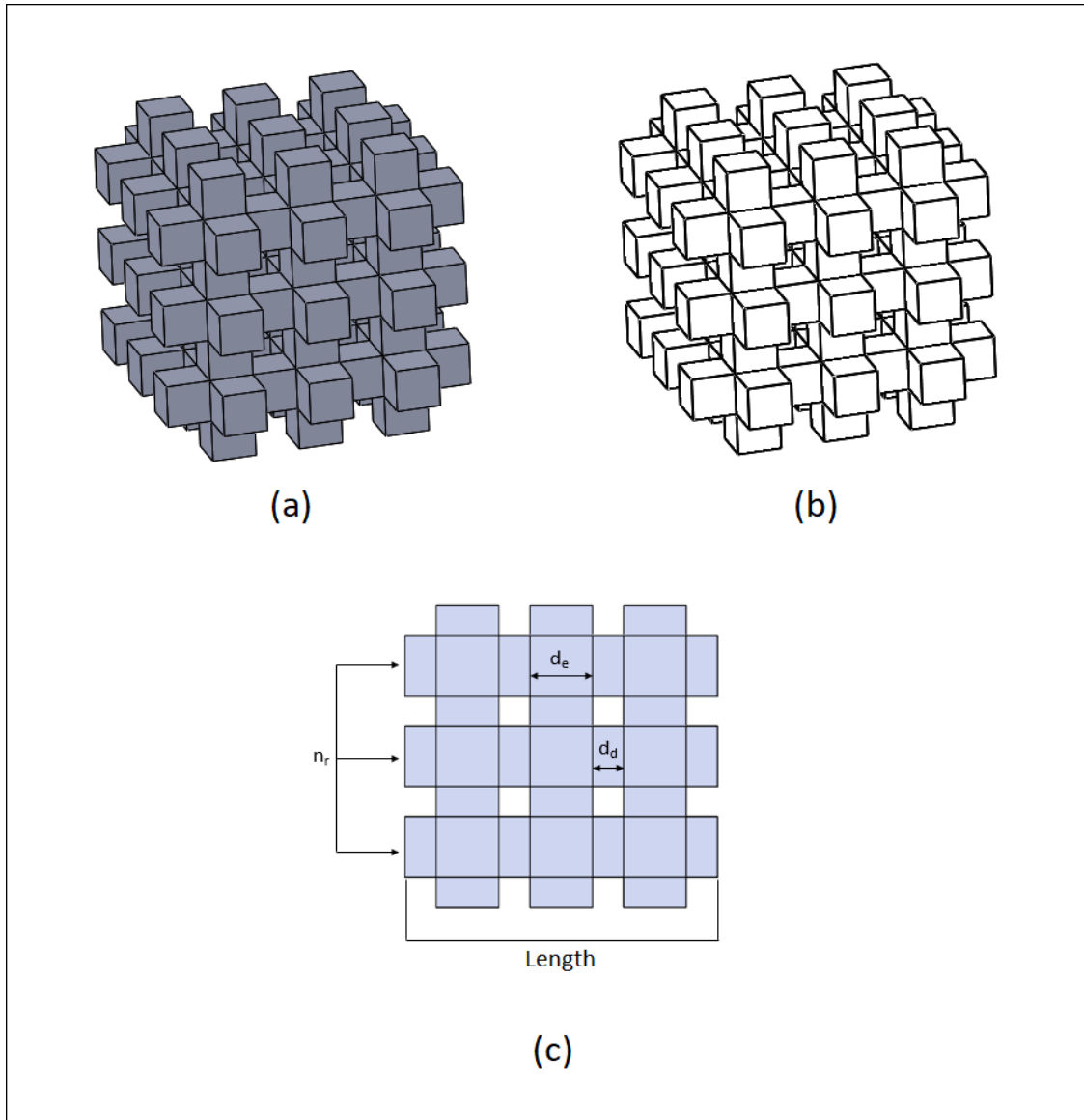


**Figure 5.2.** Schematic representation of a lattice structure which has dimensions of 5\_2.5\_3, where (a) shows the actual view of the lattice structure, (b) shows the transparent image of it and, (c) represents the thickness of each bar ( $d_e$ ), void thickness between two bars ( $d_d$ ), and the number of lines ( $n_r$ ) respectively.

**Table 5.1.** The dimensions of all lattice structures.

The Code of Geometry	$d_e$ [mm]	$d_d$ [mm]	$n_r$	Length [mm]
5_5_6	5	5	6	65
5_5_3	5	5	3	35
5_2.5_6	5	2.5	6	47.5
5_2.5_3	5	2.5	3	25
2.5_2.5_6	2.5	2.5	6	32.5
2.5_2.5_3	2.5	2.5	3	17.5
2.5_1.25_6	2.5	1.25	6	23.75
2.5_1.25_3	2.5	1.25	3	12.5

The purpose of the dimension of the element  $d_e$  (5 – 2.5 mm) is both to test the limits of the BJ technology in making small-sized parts (i.e., to be able to easily extract the accumulated powder that has not taken part in the process) and to understand if it is possible to pour into the molten metal. On the other hand size of the distance of an element from the next one  $d_d$  (100 % – 50 %  $d_e$ ) is to evaluate both the resistance of the element in contact with molten aluminum and to understand the contractions of the metal during solidification. The number of repetitions of the element in XYZ  $n_r$  (3 – 6) is to figure out the influence of the size of the component as a function of its correct filling based on the filling/solidification time of the molten metal.

### 5.1.2. Design of the gating systems

To fill up the mold in the desired time without any casting defects such as boiling point or turbulence, three different gating systems realized. Each has its advantages and disadvantages.

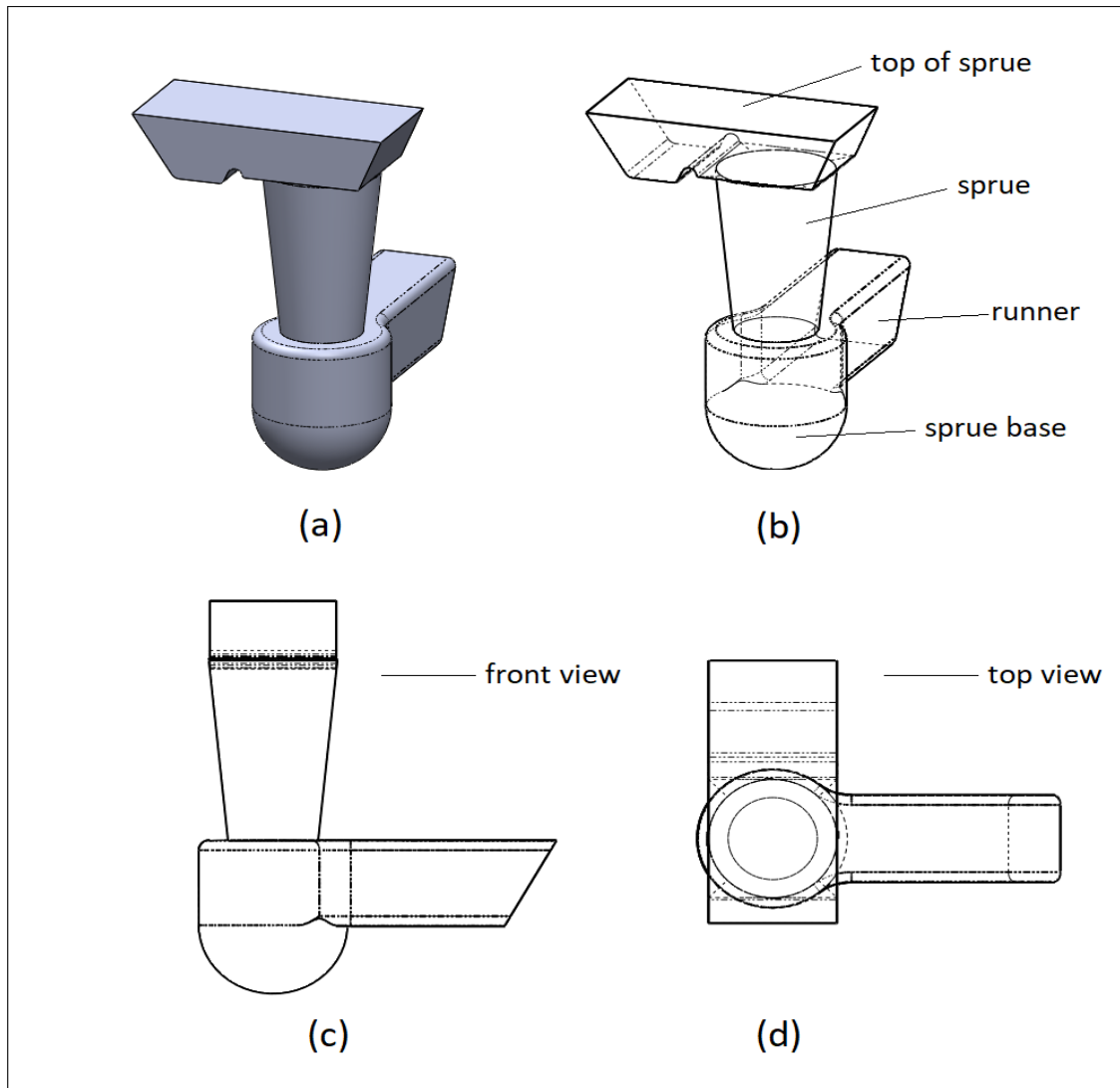


**Figure 5.3.** The representation of the first gating system was designed to overcome several casting problems; filling, hot-point, and turbulence. Where (a) shows the actual image of the whole system, (b) the transparent illustration of the gating system, where shows the top of sprue, sprue, sprue base, and runner, (c) front view, (d) top view.

The first gating solution design where can be seen in Figure 5.3, was generated to fill up the mold as fast as possible. However, the main disadvantage of this solution is that it needs excessive material to fill the mold. The gating system is realized based on some mathematical calculations. It can only be generated, taking into account the volume of the lattice structure dimension. During the calculations, two theorems were used;

## 1. Bernoulli's Theorem

This theorem is based on the law of conservation of energy and relates to pressure, friction, velocity, and height. The equation of Bernoulli's Theorem is given below;

$$h + \frac{p}{\rho g} + \frac{v^2}{2g} = \text{constant} \quad (5.1)$$

Where  $h$  is the height/altitude,  $p$  is the pressure at a certain height,  $v$  is the velocity at a certain height,  $\rho$  is the density, and  $g$  is the gravity. The law of conservation of energy requires that the following equation be established at each point.

$$h_1 + \frac{p_1}{\rho g} + \frac{v_1^2}{2g} = h_2 + \frac{p_2}{\rho g} + \frac{v_2^2}{2g} + f \quad (5.2)$$

Where 1 and 2 represent two different altitude,  $f$  is the loss of the energy due to friction. In this study, pressure and friction are neglected.

## 2. Continuity Theory

The continuity law requires a constant flow rate in the system for an incompressible fluid. The equation of Continuity Theory is given below;

$$Q = A_1V_1 = A_2V_2 \quad (5.3)$$

Where  $Q$  is the flow/flow rate ( $\text{mm}^3/\text{s}$  or  $\text{m}^3/\text{s}$ ),  $A$  is the cross-section of the liquid ( $\text{mm}^2$  or  $\text{m}^2$ ),  $V$  is the velocity of the liquid at a particular cross-section.

One of the most important consequences of applying these two flow laws in casting processes is the conical design of the sprues. If we omit the pressure difference ( $p_2 - p_1$ ) between the upper part and the lower part of the sprue and the friction losses ( $f$ ) in the sprue wall, we find the following relationship between the sprue height ( $h$ ) and the areas ( $A$ );

$$\frac{A_1}{A_2} = \sqrt{\frac{h_2}{h_1}} \quad (5.4)$$

Here, (for a liquid metal flowing from top to bottom), the subscript 1 indicates the peak of the sprue, and sub-symbol 2 represents the sprue base. Accordingly, the cross-sectional area of the sprue has to reduce gradually.

This is why the cross-sectional area of the sprue has to decrease consistently. The cross-section of a fluid released from any height will taper as the speed increases downward. It will be seen that as the fluid falls further downward, it breaks away from the central flow mass and becomes droplets. If the sprue cross-sectional area is designed as fixed from top to bottom, the flowing liquid in the sprue will undergo cross-sectional constriction as the alloy goes down. As a result, the liquid will be separated from the wall of the sprue, and aspiration will occur. In other words, it will start pumping air into the mold. In order to avoid such problems, the sprues should be designed as conical.

Here some equations could be useful:

$$v_2^2 = 2gh_2 \quad (5.5)$$

$$d = \frac{m}{v} \quad (5.6)$$

Assumed variables;

- $h_2 = 52,5mm$
- $d = 2,71kg/m^3$  of Aluminum
- $g = 9,81m/s^2$
- $t = 5sn$  (we want to fill the mold in 5 sec on an average)
- $v_1 = 0,5m/s$

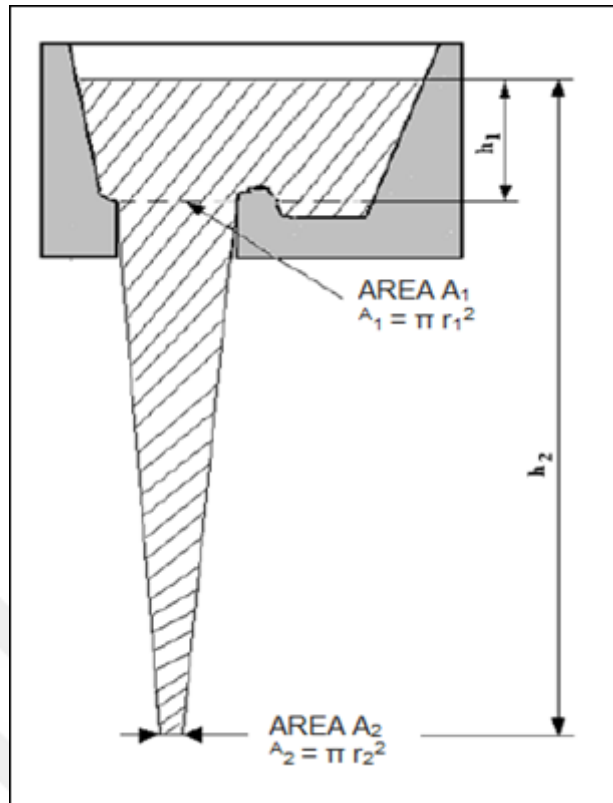


**Figure 5.4.** Schematic representation of the sprue system where illustrates  $h_1$ ,  $h_2$ ,  $A_1$ ,  $A_2$  that are assumed variables.

```

Mass properties of #2 CUBE NUMBER 1 XYZ_2,5 2,5 2,5_VOID_1,25
Configuration: Varsayilan
Coordinate system: -- default --

Density = 1.00 grams per cubic centimeter
Mass = 1.27 grams
Volume = 1.27 cubic centimeters
Surface area = 1687.50 square millimeters

Center of mass: ( millimeters )
X = 5.00
Y = 6.25
Z = -2.50

Principal axes of inertia and principal moments of inertia: ( grams * square millimeters )
Taken at the center of mass.
Ix = ( 1.00, 0.00, 0.00)   Px = 29.44
Iy = ( 0.00, 1.00, 0.00)   Py = 29.44
Iz = ( 0.00, 0.00, 1.00)   Pz = 29.44

Moments of inertia: ( grams * square millimeters )
Taken at the center of mass and aligned with the output coordinate system.
Lxx = 29.44      Lxy = 0.00      Lxz = 0.00
Lyx = 0.00      Lyy = 29.44      Lyz = 0.00
Lzx = 0.00      Lzy = 0.00      Lzz = 29.44

Moments of inertia: ( grams * square millimeters )
Taken at the output coordinate system.
Ixx = 86.79      Ixy = 39.55      Ixz = -15.82
Iyx = 39.55      Iyy = 68.99      Iyz = -19.78
Izx = -15.82     Izy = -19.78     Izz = 110.52

```

**Figure 5.5.** Dimensions of the sample lattice structure.

As seen in Figure 5.5, after obtained the volume of the part (lattice structure) via Solidworks, the total mass that we need to cast was calculated;

$$d=m/v$$

$$m=d*v$$

$$m=1,27\text{cm}^3 * 2,76\text{gr/cm}^3$$

$m=3,50\text{gr}$  (Total amount of weight that we need to fill the mold up. Sprue and runner cavity are neglected)

After that;

$$Q=\text{total casting weight}/\text{total casting time}$$

$$Q=3,50\text{gr}/5\text{sec}$$

$Q=0,70\text{gr}/\text{sec}$  (The flow rate required to fill the mold, however, we do not need to identify the weight of the liquid metal passing through the unit area per unit time, we need volume passing through the unit area per unit time)

$$Q=(0,70\text{gr}/\text{sec})/(2,71\text{kg/m}^3)$$

$$Q=2,58*10^{-4}\text{m}^3/\text{s}$$

First, we need to compute velocity to identify  $A_2$ ;

$$Q=A_2*v_2$$

$$v_2 = 1,01\text{m/s}$$
 (velocity at sprue base)

So;

$$A_2=2,58*10^{-4}\text{m}^2$$
 (sprue base cross-section)

From the value of cross-section of  $A_2$ , we can evaluate  $r_2$  which is the Radius of the sprue base;

$$A_2= \pi r_2^2 , r_2=8,9\text{mm}$$

$$\text{From } A_1*v_1 = A_2*v_2$$

$$A_1=5,15*10^{-4}\text{m}^2 , r_1=12,81\text{mm}$$

The last value that we need to calculate is  $h_1$ . From the formula following;

$$A_1/A_2=(h_2/h_1)^{1/2} \quad h_1=12,74\text{mm}$$

As a result of those calculations, the cross-section of the top of sprue and cross-section of sprue base was obtained. The locations of the sprue top and base were also identified by the result of those calculations with the help of  $h_1$  and  $h_2$  values.

In the second gating solution design where can be seen in Figure 5.6, it is aimed to let molten metal penetrate to every region of the lattice structure to avoid filling problems.

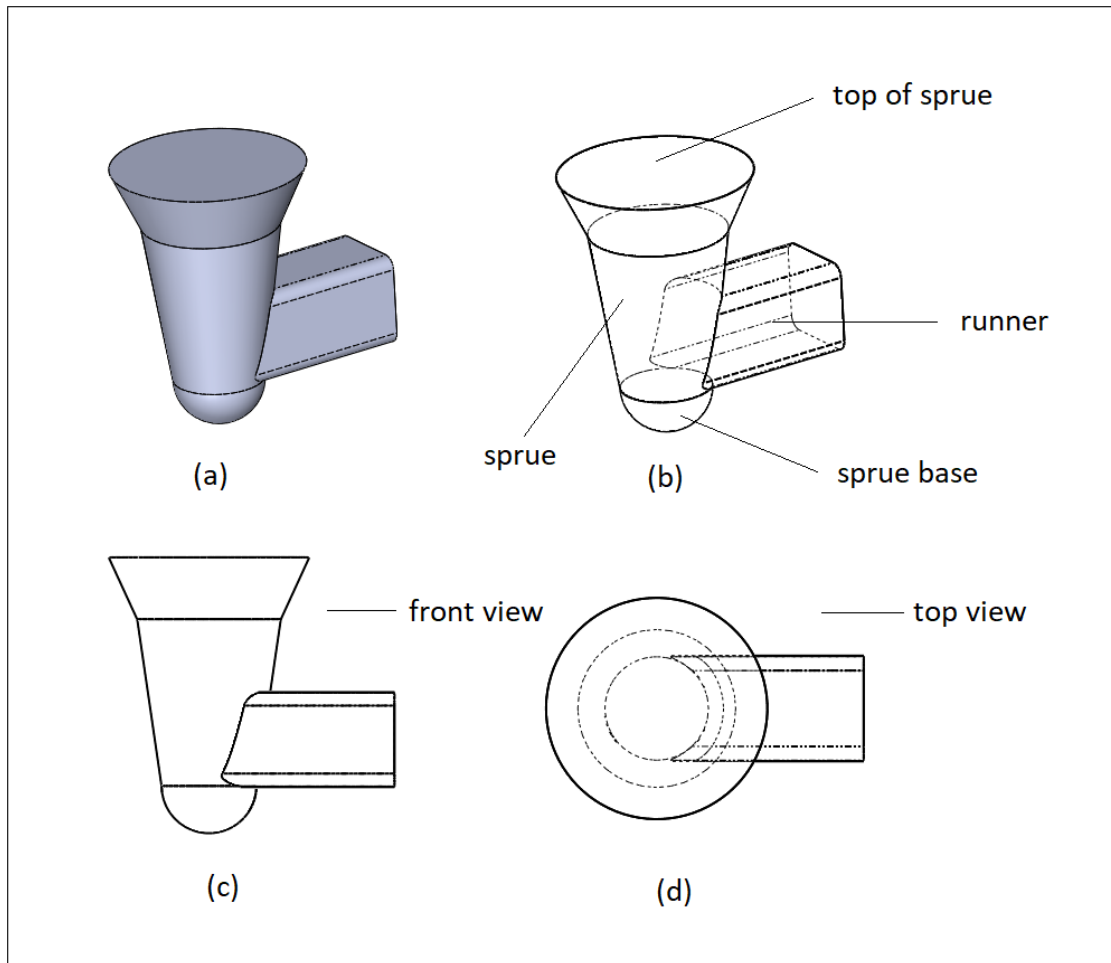


**Figure 5.6.** The illustration of the second gating solution employing the strategy of side-attack to let molten metal penetration. Where (a) represents the actual view of the gating design, (b) shows the transparent image of it, (c) shows the front view, (d) represents the top view of the system.

It designed to reduce waste of casting material and present a different perspective about fill up the mold. The purpose of this design is to enter the mold from the middle and be able to reach the regions that it would be hard.

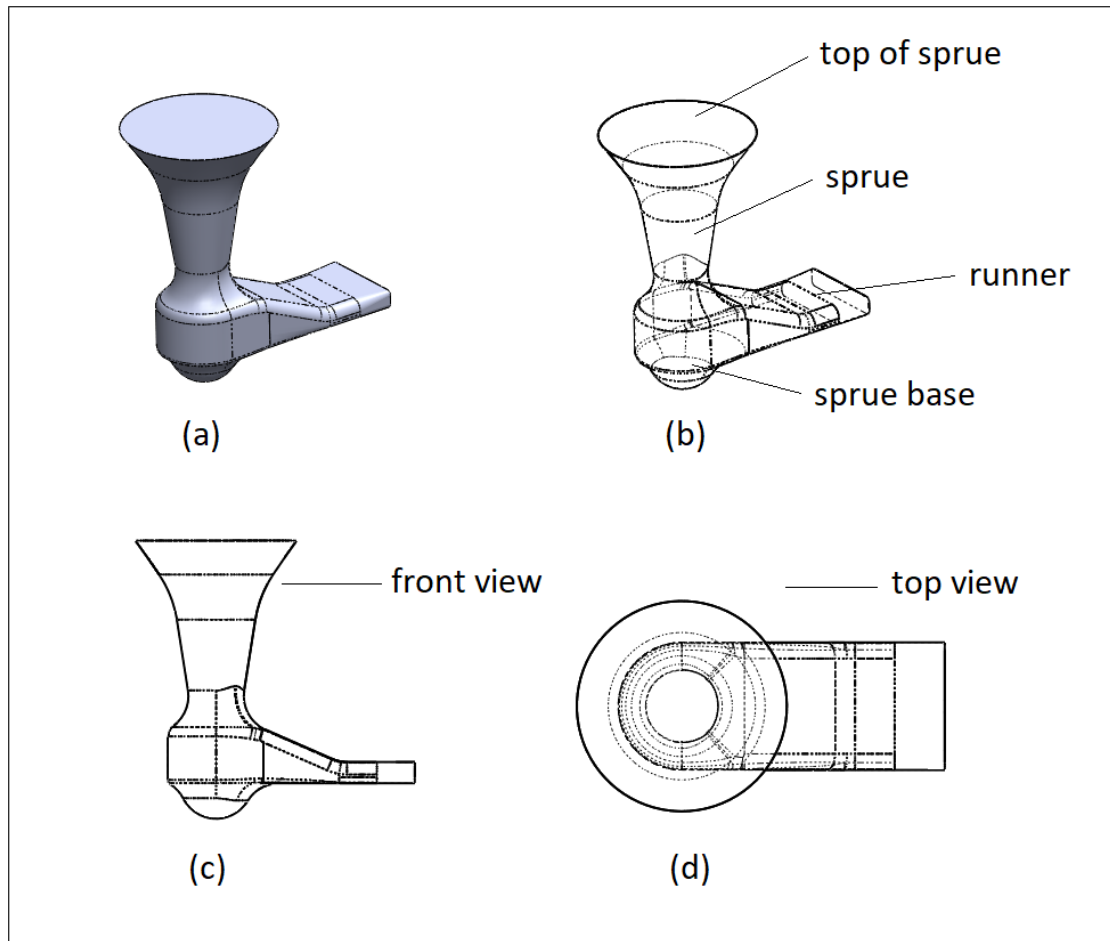


**Figure 5.7.** The depiction of the third gating system utilizing the strategy of base-attack to fill the Mold in time. Where (a) shows the actual view, (b) represents the transparent of a, (c) shows the front view, (d) illustrates the top view of the system.

As can be seen from Figure 5.7, the size of the feeding channel is reaching to the part as decreasing. Apart from the previous two designs, it is aimed to fill the mold with minimum material loss and control the velocity of the molten metal. In the third gating solution approach, the molten metal starts filling from the bottom of the part to the up as it happens in the first gating system. The difference between those two designs, in this approach, the molten metal does not enter from the bottom. An illustration is given to make this idea clear in Figure 5.8.

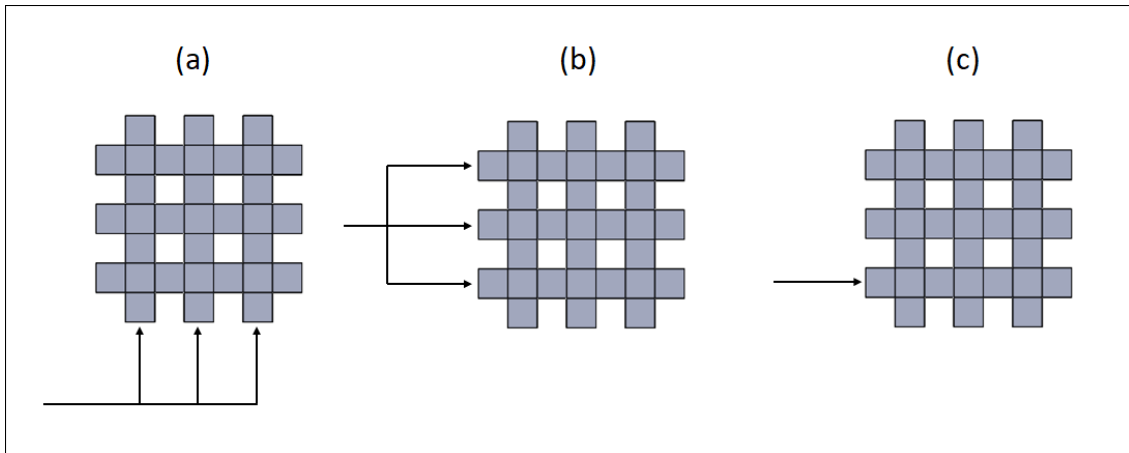


**Figure 5.8.** An expression, which regions where molten metal starts to fill the lattice structure up. In the first gating system, (a) shows the molten metal entered the part from the bottom. In the second gating system, (b) represents the molten metal entered the part from the middle. In the third gating system, (c) illustrates the molten metal entered the part from the left-base side.

### 5.1.3. Assembling of gating systems and lattice structures into the mold

Solidworks 2018 program licensed by the university was used for mold design as well as happen in all design processes. The mold cavity was achieved by subtracting the positive design of the lattice structure assembled with the gating system from the mold. During the casting process, the thickness between the surface of the lattice structure and the mold shell was adjusted 10mm as a minimum from each region to resist the initial effect of molten aluminum. The first step of followed strategies for generating of molds is illustrated in Figure 5.9.

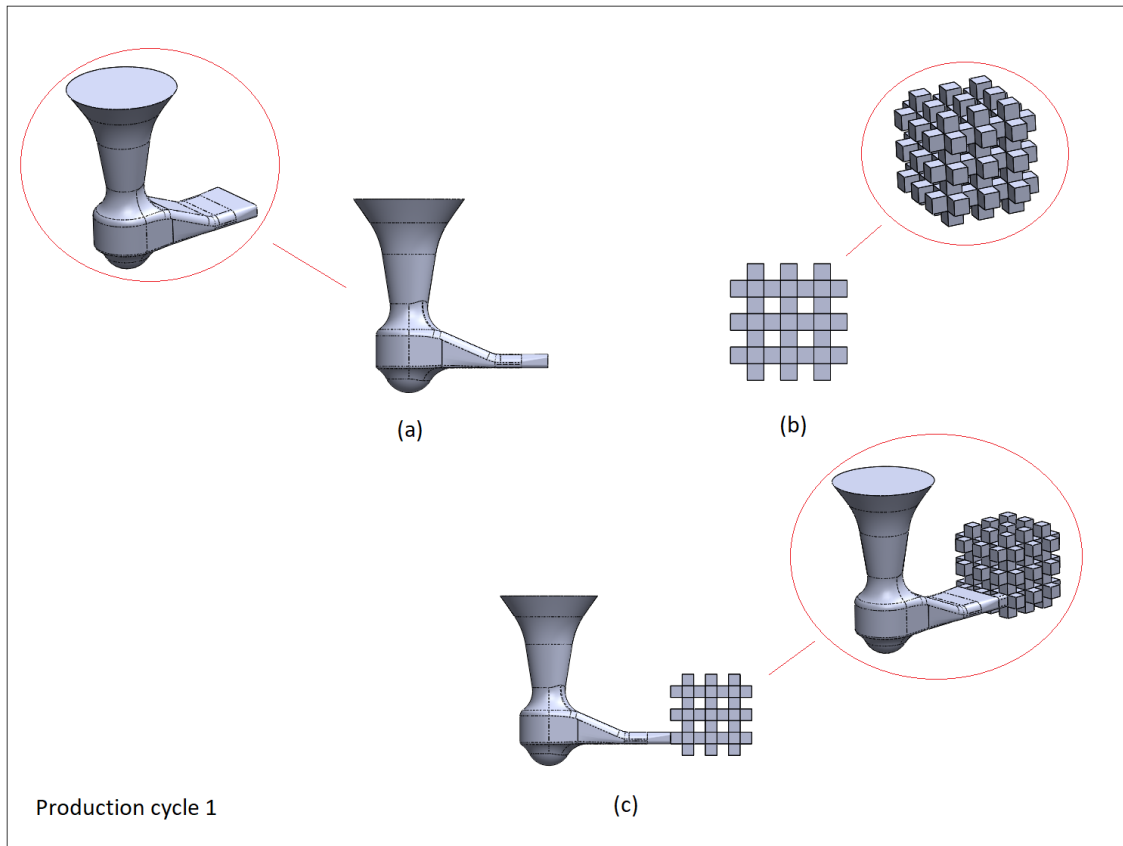


**Figure 5.9.** Schematic illustration of the assembling of the gating systems and components into the mold. (a) represents the third gating system, (b) represents the component, and (c) shows the assembled part of them called ‘positive.’

Basically, the generation of the molds begins with the integration of the gating systems and components, as illustrated above. This strategy followed in all gating systems and components integration. Later on, the mold generation continues with the removing process of the positive from the mold. Moreover, the mold is built on the positive part. The mold cavity called ‘negative’ is obtained by extruding the positive part from the mold. In order to adjust the thickness between the surface of positive and mold shell as a minimum 10 mm, some useful Solidworks feature has been used.

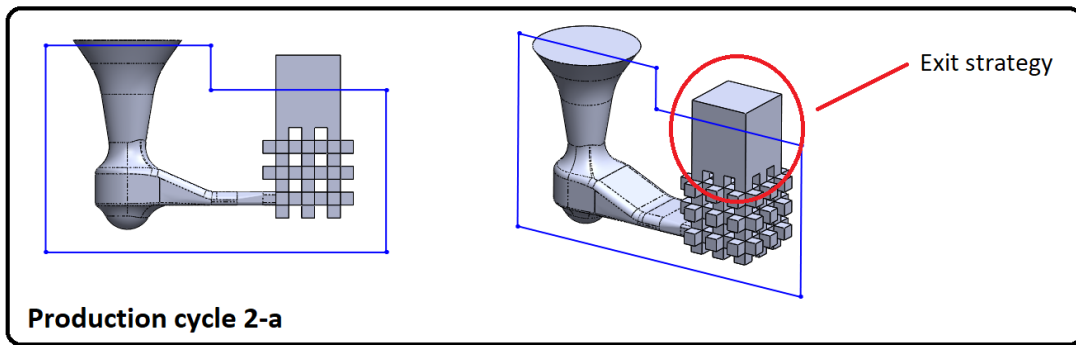


**Figure 5.10.** Schematic representation of the drawing of the mold-boundaries.

First, as shown in Figure 5.10, by assigning a reference plane to the center of the positive part, mold boundaries are drawn. An exit strategy generated to let air passing through the mold cavity towards outside.

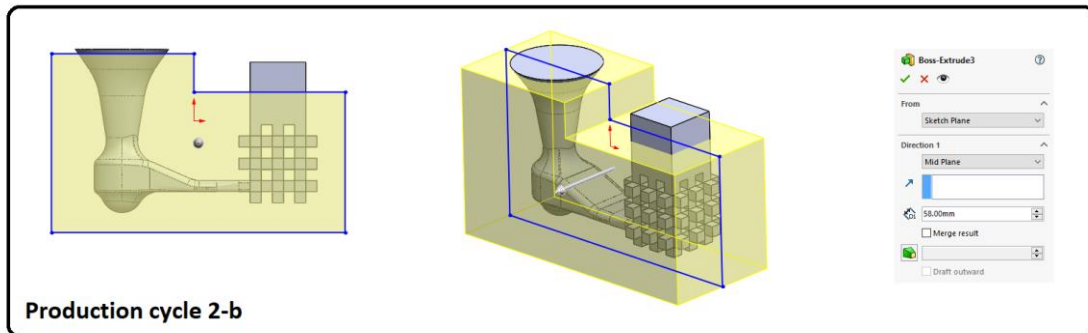


**Figure 5.11.** Schematic representation of the solid-Boss-Extrude.

Then, as illustrated in Figure 5.11, the whole drawing is selected and giving substantial thickness by Boss-Extrude.

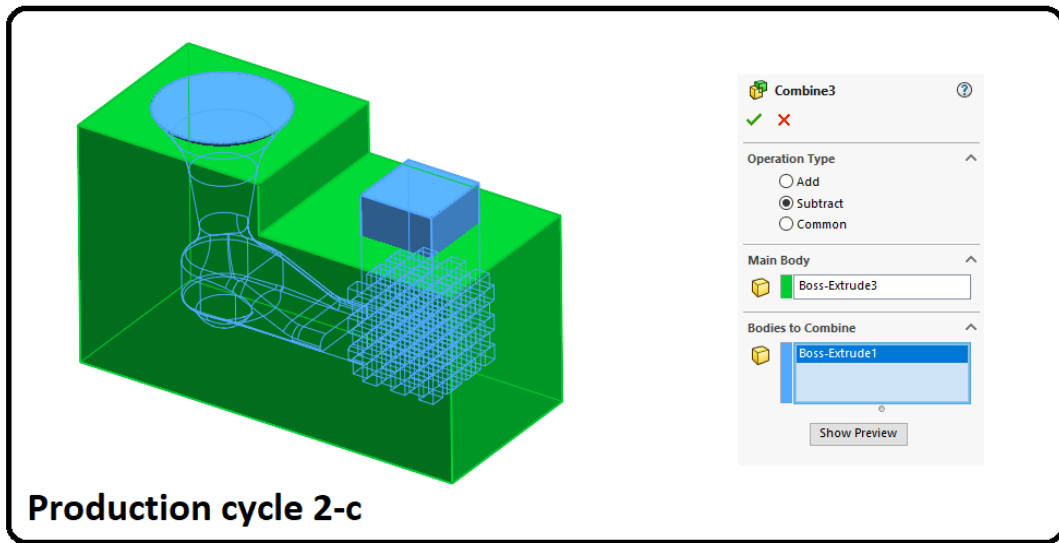


**Figure 5.12.** The depiction of the Combine process.

The process continues with the subtract of the positive from the mold. As illustrated in Figure 5.12, the Combine feature of Solidworks software helps us to do it quickly.

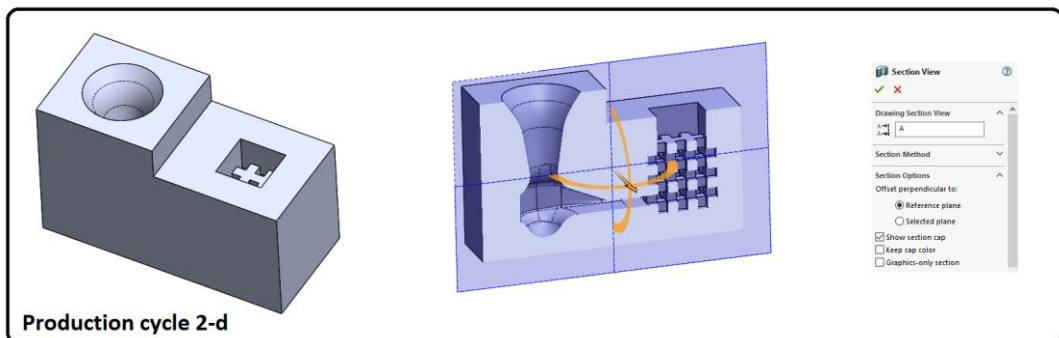


**Figure 5.13.** Schematic representation of the mold and its section view.

The design process ends when the mold cavity is obtained. As can be seen in Figure 5.13, it is proved that the mold cavity was obtained based on the section view property of Solidworks. After the generation of the molds, the mold dimensions were calculated to take into account XYZ. This calculation aimed to have an idea about dimensions and discuss the build chamber volume capacity of the 3D printer.

## 5.2. Production Activities

### 5.2.1. The Projet CJP 460Plus

The used printer during printing processes was a Projet CJP 460 Plus, which is a 3DSystem product. It is able to use various input format files such as .stl, .step, .x\_t, .3ds, .obj, .ply, and more. The Projet CJP 460Plus that is using BJ technology can print fully colored parts up to 10x faster than other technologies. In addition to its full-color part printing capability, up to 7x cost-effective part production, no need for supporting materials, and recycling of non-stick materials makes it one step ahead of its competitors.



**Figure 5.14.** Schematic representation of the Projet CJP 460 Plus.

The Projet CJP 460 Plus supports two different software called as 3DSprint and 3Dprint. 3DSprint can modify the appearance of pieces as well as employing many input files, as mentioned above. It has a broad range of interface functions to modify parts such as fix, scaling by unit, triangle reduction, measure, and more. 3DPrint is software that enables us to display the parts desired in real-time and adjust their positions in the build chamber. Production time, the amount of binder and powder, the number of layers, and height can also be displayed and control with the employing of this software. It is the last step-program before the printing process start.

One of the most important things is that the printer needs to keep being connected with a computer during the printing process. This is because the computer continues to send each layer to the printer individually via 3DPrint software. To avoid delay and production

errors, the connection cable called ethernet must preserve with durability and connected. It is also recommended that internal and external security software should keep closed during production.

**Table 5.2.** Technical specifications of the ProJet CJP 460Plus [133].

The Printer	Manufacturer	Print Resolution	Net Build Volume (XYZ, mm)	# of Print Heads	# of Jets	Part Cleaning (Accessory /Integrated)	Layer Thickness (mm)	Max. Vertical Build Speed (mm/hour)
ProJet CJP 460Plus	3D SYSTEMS	300 x 450 DPI	203 x 254 x 203	2	604	Integrated	0.1	23

### 5.2.2. Mold production

Three of eight different geometries were selected for the printing of molds before the casting process performed. Each geometry was aimed to be printed three times, integrated with three different gating systems. Nevertheless, as can be seen in Table 5.3, the geometries integrated with the gating system 1 needs the over-printing and casting specifications such as printing volume and casting weight. Because of this situation, only the geometry of 2.5\_2.5\_3 combined with the gating system 1 found proper to be printed. The other two geometry were eliminated.

**Table 5.3.** Technical pieces of information about printed molds.

The Code of Geometry	Lattice Design Parameters				Mold dimensions [mm]			Whole Cast information		
	Thickness [mm]	Void [mm]	# of line	Gating System	X	Y	Z	Volume [cm <sup>3</sup> ]	density [g/cm <sup>3</sup> ]	Weight [g]
2.5_1.25_6	2.5	1.25	6	1	132	120.57	149.58	247.03	2.67	659.57
2.5_2.5_3	2.5	2.5	3	1	89	76.89	94	70.3	2.67	187.71
5_2.5_3	5	2.5	3	1	120	111.96	146.91	240.56	2.67	642.3
2.5_1.25_6	2.5	1.25	6	2	67.83	35	45.41	22.19	2.67	59.25
2.5_2.5_3	2.5	2.5	3	2	60.18	28	32.1	8.29	2.67	22.14
5_2.5_3	5	2.5	3	2	91.78	45	56.17	31.25	2.67	83.44
2.5_1.25_6	2.5	1.25	6	3	79.34	35	53.96	15.9	2.67	42.5
2.5_2.5_3	2.5	2.5	3	3	65.12	34	44.82	5.24	2.67	14
5_2.5_3	5	2.5	3	3	107.3	40	70.58	26.3	2.67	70.2

As a result, seven geometry were printed for the casting process.

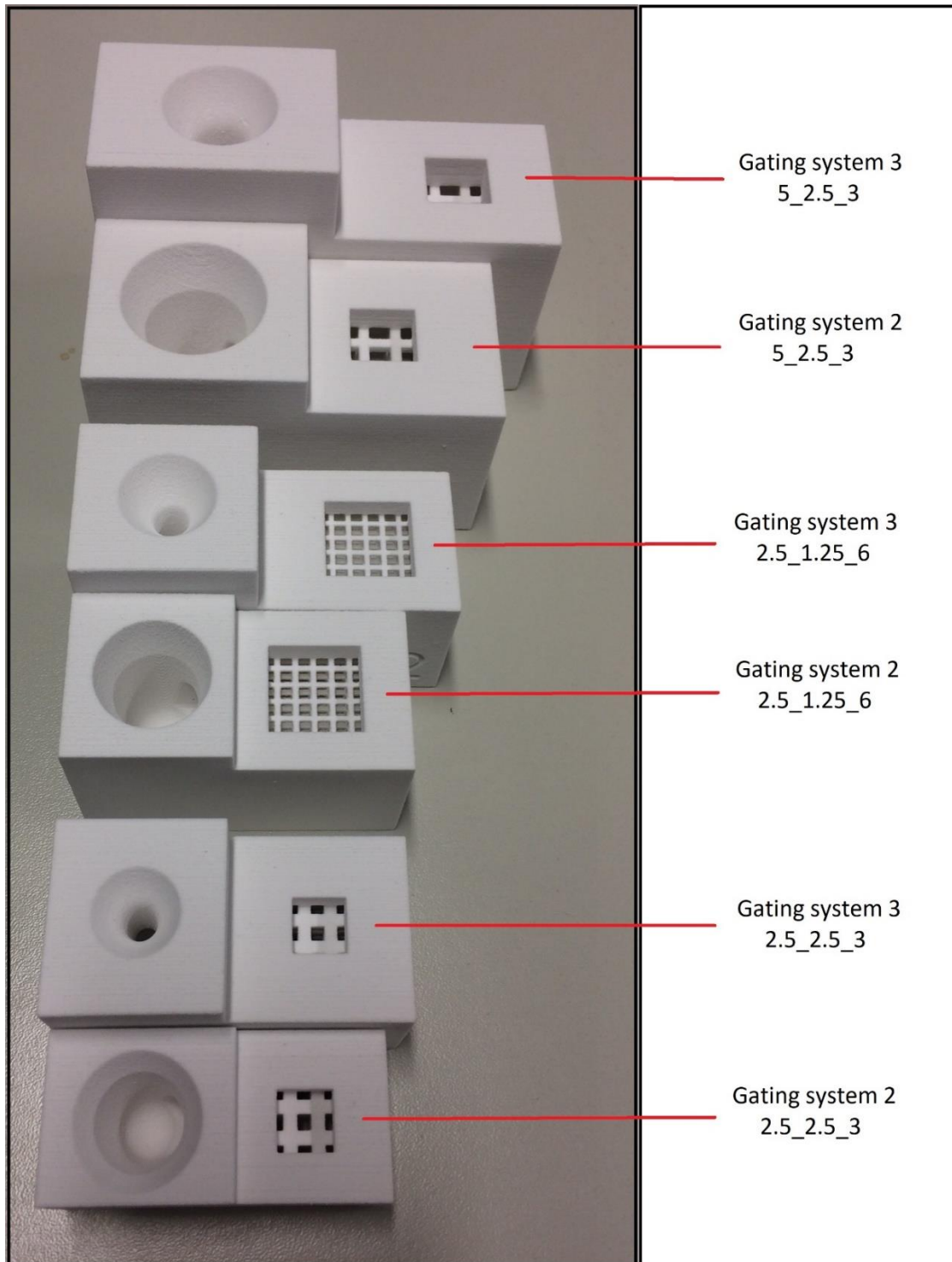


**Figure 5.15.** The images of the printed molds. The representation of the geometry of 2.5\_2.5\_3 combined with the gating system 1 is given in Figure 6.16.

### 5.2.3. Used powder and binder in printing

In this research, gypsum known as also Calcium Sulphate Hemihydrate was used as a feedstock in BJ experiments. Projet 460 manufacturer supplies the powder, which has a spherical shape in 0.1 mm diameter. It is a ceramic-based material that can use by machine in printing processes. On account of it is a ceramic-based powder, it has a high melting point around 1450 °C, which gives the ability to resist high casting applications.

Calcium Sulphate Hemihydrate powder has a density of something between 2,6-2,7 g/cm<sup>3</sup> according to the guidelines provided by 3D Systems. The color of it is white, and solubility properties are shown in Table 5.4.

**Table 5.4.** Physical and Chemical Properties of Calcium Sulphate Hemihydrate Powder.

Physical and Chemical Prop.	Color	Density (g/cm <sup>3</sup> )	Water solubility (20°C in g/l)	Melting point/range (°C)	Acute effects (toxicity tests)	
					LD <sub>50</sub> Oral	LD <sub>50</sub> Dermal
Calcium Sulphate Hemihydrate	White	2.6-2.7 g/cm <sup>3</sup>	0.83% (3°C)	1450°C	> 5000mg/kg (rats)	NA

The 2-pyrrolidone, which has an organic compound, was used as a liquid bonding agent that is using by the machine to combine layers. The boiling point of it is 100 °C and shows soluble property when it touches with water. Owing to the ability toxic fumes out, such as carbon dioxide, carbon monoxide in high-temperature tests, we used unique masks for protection. The density of 2-pyrrolidone is 1 (g/cm<sup>3</sup>) like water.

### 5.2.4. Post processing

The powder-removal process in BJ technology can be accepted as the most critical step in post-processing. With the increase of the internal complexity of the part that is desired to be produced, this process becomes more laborious.

In this study, after the printing process is done, the parts took from the building chamber of the printer (left) and put to the cleaning box (right) (Figure 5.14). Two guns that have different pressure levels were used to remove the non-stick powder from the molds. The first one is the regular pressure gun located in the cleaning part of the Projet CJP 460 Plus, and the other is the high-pressure gun connected to the laboratory pressure network.

### 5.3. Mold Cavity Verification

All eight geometries, combined with a pure mold perspective (demo), were printed to verify that the mold cavity was obtained correctly. As illustrated in Figure 5.16, those molds do not have sprue and runner, briefly gating system.

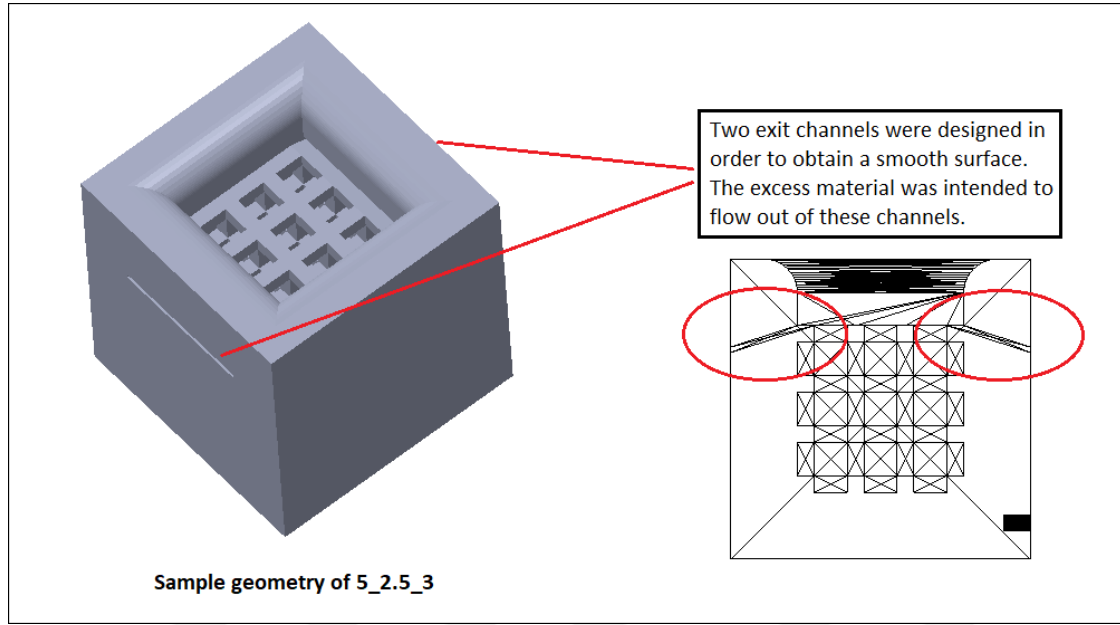


**Figure 5.16.** Schematic view of a demo mold of 5\_2.5\_3.

To understand that the loose powder was removed from the molds correctly, rubber was poured into them by gravity casting. After the mold was destroyed, and a visual inspection was carried out to evaluate the feasibility of the pieces obtained. The purpose of this experiment was to have an idea about the powder-removal process before printing real-mold production.

### 5.4. Temperature Test

In the heat treatment test, the durability of the smallest parts was tested to understand which temperature is the best. For this experiment, three different geometries selected and produced three times each. The followed strategy was the same as in the Mold Cavity Verification section. An identical mold type used. After the heat treatment test, gravity casting performed into the molds employing rubber. Then the molds destroyed.

As shown in Table 5.5, the molds were kept in a heat treatment furnace for 10 minutes at three different temperatures. Our aim in this experiment was to evaporate the binder from

the structure of mold by evaporation. The purpose of adopting such an approach is to obtain a more fragile structure while, removing the desired part from the mold efficiently after the casting process.

**Table 5.5.** Heat treatment experiment values.

#selected geometries	Time	Temperature (°C)
5_2.5_3	10 min	300 °C
2.5_2.5_3	10 min	500 °C
2.5_1.25_6	10 min	700 °C

### 5.5. Aluminum Casting

The alloy selected as aluminum during the casting applications. The composition of aluminum alloy was given in Table 5.6.

**Table 5.6.** Composition of the Aluminum alloy used in this study.

element	Al	Cu	Mg	Si	Fe	Mn	Ni	Zn	Altri
Percentage [% ,weight]	86.93	2.11	0.17	8.39	0.85	0.23	0.08	0.96	0.28

Basically, the casting method was performed as a conventional gravity casting. During the casting processes, a heat treatment oven, which has no vacuum feature, used as a heat source to melt aluminum alloy and keep at that temperature. In order to avoid casting errors due to the temperature difference between the molds and the molten aluminum during casting, the molds were also heated to a predetermined temperature inside a second heat treatment furnace. The casting process was carried out within 10 seconds after being removed from the furnace. After the casting finished, the molds left for a particular time to cool and then placed in a container filled with water. Then the molds were destroyed then the removed pieces were collected for inspection.

## **6. RESULTS AND DISCUSSION**

### **6.1. Mold Cavity Verification**

According to the author of the thesis, the powder-removal process is the most significant step of the BJ mold production approach. If the loose powder does not remove from additively produced molds, then this approach, specifically mold production, becomes useless. To overcome this obstacle, the molds could be produced in two parts and then combined. However, this approach is contrary to the spirit of one-piece production in one step, which additive manufacturing technology offers. As a result, before the printing process of the real molds, a step that is called 'Mold Cavity Verification' generated. It is important to note that the powder-removal process has a direct relationship with the internal design complexity of the part. As mentioned in chapter one, some critical design parameters must take into account during the design process.

#### **6.1.1. Demo mold production**

In this experiment, as shown in Figure 6.1, eight lattice structures, which have no gating systems, were printed with a simple mold approach.

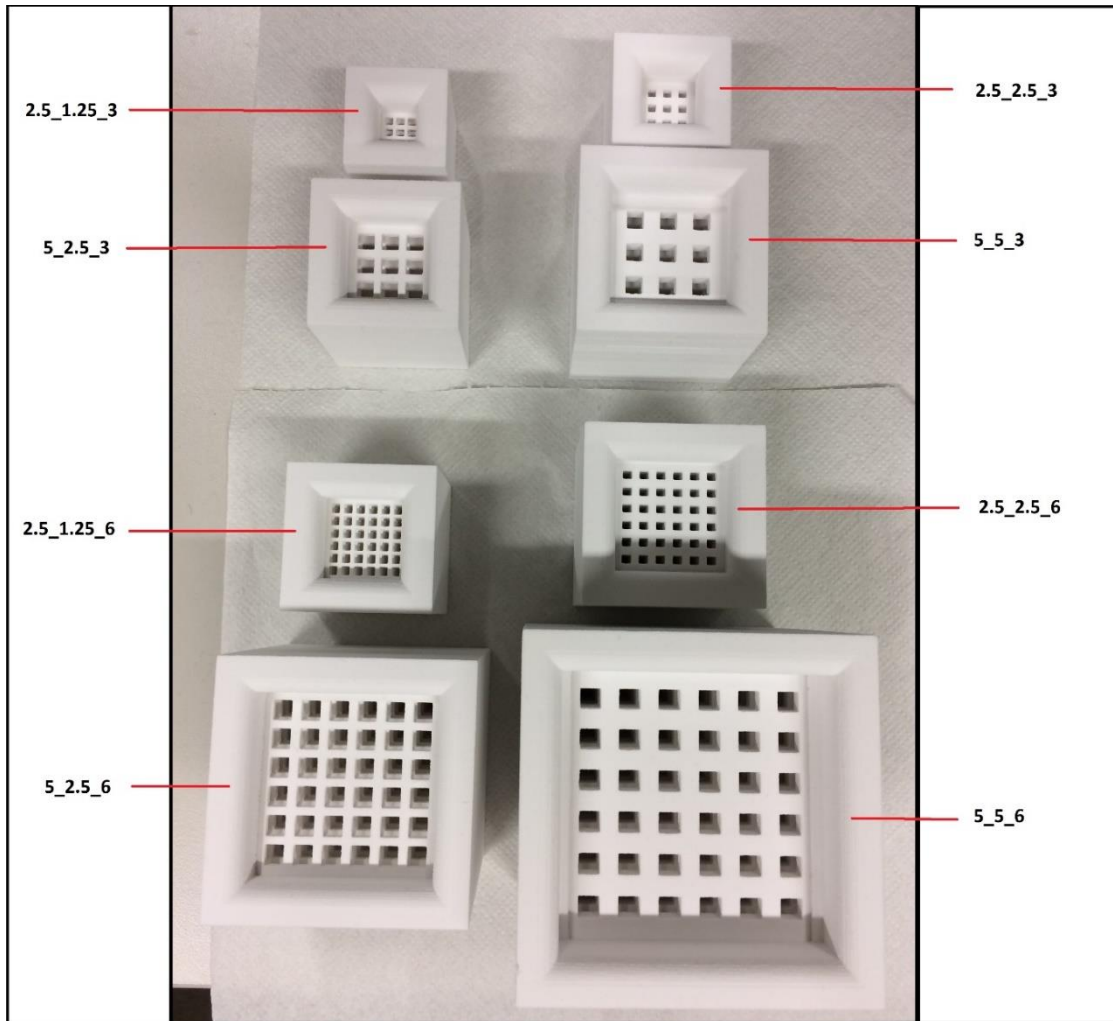


**Figure 6.1.** Printed demo molds to check powder-removal behaviors of the lattice structures.

During the powder-removal process, two different air pressure guns used. In most cases, the gun where inside the Printer is quite enough for powder-removal. However, in order to make sure that the loose powder took out, another high-pressurized gun used.

### **6.1.2. Silicone rubber casting**

After the powder-removal process with pressurized air, a composition comprised of silicone rubbers prepared. An illustration of the silicone rubbers used is given in Figure

6.2.



**Figure 6.2.** An illustration of the silicone rubbers of R PRO 30 A and R PRO 30 B.

Silicone rubbers were stirred with the help of a stick in a plastic container. The composition of this mixture was %50 from R PRO 30 A type of silicon rubber and %50 from R PRO 30 B type of silicon rubber. This solution was mixed until the color turns out a uniform shape, then casting performed.

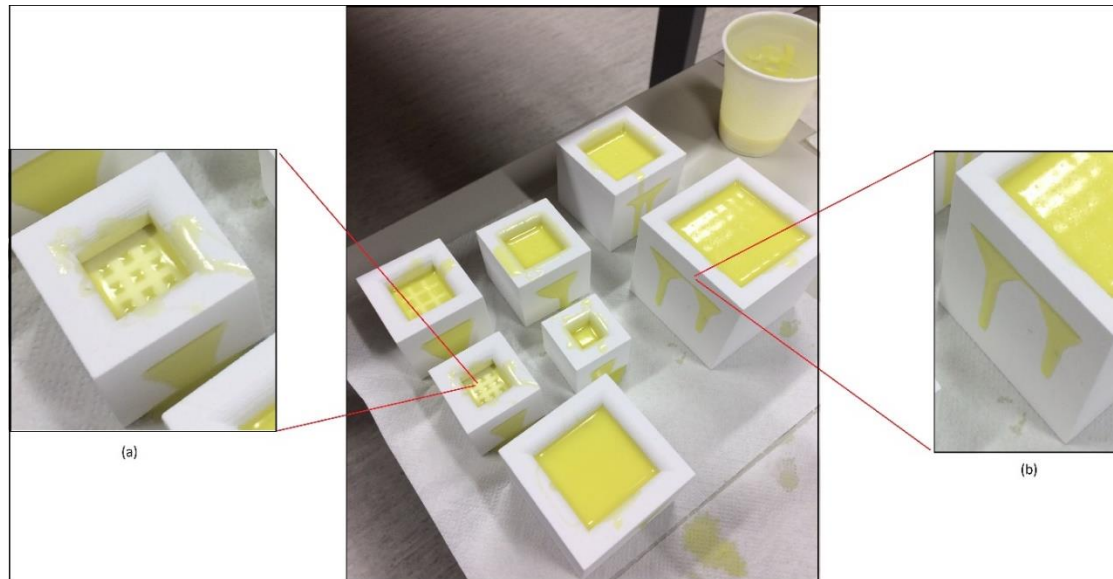


**Figure 6.3.** Representation of the demo molds after silicone rubber casting. Where (a) shows that the excess mixture flow towards the outside, where (b) shows that the exit tunnels strategy was successful.

After casting, demo molds were placed in a plastic container filled with water. It is known that the feedstock, which is calcium sulfate hemihydrate, has an excellent dissolving relation with water. After a waiting period of around 2-3 minutes, the silicone parts were removed from the molds by applying pressure. Then the parts were put in another box for the detailed cleaning process to make their surfaces more visible.

### 6.1.3. Results of the mold cavity verification

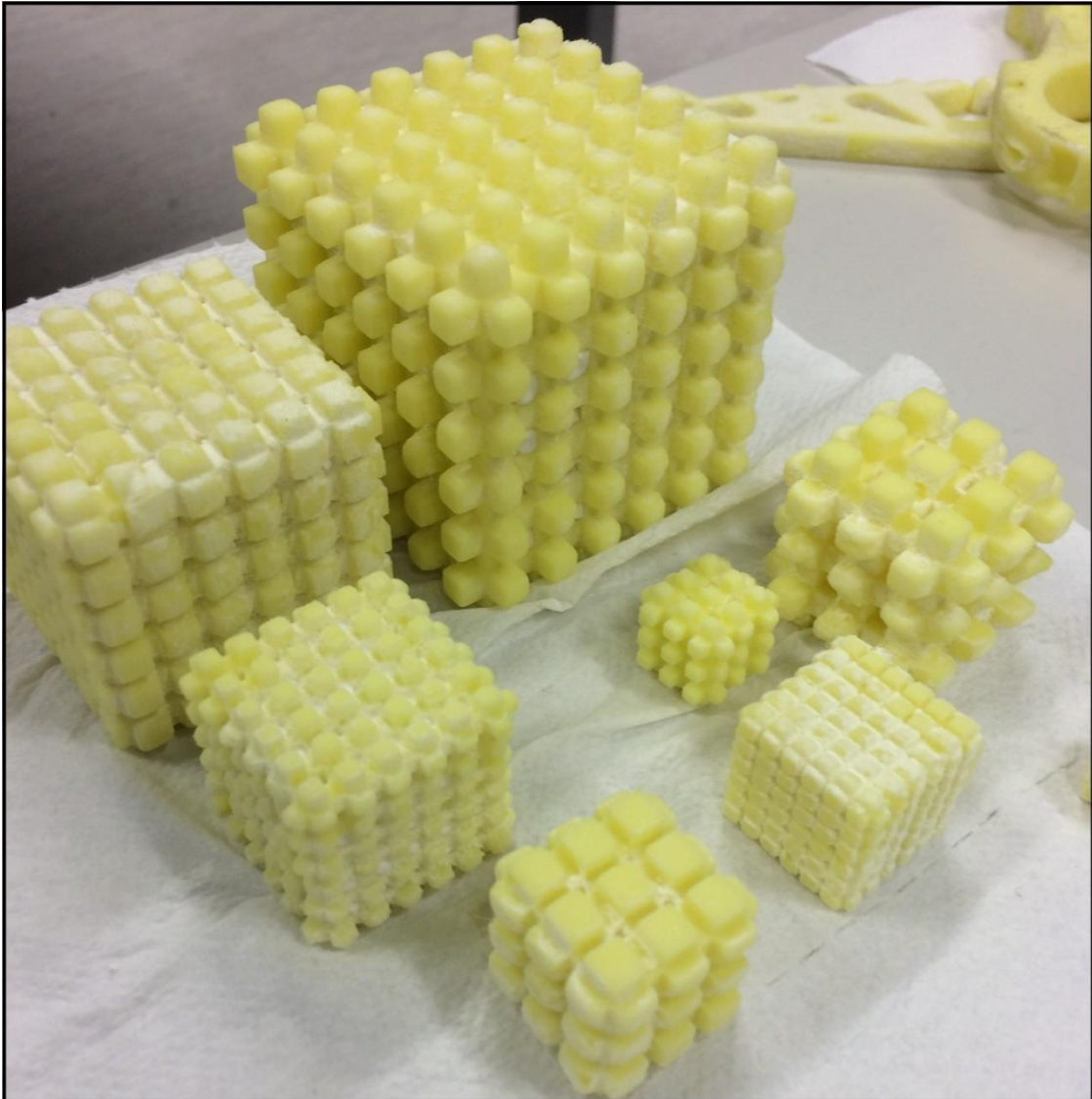


**Figure 6.4.** The parts extracted from the demo molds.

As can be seen in Figure 6.4, the results were quite clear. There were no casting errors, such as a filling. The primary purpose of this experiment was to check whether the powder removal process is possible. It has been proven that after the visual inspection, the powder-removal process has been successfully carried out. It is also checked that the relation between the powder-removal process and the internal design complexity of the molds. The results also proved that the design complexity of the molds realized in this study was not an obstacle in front of the aluminum casting.

It is also worthy of mentioning that the feedstock hardened by the binder effect was difficult to remove from the inner parts of some lattice structures. It is because of the void dimension was not enough between the elements. Besides, more pressure that could be applied by hands was not possible because of the elastic properties of the silicon rubbered parts. It should not be forgotten that this process performed before heat treatment. We know that the heat treatment results in binder evaporation enable ease of feedstock-removal process after casting.

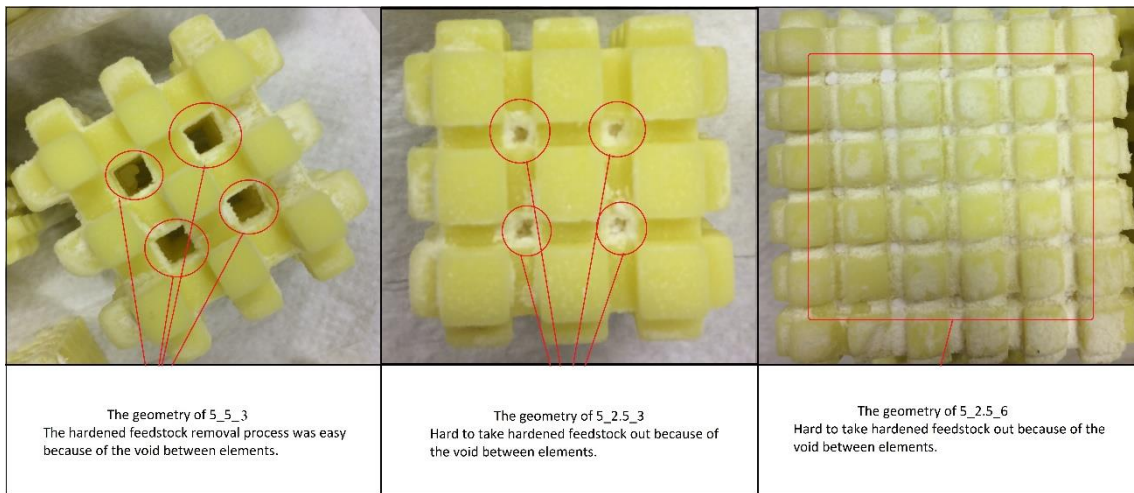


**Figure 6.5.** Schematic representation of the silicone rubber parts.

The geometries which have 2.5 mm void thickness between elements showed more resistance to the hardened powder-removal process. As a result, it is verified that real molds could produce for aluminum casting.

## 6.2. Temperature Test

In the heat treatment experiment, it is aimed to obtain a more fragile mold structure. Because no matter how it is easy to destroy the mold with the help of water, the structure still rigid and durable. It needs more human efforts compared to the conventional part removing styles. In order to reduce this effort, a heat treatment experiment was performed at three different temperatures. The temperatures are 300, 500, and 700 C, respectively. The time that the molds are kept in the heat treatment furnace is 10 minutes. For the heat treatment test, the same approach was used in the Mold Cavity Verification. Three geometry, which has the same mold perspective with the previous test, produced three times each. After the heat treatment of those molds, silicone rubber casting was performed.

### 6.2.1. Demo mold production

As it is illustrated in figure 5.6, selected geometries were 2.5\_1.25\_6, 5\_2.5\_3, and 2.5\_2.5\_3.

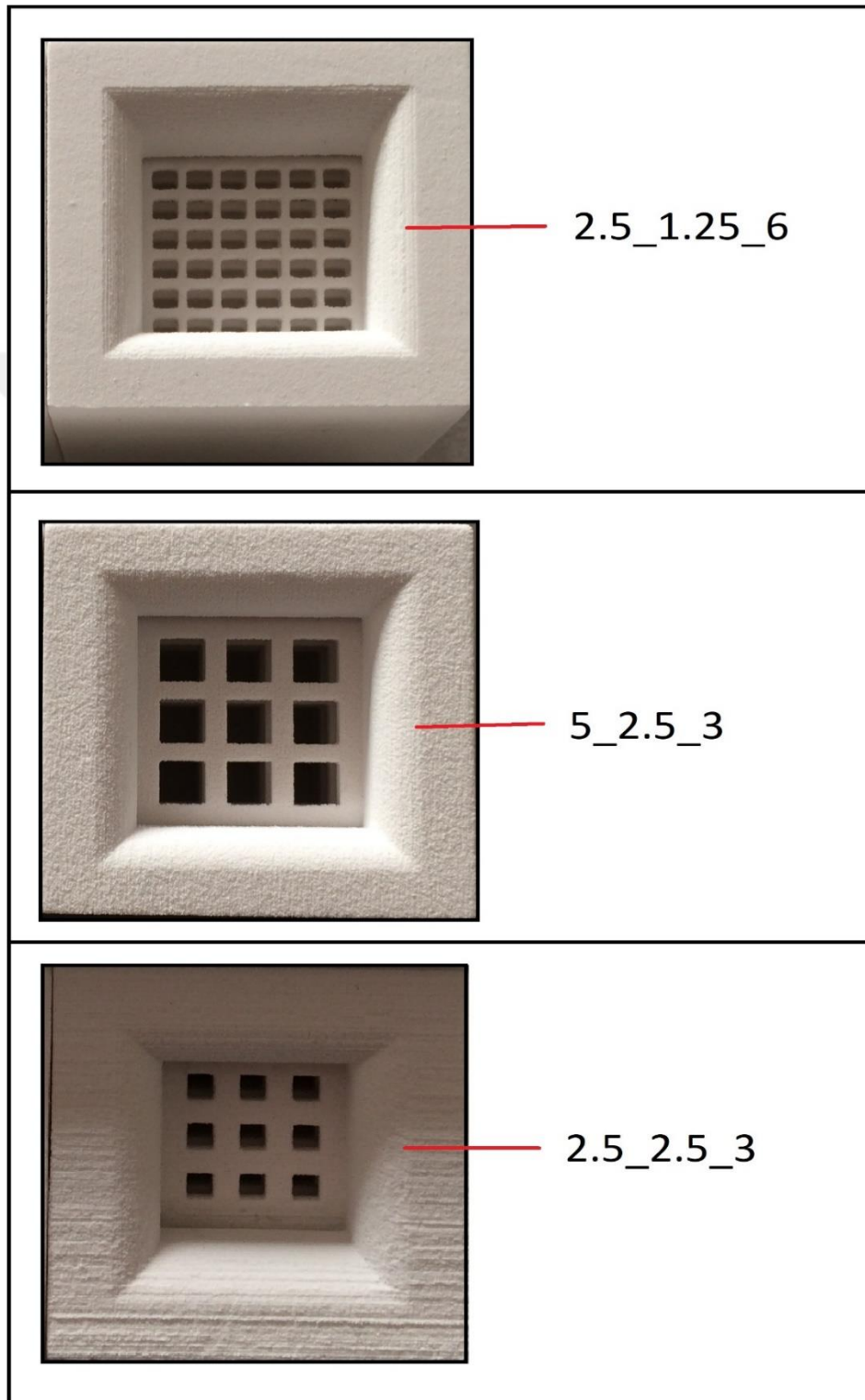


**Figure 6.6.** Schematic representation of the sample geometries.

### 6.2.2. Heat treatment

The produced molds were put into the heat treatment furnace. First, the temperature was set at 300 °C. This process was followed by 500 and 700 °C, respectively. After removing the molds from the furnace, they were left to cool at room temperature. Images of the groups after heat treatment are given in Figures 6.7, 6.8, 6.9, respectively.

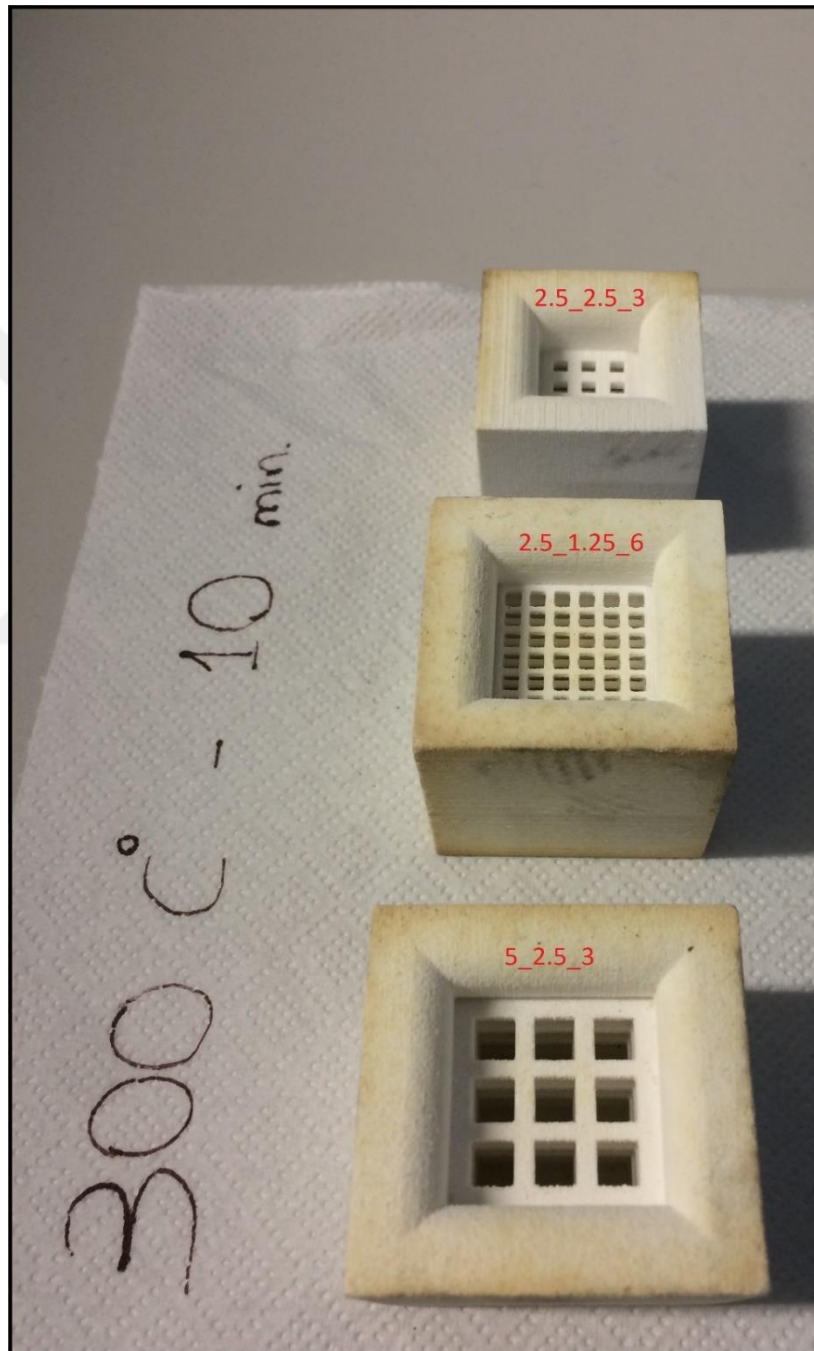


**Figure 6.7.** Depiction of the first test group of geometries after heat treatment.

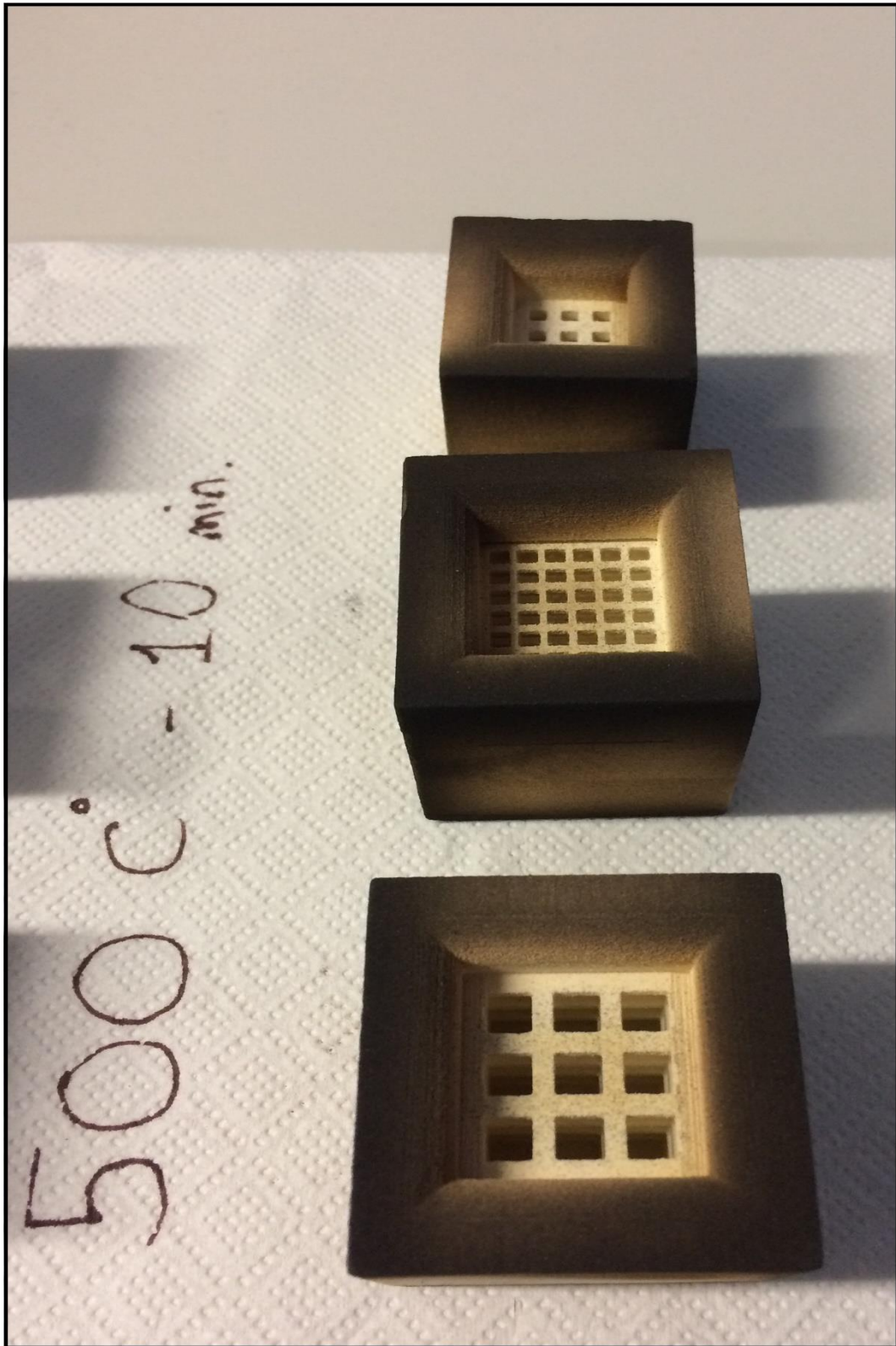


**Figure 6.8.** Depiction of the second test group of geometries after heat treatment.

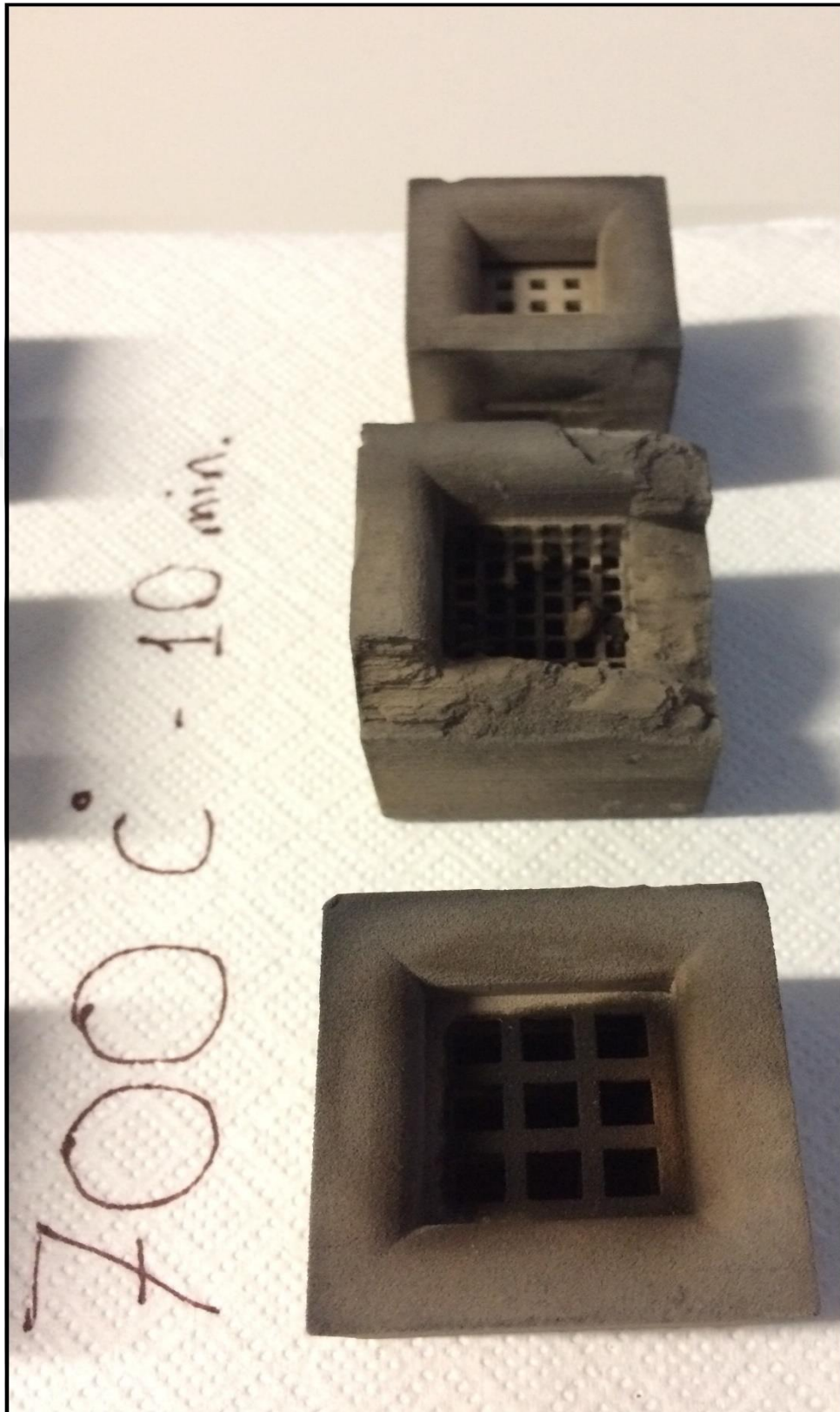


**Figure 6.9.** Depiction of the third test group of geometries after heat treatment.

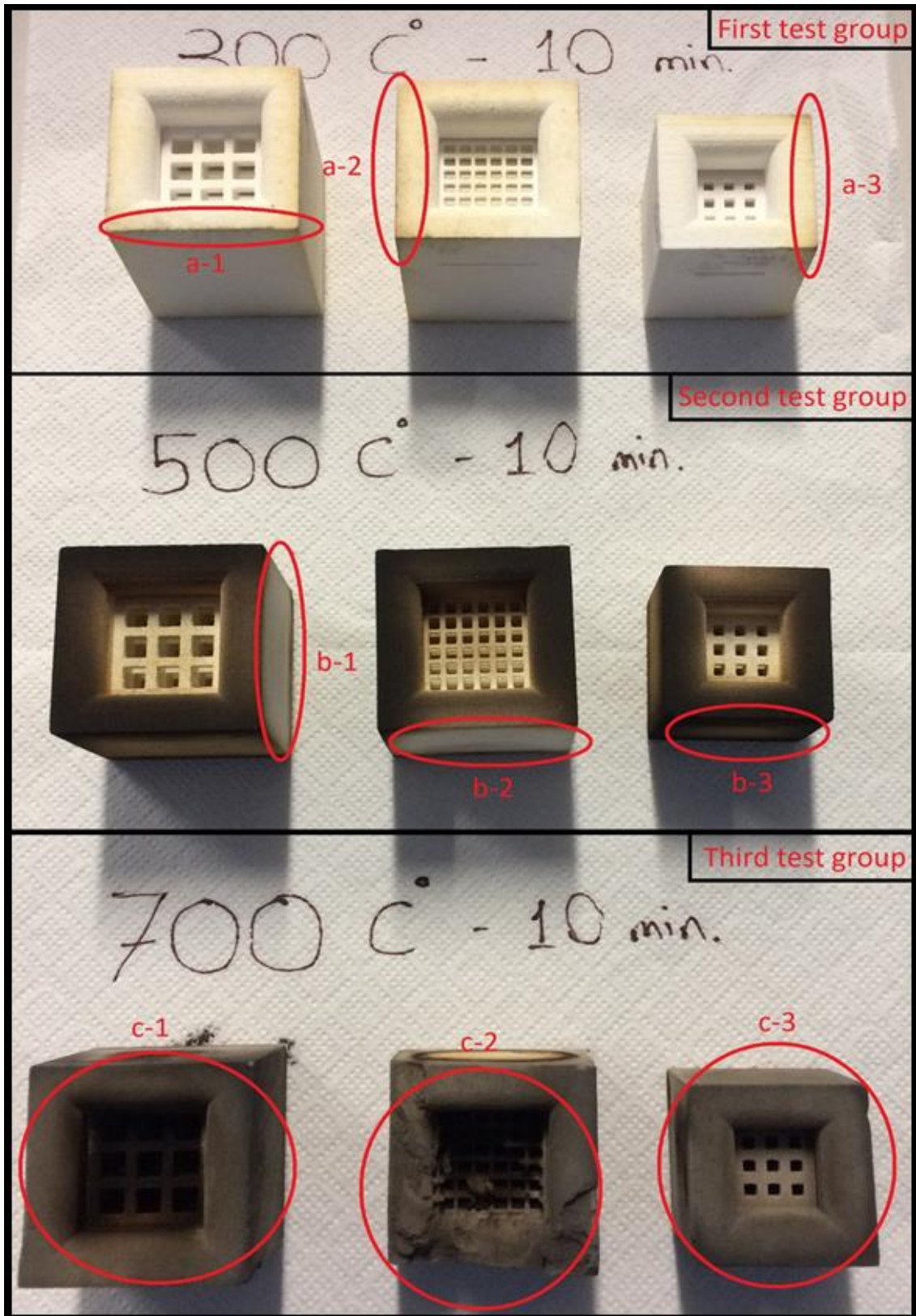


**Figure 6.10.** A comparison of the temperature test results of each group.

General observations of the temperature test were given in Table 6.1.

**Table 6.1.** General observations of the temperature tests.

#test results	First test group	Second test group	Third test group
Test settings	– 300 °C – 10 minutes	– 500 °C – 10 minutes	– 700 °C – 10 minutes
Level of fumes	Less	Middle	High
Mold durability	High	High	Poor
Level of color change	The color of molds transformed into a little bit brown in which at the point of junctions of corners.	Starting from the corners where black tones, it turned to brown towards the middle of the surfaces.	The color of molds transformed into a tone of black in every region.
General results	<ul style="list-style-type: none"> <li>– It is observed that the color change started from the corners.</li> <li>– It is also observed that the fumes come out from the molds during the temperature tests as we expected.</li> </ul>		

### 6.2.3. Silicone rubber casting

After the heat treatment test, silicone rubber casting performed to check the durability of the molds during the part-removal process from the molds. It was aimed to obtain a mold structure with a brittle phase but, at the same time, a structure that has the durability to resist the first impact of the molten aluminum casting. A comparison of the molds after casting was given in Figure 6.11.

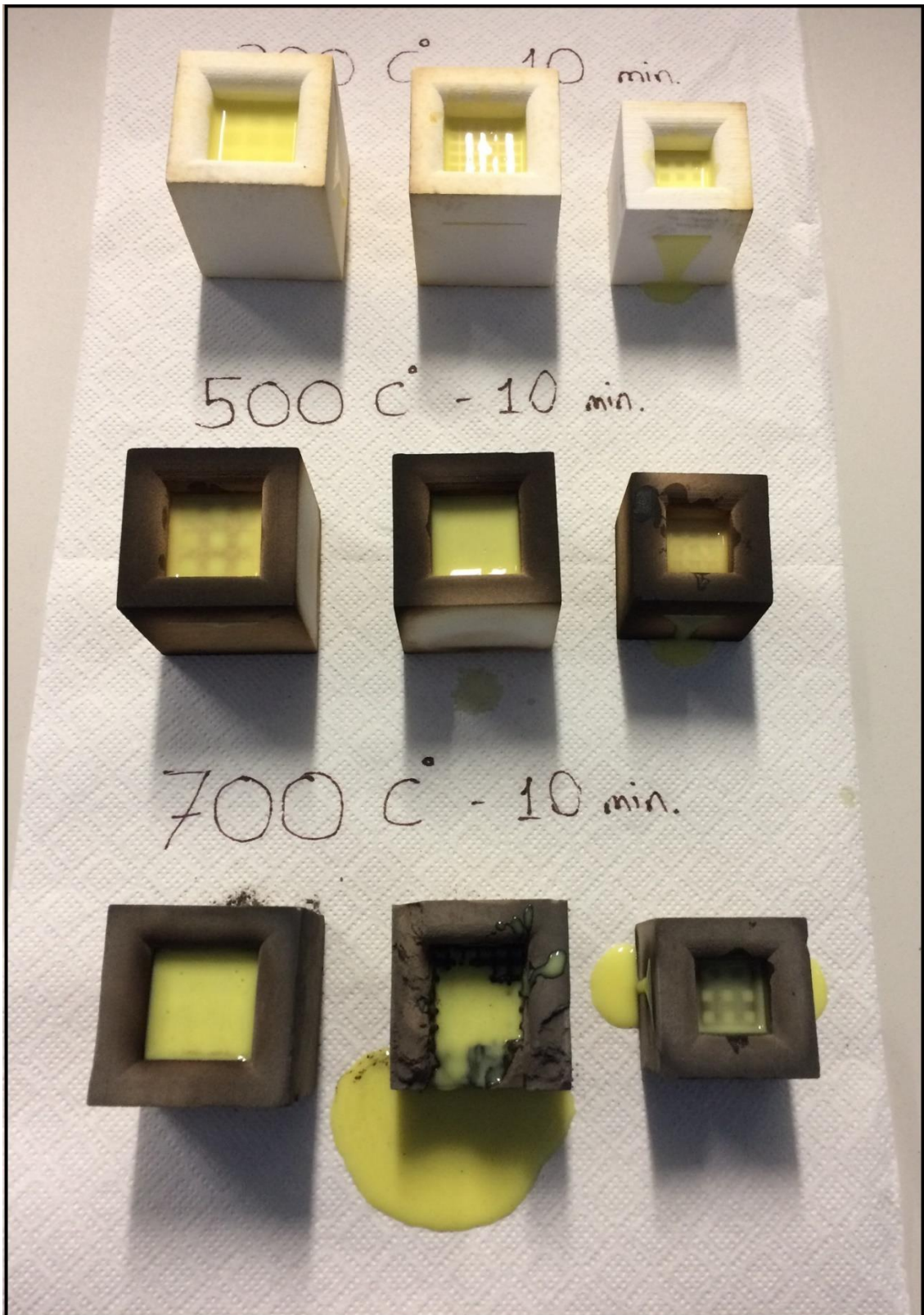


**Figure 6.11.** The representation of the molds after silicone rubber casting.

#### 6.2.4. Results of the temperature test

After silicone rubber casting, the molds were destroyed, and visual inspection carried out. Removed silicone lattice structures were illustrated in Figure 6.12.

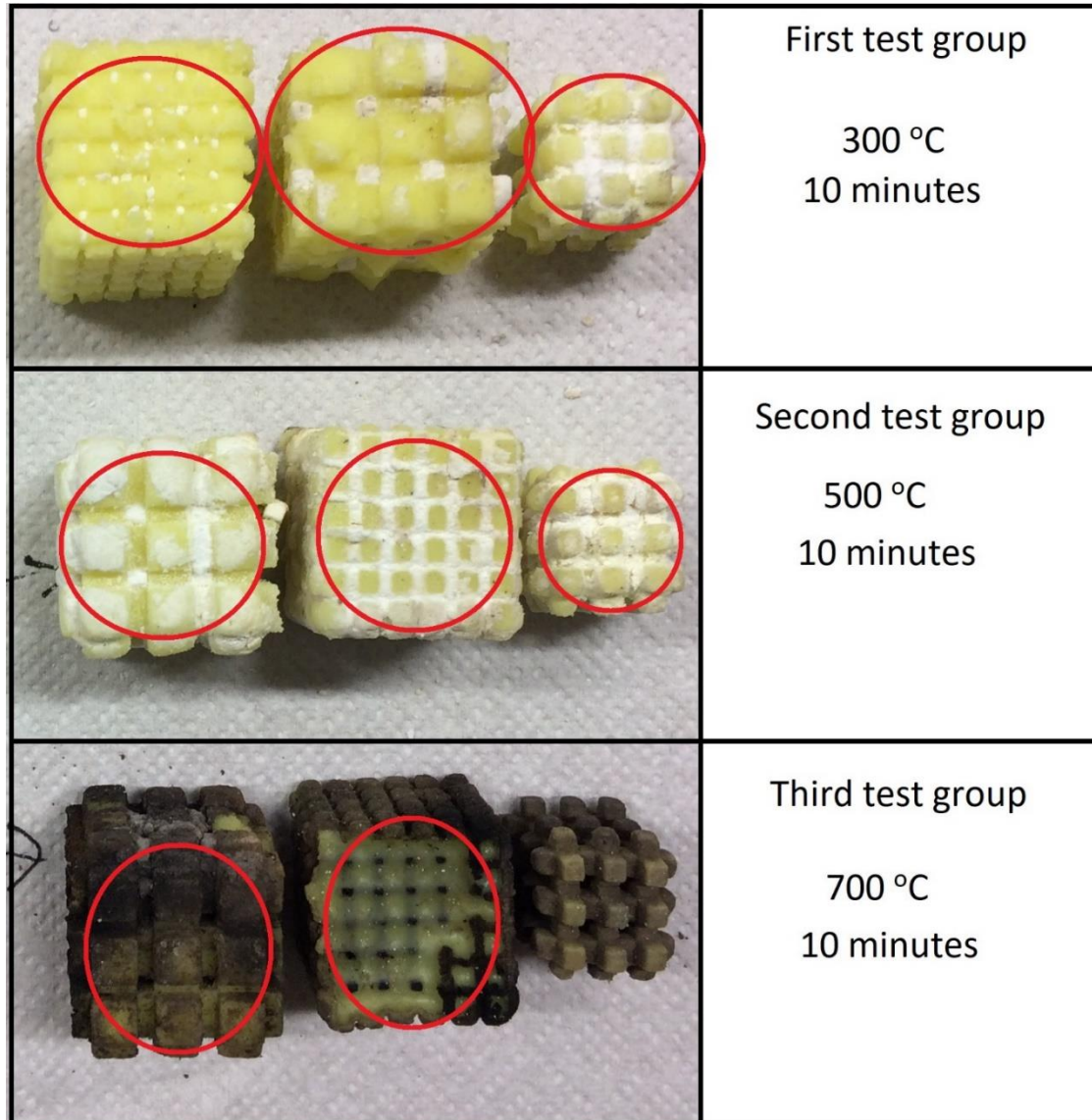


**Figure 6.12.** Depiction of the extracted parts from the molds.

The results of the first test group showed that after the heat treatment test, the mold durability became slightly softer when the molds take out from a water-filled box. This softness comment observed during the disintegration of the molds was obtained by comparing it with the mold disintegration made in the mold cavity verification test. The difference between the two part-removal processes is the heat treatment test. As can be seen in Figure 6.12, it is still difficult to remove powder from the inner regions of the

parts.

The results of the second test group were somewhat surprising compared to the results of the first test group. In this test group, more binder evaporation was observed during the temperature test compared to the first test group as expected. As a result, the fragility in the structure was expected to be higher. However, it was observed that the mold resistance was almost equal with the first test group during the removal of the parts from the molds. Nevertheless, the difficulty in removing parts was more comfortable than removing the part in the mold cavity verification test.

The parts were extracted from the molds easily. It is because of the binder evaporation was quite high when compared to the previous two test groups. Nevertheless, it is essential to mention that the durability of the molds before casting was typical. The test sample of c-2 presented in Figure 6.10 was looking like it damaged because of the less mold durability, but it was just a drop error that happens accidentally by the operator. It can be said that removing powder from the inner regions of the parts is more relaxed in this test group than the previous ones.

As a result of the heat treatment test, it is decided to apply the second test parameters in the real heat treatment test.

### **6.3. Aluminum Casting**

The molds of geometries selected for the casting process were produced. It is illustrated in Figure 5.15. After the production of the molds, the heat treatment was performed with selected parameters according to the results of the heat-treated demo molds. Then aluminum casting was performed.

#### **6.3.1. Casting process**

The casting process has conventionally been carried out with the help of gravity. Images of cast molds are given in Figure 6.13, 6.14, 6.15, 6.16, respectively.

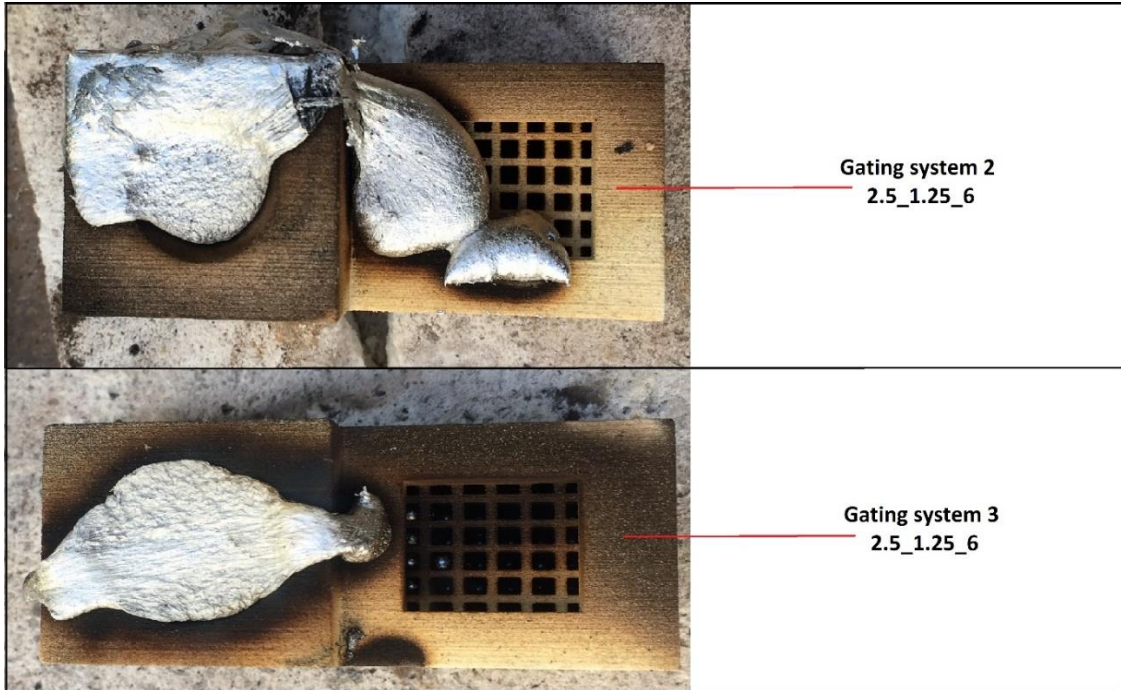


**Figure 6.13.** The illustration of the cast molds of the geometry 2.5\_1.25\_6 combined with gating systems 2 and 3.

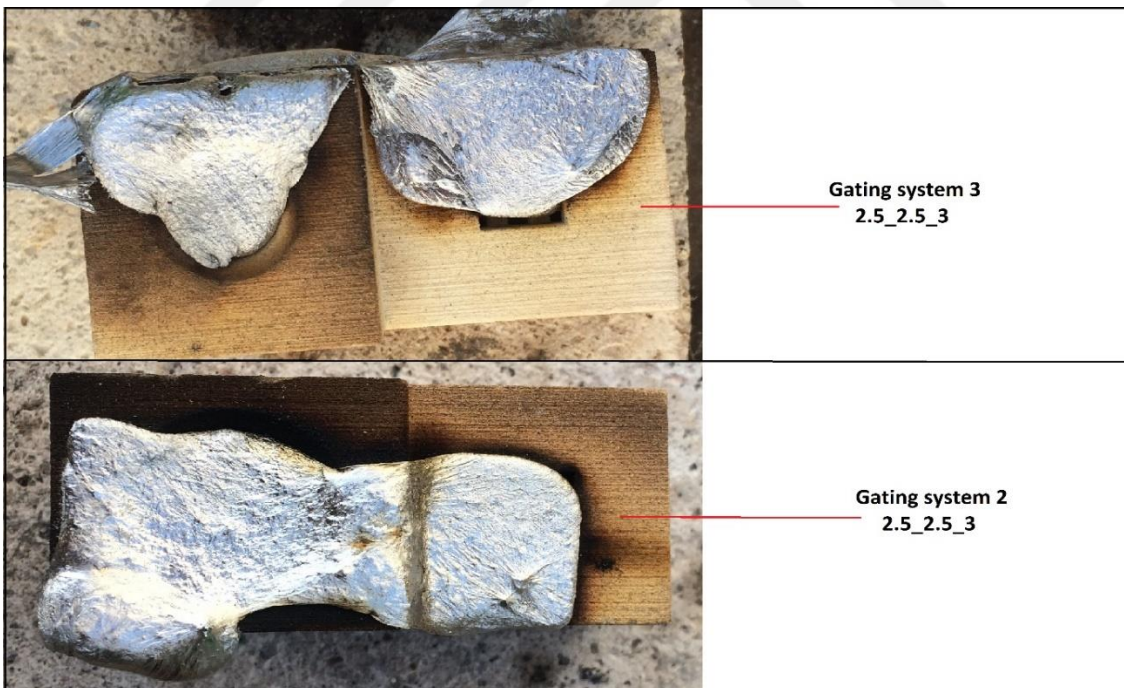


**Figure 6.14.** The illustration of the cast molds of the geometry 2.5\_2.5\_3 combined with gating systems 2 and 3.



**Figure 6.15.** The illustration of the cast molds of the geometry 5\_2.5\_3 combined with gating systems 2 and 3.

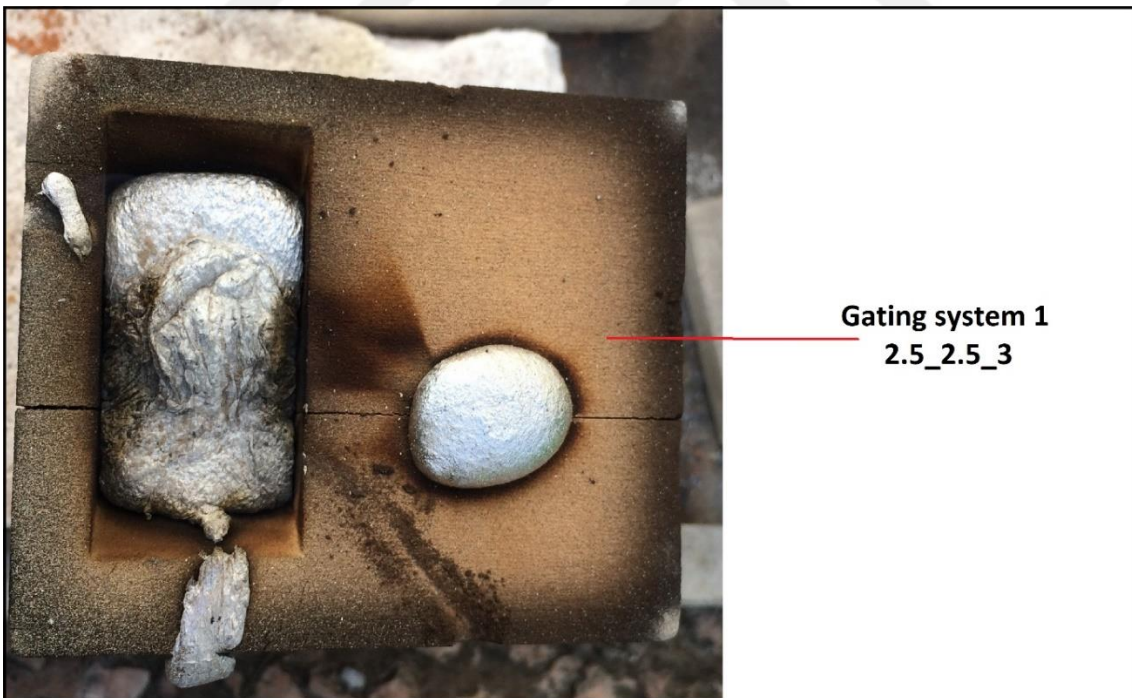


**Figure 6.16.** The illustration of the casting mold of the geometry 2.5\_2.5\_3 combined with gating system 1.



**Figure 6.17.** Schematic representation of the part-removal process of the geometry of 2.5\_1.25\_6 integrated with the gating system 2.

### **6.3.2. Results of the aluminum casting**

It is essential to mention that the molds were destroyed smoothly, as illustrated in Figure 6.17. It is because of the impact of the molten aluminum on the molds and immersing the molds in water. During the filling of the molten aluminum into the molds, some binder evaporation observed as expected because of the heat impact. It posed the more brittle mold structure. During casting, no explosion, cracking was observed in the molds. It is also known the immersing process of the molds into the water-filled container caused the change in the microstructure of the casted parts, but it is not one of the research fields of this study. So, it is ignored. An image of the 5\_2.5\_3 lattice structure integrated with the gating system 3 was given in Figure 6.18.

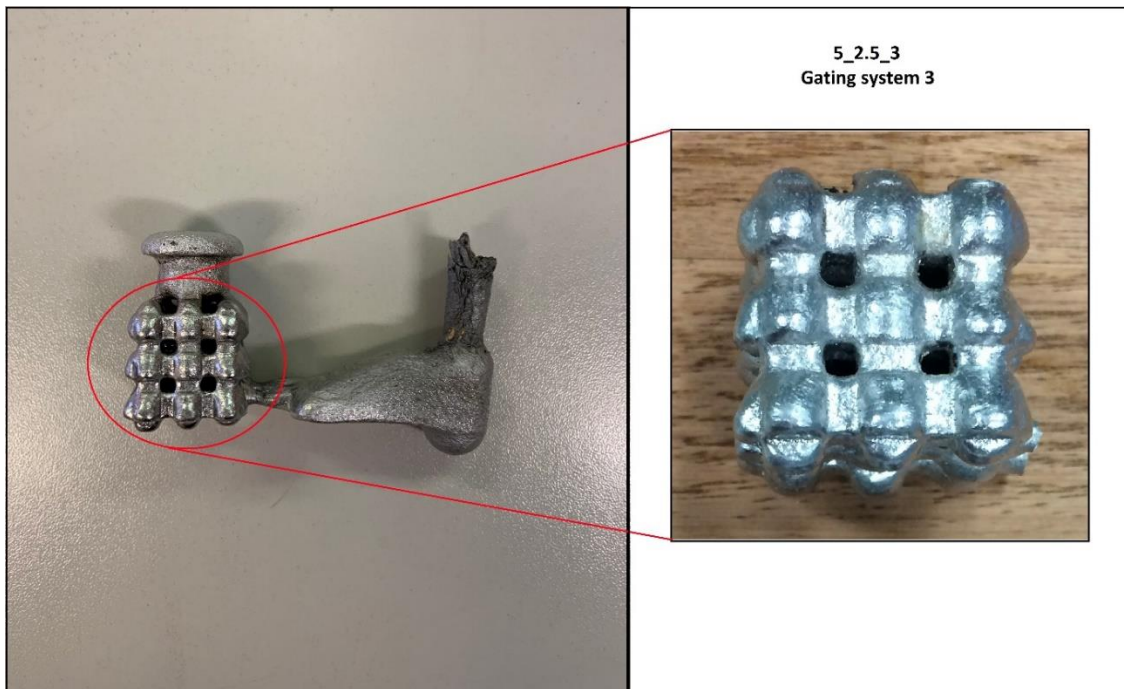


**Figure 6.18.** An illustration of the extracted 5\_2.5\_3 lattice structure integrated with gating system 3.

As can be seen from Figure 6.18, the mold filled. The performance of the gating system 3 was satisfying. However, filling in sharp corners was insufficient. The reason for this may be possible turbulence that may occur in sharp corners. The problem of air trapped could be another reason for this filling defect.

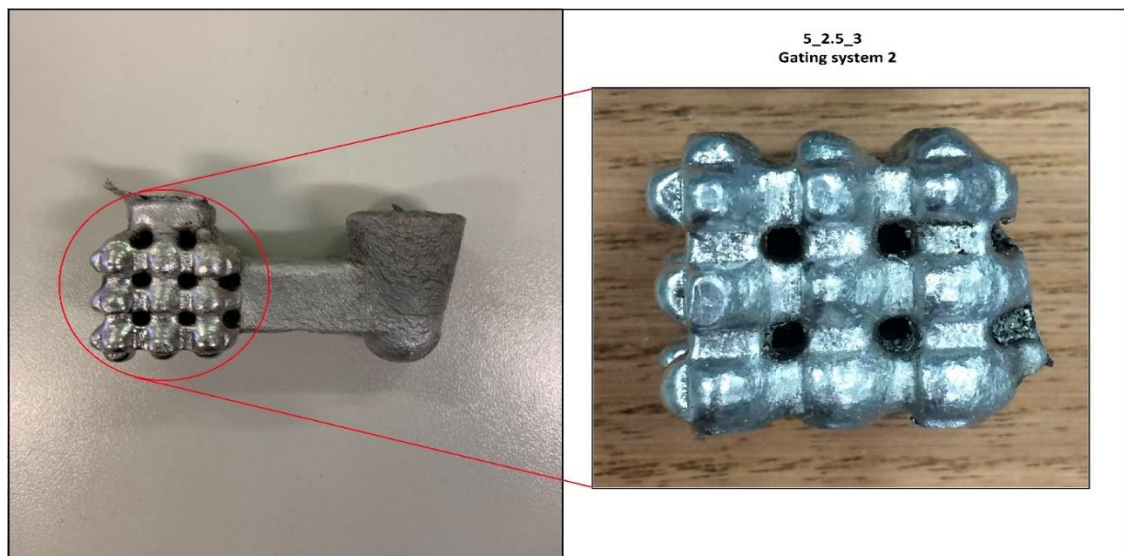


**Figure 6.19.** An illustration of the extracted 5\_2.5\_3 lattice structure integrated with gating system 2.

The fill rate of the part shown in Figure 6.19 was observed to be almost the same as the part shown in Figure 6.18. The difference between them was the gating systems used. The problem of filling the sharp corners was observed, just like it happens in the previous figure. As a result, it has been observed that the lattice structure of 5\_2.5\_3 was obtained, regardless of the gating system used.

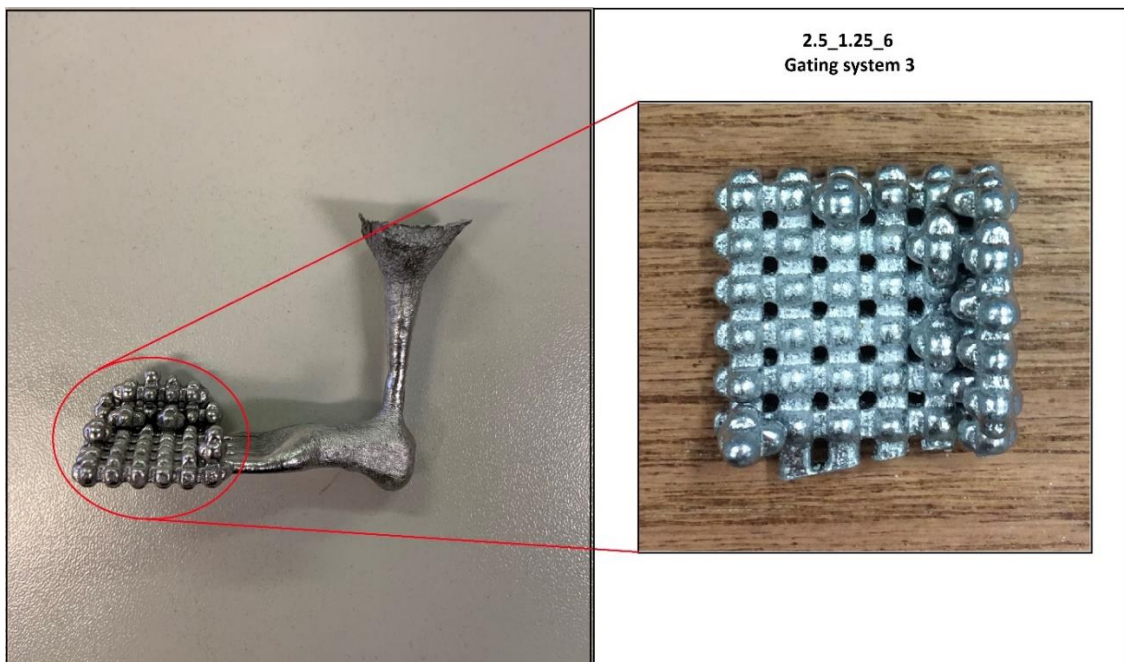


**Figure 6.20.** An illustration of the extracted 2.5\_1.25\_6 lattice structure integrated with gating system 3.

As can be seen from Figure 6.20, the lattice structure of 2.5\_1.25\_6 was not fill up by the gating system entirely. When this situation is evaluated independently of the results of the other parts, two possible causes emerge. First, the solidification rate was quite high. So, the molten metal could not have enough time to fill up the mold. Second, the gating system could not well design. Nevertheless, if we compare the result with the result of 5\_2.5\_3 illustrated in Figure 6.18, it is clear that the solidification problem is not related to the design of the gating system. Although both (Fig 6.18 and Fig 6.20) employed the same gating system, only one of them resulted in success. This failure results from the complexity of the lattice structure, as shown in Figure 6.20.

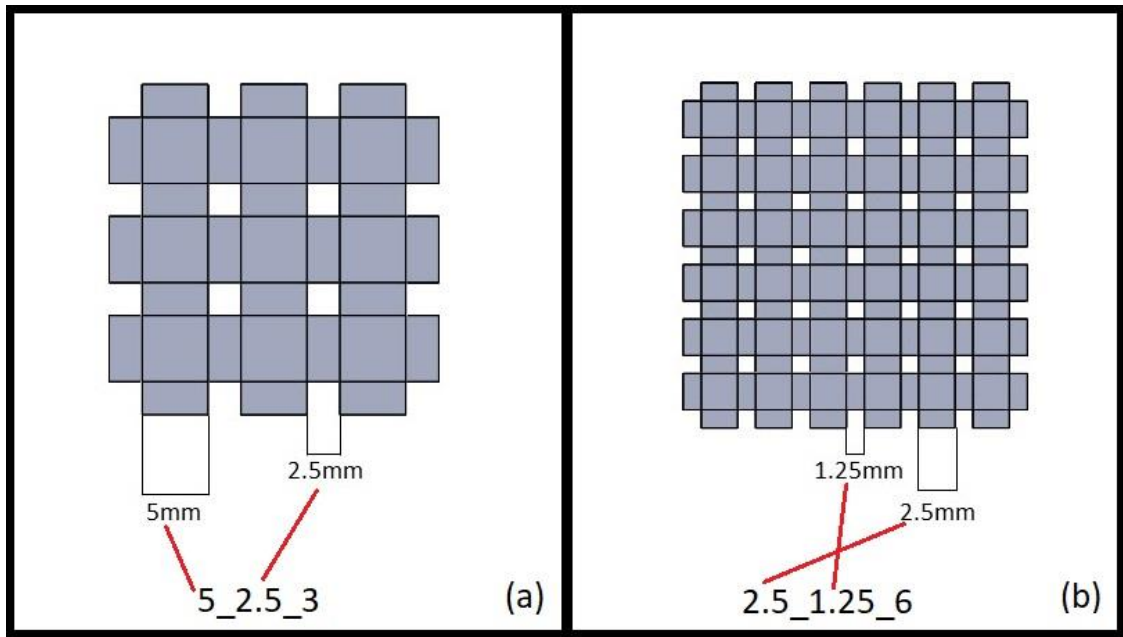


**Figure 6.21.** A comparison between geometries of 5\_2.5\_3 and 2.5\_1.25\_6.

The complexity of the geometry illustrated in (a) in Figure 6.21 has lower than the other one where shows in (b) the same figure. The thickness of the elements and void among them is higher. As a result, it has been revealed that the mold filling problem is associated with the complexity of the lattice structure.

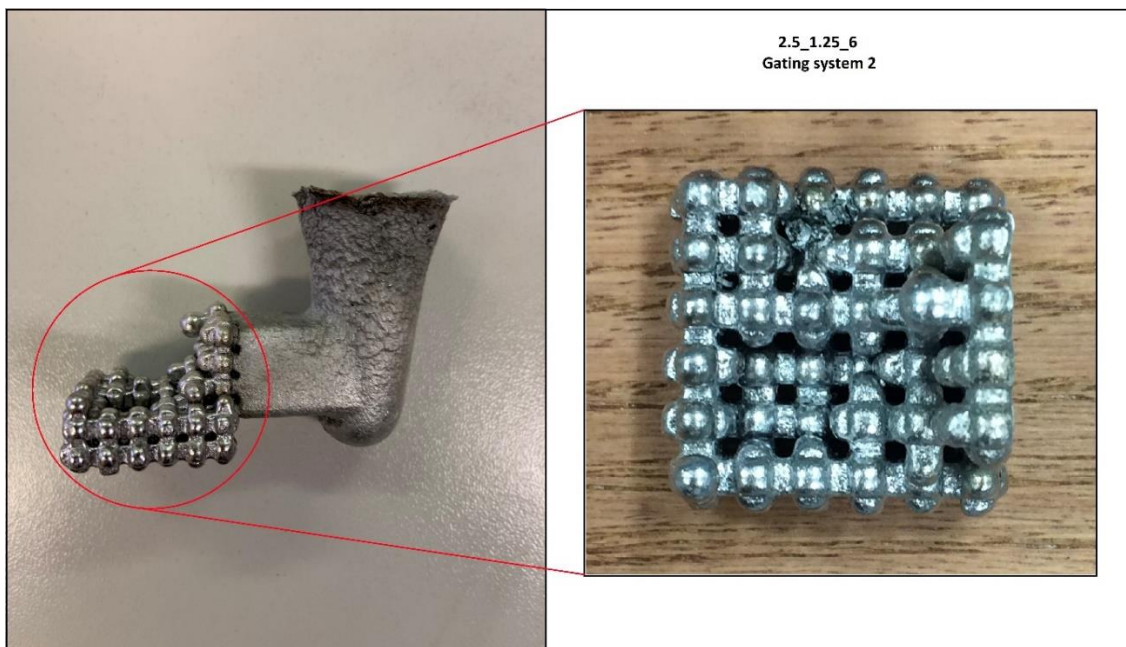


**Figure 6.22.** An illustration of the extracted 2.5\_1.25\_6 lattice structure integrated with gating system 2.

As can be seen in Figure 6.22, the fast solidification problem was also seen in this casting

process. Compared with Figure 6.20, it has been proven that the filling problem of the mold is related to the design complexity, not the gating system used. Nonetheless, as it is illustrated in Figure 6.23, the filling performance of the gating system 2 is better than the gating system 3.

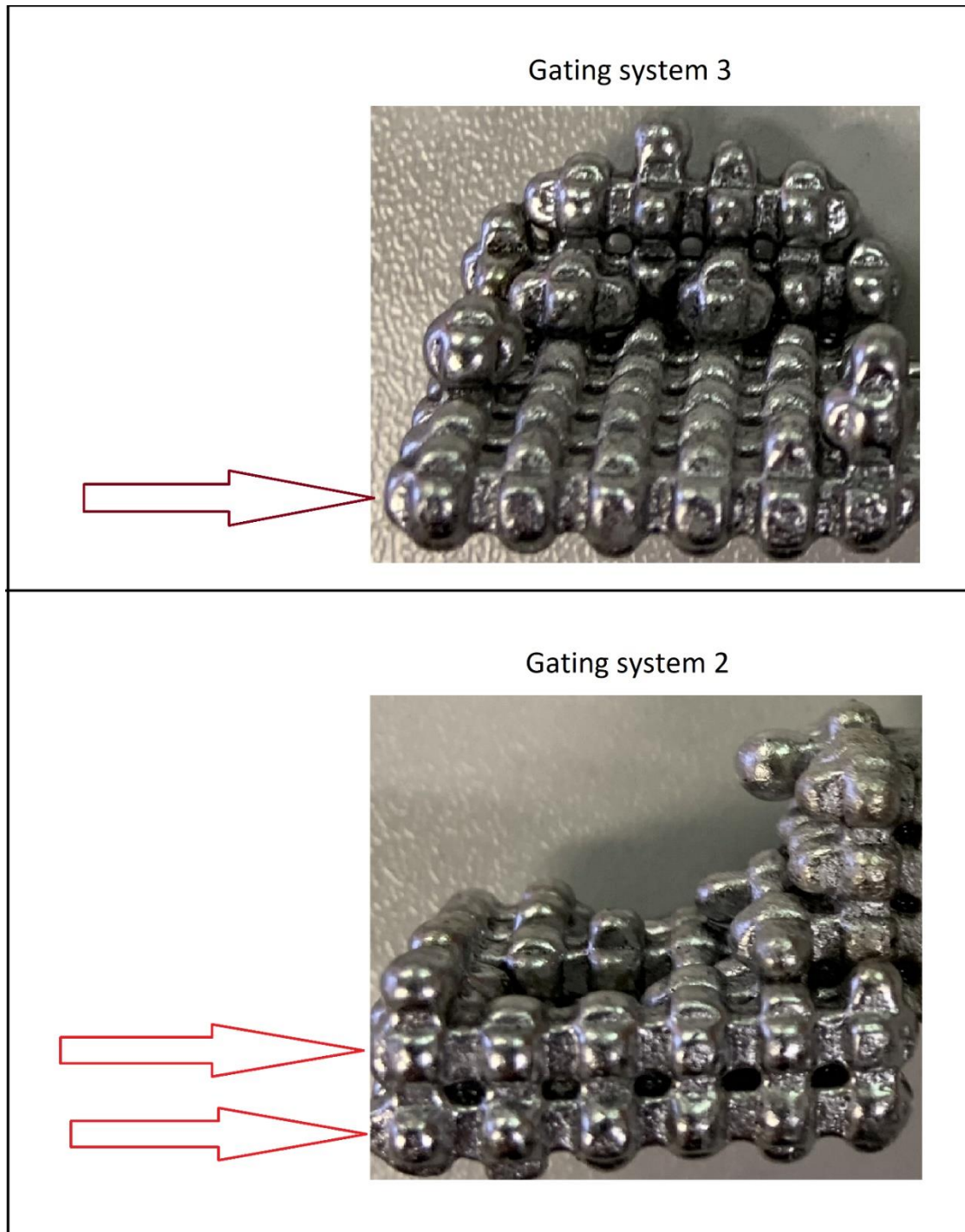


**Figure 6.23.** Comparison of the filling performance of the gating systems.

As shown in Figure 6.23, almost two layers were filled by the gating system 2, while just one layer was filled by the gating system 3. Rapid solidification was also observed in Figures 6.24, 6.25, 6.26.



**Figure 6.24.** An illustration of the extracted 2.5\_2.5\_3 lattice structure integrated with gating system 3.

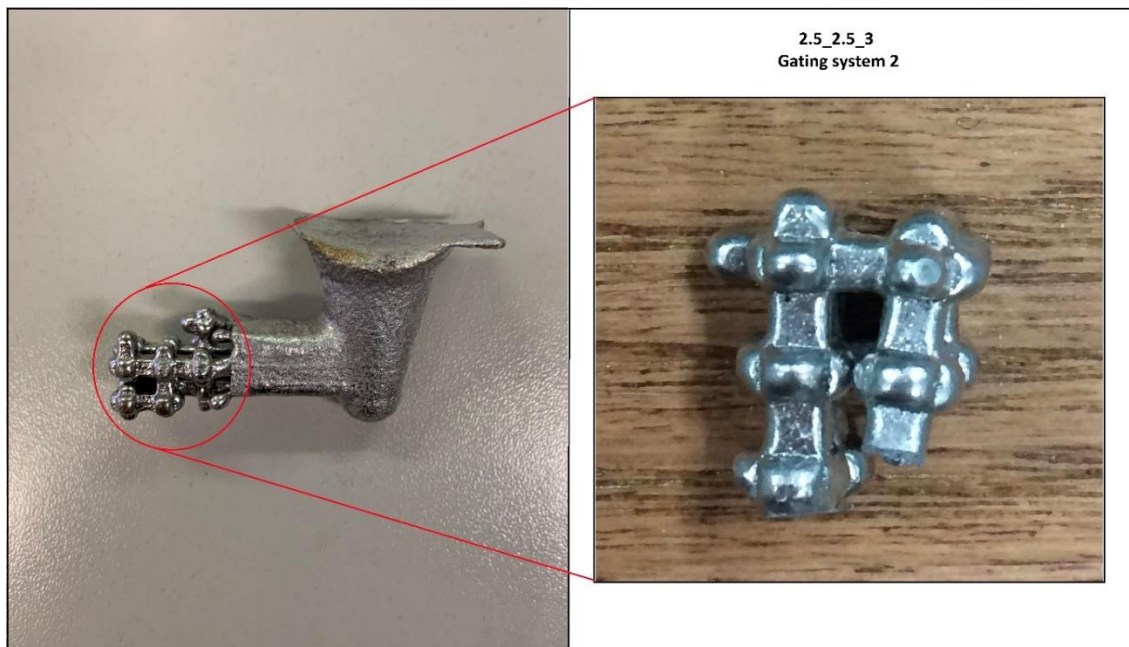


**Figure 6.25.** An illustration of the extracted 2.5\_2.5\_3 lattice structure integrated with gating system 2.



**Figure 6.26.** An illustration of the extracted 2.5\_2.5\_3 lattice structure integrated with gating system 1.

In Figure 6.26, the gating system was designed to fill the mold quickly. However, due to the high speed, the hot metal has reached the surface and solidified without being able to penetrate the internal regions of the lattice structure.

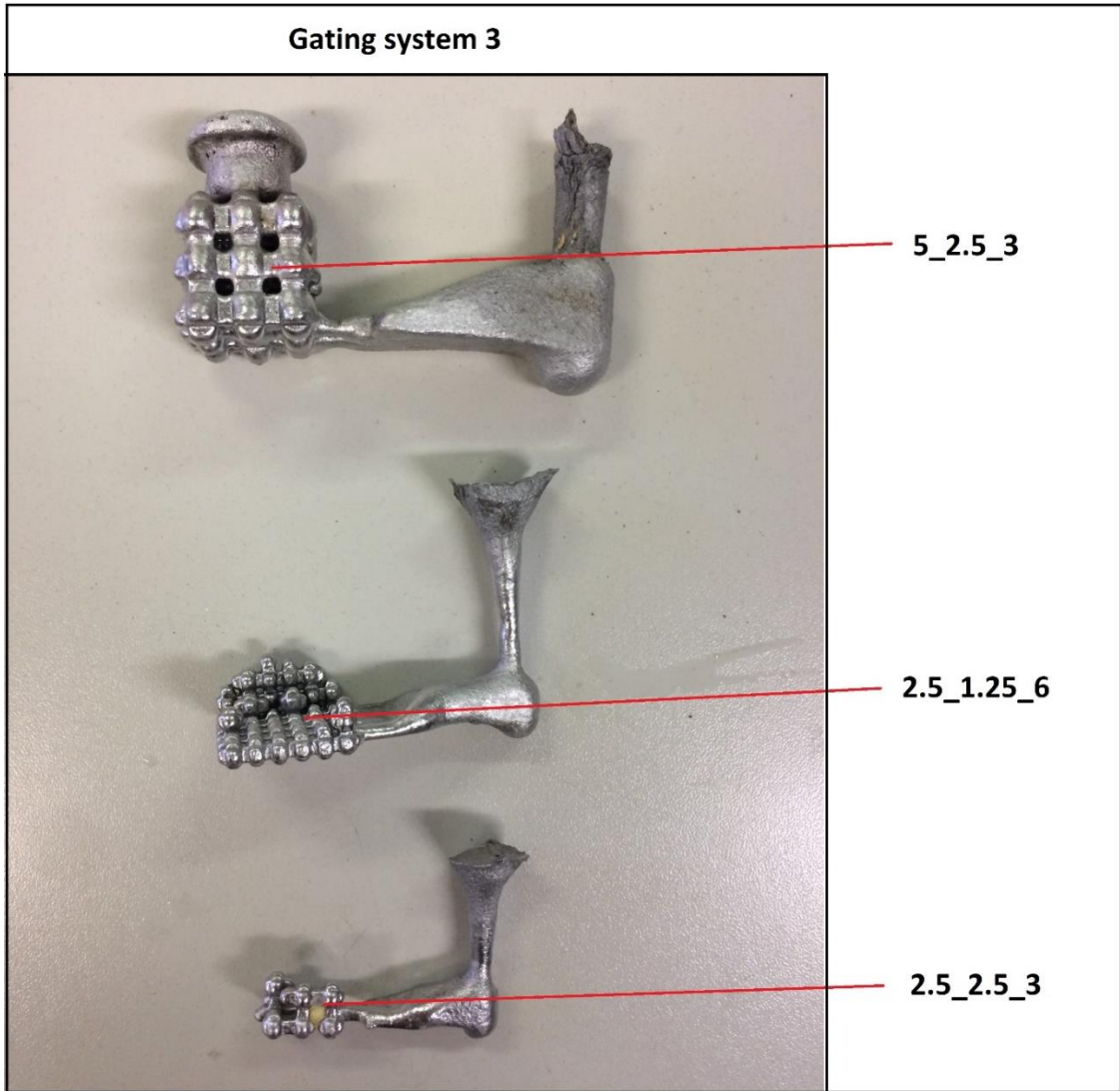


**Figure 6.27.** A comparison of the extracted parts integrated with gating system 3.

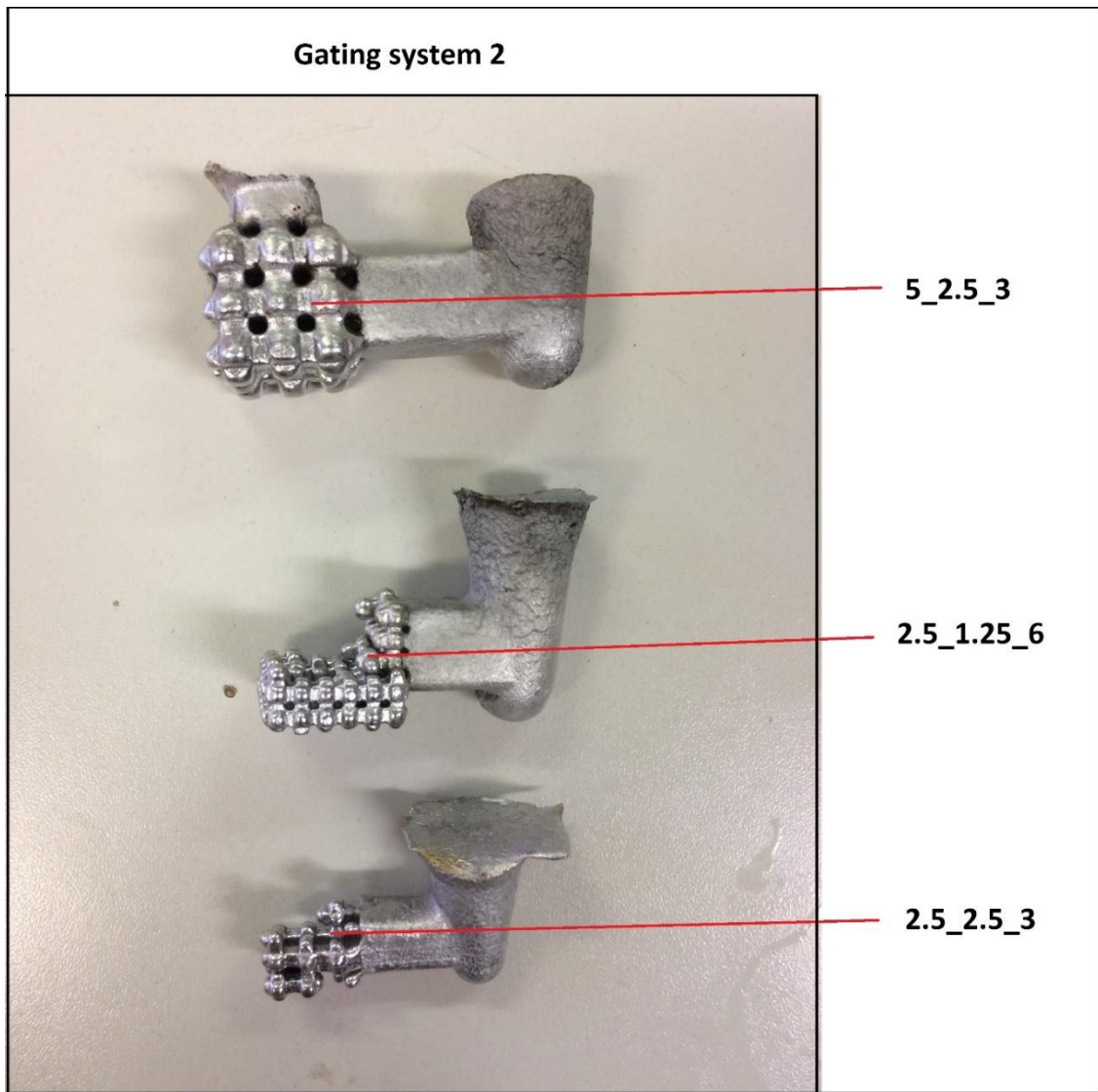


**Figure 6.28.** A comparison of the extracted parts integrated with gating system 2.

As can be seen from figure 5.27 and 5.28, the filling performance of the gating systems 2 and 3 only worked with the geometry of 5\_2.5\_3.

As a result, it is important to note that the presence of sharp corners inside the mold has influenced the filling performance. To overcome this problem, a new design approach was realized. In this experiment, only the component geometry of 5\_2.5\_3 was chosen because of its satisfactory performance in the previous experiments. Gating system 3 was chosen for the casting process. The mold was just produced one time. To follow the same path with the previous samples, heat treatment of the mold was performed at 500 °C along 10 minutes.

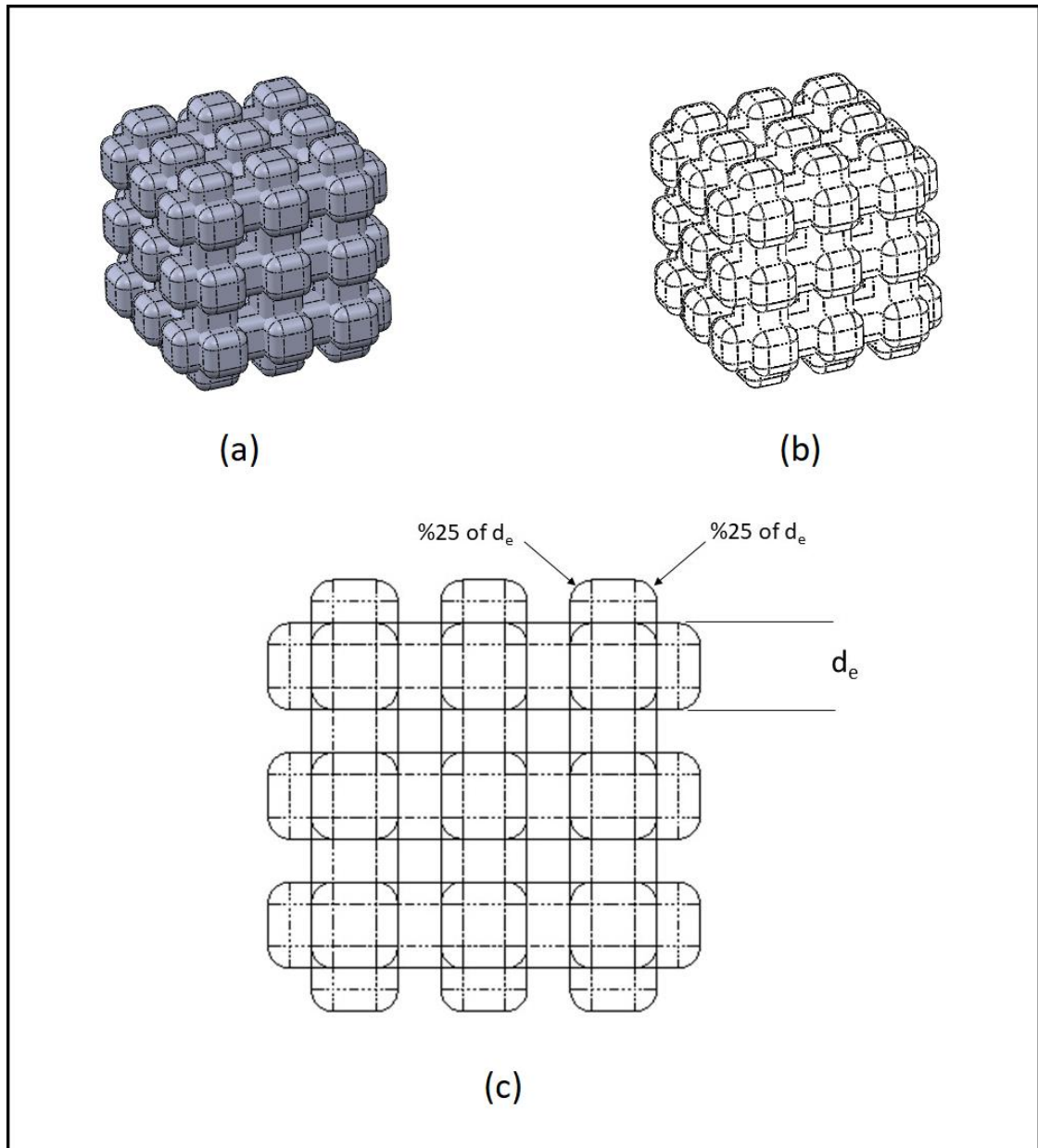


**Figure 6.29.** Depiction of the new design strategy of sample geometry of 5\_2.5\_3. Where (a) and (b) shows the actual and transparent view of the lattice structure respectively. Where (c) shows the detail of the new design strategy.

As it is illustrated in Figure 6.29, sharp corners of the lattice structure have been redesigned by reducing a radius of equal to 25% of  $d_e$ .

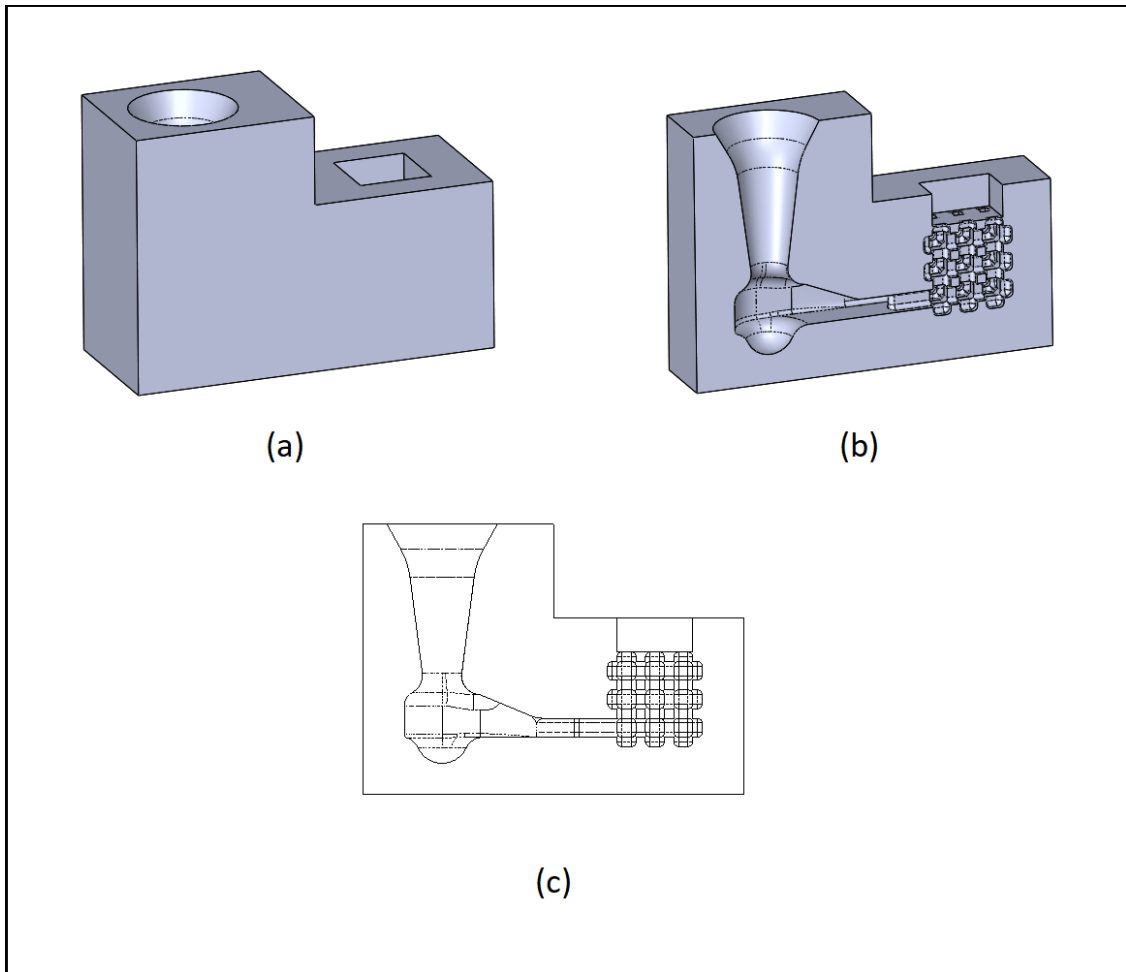


**Figure 6.30.** Representation of the mold from different aspects. Where (a) shows the actual view of the mold, (b) illustrates the mold cut in half by employing a feature of Solidworks, and (c) shows the front view of the mold as transparent.

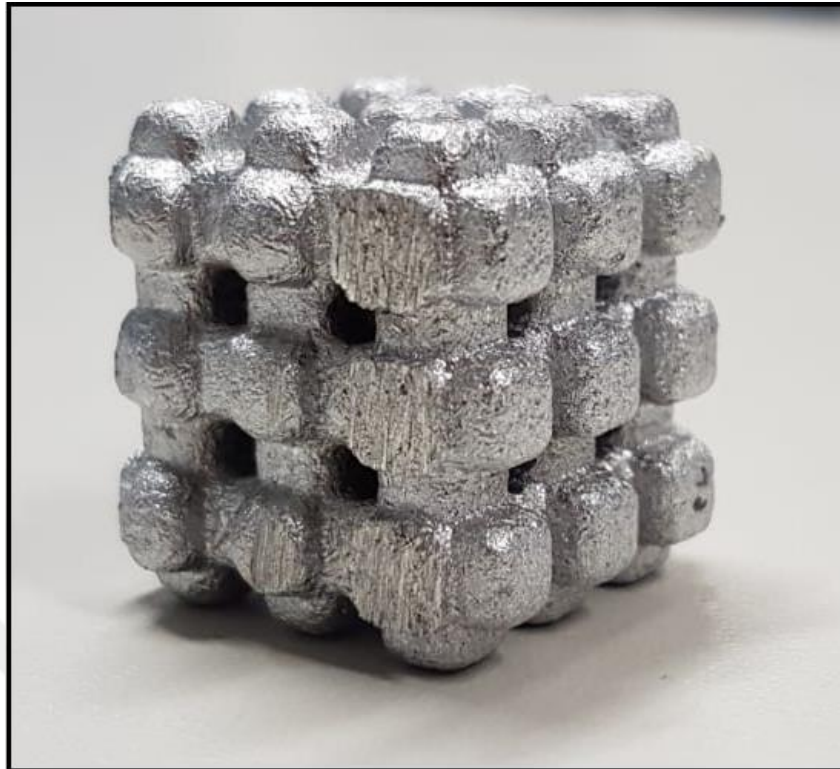


**Figure 6.31.** An illustration of the lattice structure of 5\_2.5\_3 after casting performed.



**Figure 6.32.** An image of the lattice structure of 5\_2.5\_3.

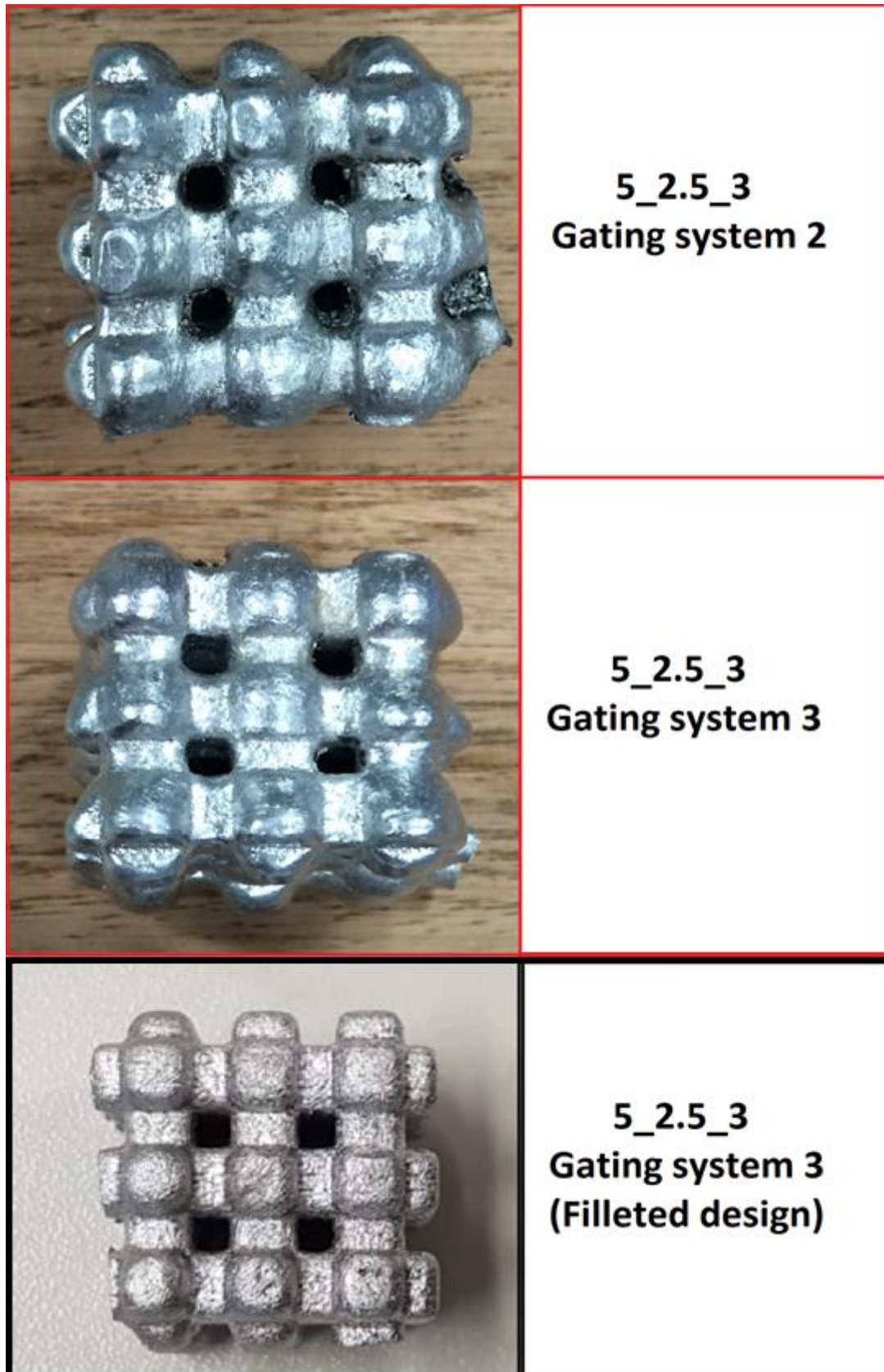


**Figure 6.33.** A comparison of the 5\_2.5\_3 sample results.

As can be seen in Figure 6.33, it has been observed that the filling performance is improved when the results of the two previous geometries are compared with the filleted design. It was seen that the surface quality improved in parallel with the increased filling performance.



## 7. CONCLUSIONS

By employing the Binder Jetting technology to produce complex parts is essential for the future of the casting industry because of its remarkable benefits when benchmarked against other Additive Manufacturing methods. However, the molds produced with this technology have been used in the experimental studies of simple parts up to today. Although, understandably, these pioneering studies shed light on future studies, it has caused missing information in today's literature. Briefly, the Binder Jetting technology has not been individually tested on the production of complex parts that the industry needs. In this master's thesis, utilizing this technology, the molds needed to obtain complex parts were produced, and satisfactory results were obtained by making an aluminum casting.

As stated previously, experiments show that designed components and runner systems were combined in a digital environment then produced without any problem. In addition to the eight complex shaped components that have been designed, taking into account three crucial critical parameters, three different runner systems are realized. The results also showed that a complex lattice structure could be achieved utilizing two different runner systems. The temperature test led to increased mold fragility as expected, facilitating the post-casting part removal process. Finally, some critical design parameters have been obtained to remove loose powder from produce molds then for a defect-less casting that could affect the filling process.

Nonetheless, in future studies, to obtain a casted part, which has more surface precise, quality, and filling rate, the sharpness of inner regions of the mold should reduce as much as possible. Also, to avoid problems such as turbulence and hot-point, more exit strategies should be generated. Simulation programs could be useful to have a piece of knowledge before casting performed. It is also worthy that keeping the molds inside the heat treatment furnace for a longer time by lowering the temperature may provide more convenience after the casting process to remove parts.

## 8. REFERENCES

- [1] Sama, S. R., Wang, J., & Manogharan, G. (2018). Non-conventional mold design for metal casting using 3D sand-printing. *Journal of Manufacturing Processes*, 34(01), 765–775.
- [2] Hodder, K. J., & Chalaturnyk, R. J. (2019). Bridging additive manufacturing and sand casting: Utilizing foundry sand. *Additive Manufacturing*, 28(06), 649–660.
- [3] Voigt, R., & Manogharan, G. (2018). 3D Printed Sand Molds-An Opportunity for Investment Casters. The 65<sup>th</sup> Annual ICI Technical Conference, October 21-24, Kansas City, USA.
- [4] Strano, G., Hao, L., Everson, R. M., & Evans, K. E. (2013). A new approach to the design and optimisation of support structures in additive manufacturing. *International Journal of Advanced Manufacturing Technology*, 66(9–12), 1247–1254.
- [5] Ziaee, M., & Crane, N. B. (2019). Binder jetting: A review of process, materials, and methods. *Additive Manufacturing*, 28(12), 781–801.
- [6] Snelling, D. A., Williams, C. B., & Druschitz, A. P. (2019). Mechanical and material properties of castings produced via 3D printed molds. *Additive Manufacturing*, 27(03), 199–207.
- [7] Hull, C. W., Arcadia, & Calif. (1984). Apparatus for Production of Three Dimensional Objects by Stereolithography, United States Patent (19), 16.
- [8] R. Baker. (1925). Method of making decorative articles. US Patent, 1–3.
- [9] Guo, N., & Leu, M. C. (2013). Additive manufacturing: Technology, applications and research needs. *Frontiers of Mechanical Engineering*, 8(3), 215–243.
- [10] ASTM International. (2013). F2792-12a - Standard Terminology for Additive Manufacturing Technologies. Rapid Manufacturing Association, 10–12.
- [11] Zakeri, S., Vippola, M., & Levänen, E. (2020). A comprehensive review of the photopolymerization of ceramic resins used in stereolithography. *Additive Manufacturing*, 35(March), 101177.
- [12] Bhavar, V., Kattire, P., Patil, V., Khot, S., Gujar, K., & Singh, R. (2017). A review on powder bed fusion technology of metal additive manufacturing. *Additive Manufacturing Handbook: Product Development for the Defense Industry*, (April 2016), 251–261.
- [13] Hawaldar, N., & Zhang, J. (2018). A comparative study of fabrication of sand casting mold using additive manufacturing and conventional process. *International Journal of Advanced Manufacturing Technology*, 97(1–4), 1037–1045.
- [14] Cesarano, J. (1999). A review of robocasting technology. *Materials Research Society Symposium - Proceedings*, 542, 133–139.
- [15] Upadhyay, M., Sivarupan, T., & El Mansori, M. (2017). 3D printing for rapid sand casting—A review. *Journal of Manufacturing Processes*, 29, 211–220.

- [16] Gonzalez-Gutierrez, J., Cano, S., Schuschnigg, S., Kukla, C., Sapkota, J., & Holzer, C. (2018). Additive manufacturing of metallic and ceramic components by the material extrusion of highly-filled polymers: A review and future perspectives. *Materials*, 11(5).
- [17] Fallon, J. J., McKnight, S. H., & Bortner, M. J. (2019). Highly loaded fiber filled polymers for material extrusion: A review of current understanding. *Additive Manufacturing*, 30(August), 100810.
- [18] Dass, A., & Moridi, A. (2019). State of the Art in Directed Energy Deposition: From Additive Manufacturing to Materials Design, Coatings, 29 June 2019, 1-26.
- [19] Kiran, A. S. K., Veluru, J. B., Merum, S., Doble, M., Kumar, T. S. S., & Ramakrishna, S. (2019). Additive manufacturing technologies : an overview of challenges and perspective of using electrospraying. *Nanocomposites*, 4(4), 190–214.
- [20] Calignano, F., Manfredi, D., Ambrosio, E. P., Biamino, S., Lombardi, M., Atzeni, E., Fino, P. (2017). Overview on additive manufacturing technologies. *Proceedings of the IEEE*, 105(4), 593–612.
- [21] Rosochowski, A., & Matuszak, A. (2000). Rapid tooling: the state of the art. *Journal of Materials Processing Technology*, 106, 191–198.
- [22] Lores, A., Azurmendi, N., Agote, I., & Zuza, E. (2019). A review on recent developments in binder jetting metal additive manufacturing: materials and process characteristics. *Powder Metallurgy*, 62(5), 267–296.
- [23] Celik, I., Karakoc, F., Cakir, M. C., & Duysak, A. (2013). Rapid Prototyping Technologies and Application Areas. *Journal of Science and Technology of Dumlupinar University*, 31(8), 53–70.
- [24] Additive Manufacturing / 3D Printing process flow in 7 steps. April 9, 2020, from <https://engineeringproductdesign.com/additive-manufacturing-process-steps/>
- [25] The Additive Manufacturing Process | 3D Hubs. April 9, 2020, from <https://www.3dhubs.com/knowledge-base/additive-manufacturing-process/>
- [26] 3D Printing STL files: A step-by-step guide | 3D Hubs. April 9, 2020, from <https://www.3dhubs.com/knowledge-base/3d-printing-stl-files-step-step-guide/>
- [27] Rashid, A. (2019). Additive Manufacturing Technologies. *CIRP Encyclopedia of Production Engineering*. Springer Berlin Heidelberg, Berlin, Heidelberg.
- [28] The CNC cost reduction checklist | 3D Hubs. April 5, 2020, from <https://www.3dhubs.com/get/cnc-cost-checklist/>
- [29] 3D printing trends 2020 | 3D Hubs. April 8, 2020, from <https://www.3dhubs.com/blog/3d-printing-trends-2020/>
- [30] The Additive Manufacturing Landscape 2019 [Whitepaper] - AMFG. May 1, 2020, from <https://amfg.ai/whitepaper-the-additive-manufacturing-landscape-2019/>

- [31] Murr, L. E., Gaytan, S. M., Ramirez, D. A., Martinez, E., Hernandez, J., Amato, K. N., Wicker, R. B. (2012). Metal Fabrication by Additive Manufacturing Using Laser and Electron Beam Melting Technologies. *Journal of Materials Science & Technology*, 28(1), 1–14.
- [32] Frazier, W. E. (2014). Metal additive manufacturing: A review. *Journal of Materials Engineering and Performance*, 23(6), 1917–1928.
- [33] Lewandowski, J. J., & Seifi, M. (2016). Metal Additive Manufacturing: A Review of Mechanical Properties. *Annual Review of Materials Research*, 46, 151–186.
- [34] EOS M 400-4 – the four-laser 3D printer for metals. May 3, 2020, from <https://www.eos.info/en/additive-manufacturing/3d-printing-metal/eos-metal-systems/eos-m-400-4>
- [35] DMP Factory 500 Solution - 3D Printer | 3D Systems. April 25, 2020, from <https://www.3dsystems.com/3d-printers/dmp-factory-500/>
- [36] SLM Solutions Group AG: SLM<sup>®</sup>800. April 17, 2020, from <https://www.slm-solutions.com/en/products/machines/slmr800/>
- [37] RenAM 500Q. May 3, 2020, from <https://www.renishaw.com/en/renam-500q--42781>
- [38] X Line 2000R | DMLM Machine & Metal 3D Printer| GE Additive. April 5, 2020, from <https://www.ge.com/additive/additive-manufacturing/machines/dmlm-machines/x-line-2000r>
- [39] Additive Industries - MetalFAB1 | Industrial 3D printer. June 11, 2020, from <https://www.additiveindustries.com/systems/metalfab1>
- [40] MYSINT100, Laser Metal Fusion metal 3D printing technology. May 5, 2020, from <https://www.sisma.com/en/products/mysint100/>
- [41] LASERTEC 30 DUAL SLM - ADDITIVE MANUFACTURING machines from DMG MORI. April 14, 2020, from <https://us.dmgmori.com/products/machines/additive-manufacturing/powder-bed/lasertec-30-slm>
- [42] TruPrint Series 5000 | TRUMPF. May 6, 2020, from [https://www.trumpf.com/en\\_US/products/machines-systems/additive-production-systems/truprint-5000/](https://www.trumpf.com/en_US/products/machines-systems/additive-production-systems/truprint-5000/)
- [43] Chua, C. K., Leong, K. F., & Lim, C. S. (2010). *Rapid prototyping: Principles and applications*, third edition, World Scientific.
- [44] Metal 3D Printers | Metal 3D Printing Machines | Sciaky. April 19, 2020, from <https://www.sciaky.com/additive-manufacturing/industrial-metal-3d-printers>
- [45] Spectra L | GE Additive. May 22, 2020, from <https://www.ge.com/additive/additive-manufacturing/machines/arcam-ebm-spectra-l>
- [46] DebRoy, T., Wei, H. L., Zuback, J. S., Mukherjee, T., Elmer, J. W., Milewski, J. O., Zhang, W. (2018). Additive manufacturing of metallic components – Process, structure and properties. *Progress in Materials Science*, 92, 112–224.

- [47] Sing, S. L., Tey, C. F., Tan, J. H. K., Huang, S., & Yeong, W. Y. (2019). 3D printing of metals in rapid prototyping of biomaterials: Techniques in additive manufacturing. *Rapid Prototyping of Biomaterials: Techniques in Additive Manufacturing (Second Edition)*.
- [48] Izadi, M., Farzaneh, A., Mohammed, M., Gibson, I., & Rolfe, B. (2020). A review of laser engineered net shaping (LENS) build and process parameters of metallic parts. *Rapid Prototyping Journal*, 26(6), 1059–1078.
- [49] Magic 3D printing machine and 3D printing tools - BeAM Machines. May 23, 2020, from <https://www.beam-machines.com/products/magic800>
- [50] TruLaser Cell 7040 | TRUMPF. May 11, 2020, from [https://www.trumpf.com/en\\_US/products/machines-systems/3d-laser-cutting-machines/trulaser-cell-7040/](https://www.trumpf.com/en_US/products/machines-systems/3d-laser-cutting-machines/trulaser-cell-7040/)
- [51] Gong, X., Anderson, T., & Chou, K. (2016). Review on Powder-Based Electron Beam Additive Manufacturing Technology, *International Symposium on Flexible Automation*, June 18-20, 1-9.
- [52] Sing, S. L., An, J., Yeong, W. Y., & Wiria, F. E. (2016). Laser and electron-beam powder-bed additive manufacturing of metallic implants: A review on processes, materials and designs. *Journal of Orthopaedic Research*, 34(3), 369–385.
- [53] Wu, B., Pan, Z., Ding, D., Cuiuri, D., Li, H., Xu, J., & Norrish, J. (2018). A review of the wire arc additive manufacturing of metals: properties, defects and quality improvement. *Journal of Manufacturing Processes*, 35, 127–139.
- [54] Printing the future – search to commercialise revolutionary 3D production process. May 12, 2020, from <https://www.cranfield.ac.uk/case-studies/research-case-studies/waammat>
- [55] Mireles, J., Espalin, D., Roberson, D., Zinniel, B., Medina, F., & Wicker, R. (2012). Fused deposition modeling of metals. *The 23<sup>rd</sup> Annual International Solid Freeform Fabrication Symposium - An Additive Manufacturing Conference, SFF 2012*, 836–845.
- [56] Mireles, J., Kim, H.-C., Lee, I. H., Espalin, D., Medina, F., Macdonald, E., & Wicker, R. (2013). Development of a Fused Deposition Modeling System for Low Melting Temperature Metal Alloys. *Journal of Electronic Packaging*, 135, 11008.
- [57] Vaezi, M., Drescher, P., & Seitz, H. (2020). Beamless Metal Additive Manufacturing. *Materials*, 13(4).
- [58] Michael, G., Matthias, G., & Theo, P. (1995). Fast, functional prototypes via multiphase jet solidification. *Rapid Prototyping Journal*, 1(1), 20–25.
- [59] C. Lieberwirth, M. Sarhan & H. Seitz. (2018). Mechanical Properties of Stainless-Steel Structures Fabricated by Composite Extrusion Modelling, *Metals*, 8(2), 84.
- [60] Dutta, B., Babu, S., & Jared, B. (2019). Metal additive manufacturing. *Science, Technology and Applications of Metals in Additive Manufacturing*, 1–10.
- [61] Hon, K. K. B., Li, L., & Hutchings, I. M. (2008). Direct writing technology—Advances and developments. *CIRP Annals*, 57(2), 601–620.

- [62] Gao, F., & Sonin, A. A. (1994). Precise deposition of molten microdrops: the physics of digital microfabrication. *Proceedings of The Royal Society of London, Series A: Mathematical and Physical Sciences*, 444(1922), 533–554.
- [63] Sheng, C., Daniel, A., Fu-Pen, C., Yong, Z., & C., P. R. (2004). SIEM measurements of ultimate tensile strength and tensile modulus of jetted, UV-cured epoxy resin microspheres. *Rapid Prototyping Journal*, 10(3), 193–199.
- [64] Jiang, X.-S., Qi, L.-H., Luo, J., Huang, H., & Zhou, J.-M. (2010). Research on accurate droplet generation for micro-droplet deposition manufacture. *The International Journal of Advanced Manufacturing Technology*, 49(5), 535–541.
- [65] Amirzadeh, A., Raessi, M., & Chandra, S. (2013). Producing molten metal droplets smaller than the nozzle diameter using a pneumatic drop-on-demand generator. *Experimental Thermal and Fluid Science*, 47, 26–33.
- [66] Tropmann, A., Lass, N., Paust, N., Metz, T., Ziegler, C., Zengerle, R., & Koltay, P. (2012). Pneumatic dispensing of nano- to picoliter droplets of liquid metal with the StarJet method for rapid prototyping of metal microstructures. *Microfluidics and Nanofluidics*, 12(1), 75–84.
- [67] Lass, N., Riegger, L., Zengerle, R., & Koltay, P. (2013). Enhanced liquid metal micro droplet generation by pneumatic actuation based on the starjet method. *Micromachines*, 4(1), 49–66.
- [68] Luo, Z., Wang, X., Wang, L., Sun, D., & Li, Z. (2017). Drop-on-demand electromagnetic printing of metallic droplets. *Materials Letters*, 188, 184–187.
- [69] A. P. Alkhimov, V. F. Kosarev, A. N. P. (1990). A method of “cold” gas dynamic spraying. *Dokl. Akad. Nauk SSSR*, Volume 315, 1062–1065.
- [70] Hassani-Gangaraj, M., Veysset, D., Nelson, K. A., & Schuh, C. A. (2018). In-situ observations of single micro-particle impact bonding. *Scripta Materialia*, 145, 9–13.
- [71] Moridi, A., Hassani-Gangaraj, S. M., Guagliano, M., & Dao, M. (2014). Cold spray coating: review of material systems and future perspectives. *Surface Engineering*, 30(6), 369–395.
- [72] Assadi, H., Kreye, H., Gärtner, F., & Klassen, T. (2016). Cold spraying – A materials perspective. *Acta Materialia*, 116, 382–407.
- [73] Yin, S., Cavaliere, P., Aldwell, B., Jenkins, R., Liao, H., Li, W., & Lupoi, R. (2018). Cold spray additive manufacturing and repair: Fundamentals and applications. *Additive Manufacturing*, 21(August 2017), 628–650.
- [74] Li, W., Yang, K., Yin, S., Yang, X., Xu, Y., & Lupoi, R. (2018). Solid-state additive manufacturing and repairing by cold spraying: A review. *Journal of Materials Science & Technology*, 34(3), 440–457.
- [75] Li, W.-Y., Zhang, C., Wang, H.-T., Guo, X. P., Liao, H. L., Li, C.-J., & Coddet, C. (2007). Significant influences of metal reactivity and oxide films at particle surfaces on coating microstructure in cold spraying. *Applied Surface Science*, 253(7), 3557–3562.

- [76] Wong, W., Rezaeian, A., Irissou, E., Legoux, J. G., & Yue, S. (2010). Cold spray characteristics of commercially pure Ti and Ti-6Al-4V. *Advanced Materials Research*, 89–91, 639–644.
- [77] Yu, H. Z., Jones, M. E., Brady, G. W., Griffiths, R. J., Garcia, D., Rauch, H. A., Hardwick, N. (2018). Non-beam-based metal additive manufacturing enabled by additive friction stir deposition. *Scripta Materialia*, 153, 122–130.
- [78] Dilip, J. J. S., Babu, S., Rajan, S. V., Rafi, K. H., Ram, G. D. J., & Stucker, B. E. (2013). Use of Friction Surfacing for Additive Manufacturing. *Materials and Manufacturing Processes*, 28(2), 189–194.
- [79] Liu, F. C., Hovanski, Y., Miles, M. P., Sorensen, C. D., & Nelson, T. W. (2018). A review of friction stir welding of steels: Tool, material flow, microstructure, and properties. *Journal of Materials Science & Technology*, 34(1), 39–57.
- [80] Mishra, R. S., & Palanivel, S. (2017). Building without melting: a short review of friction-based additive manufacturing techniques. *International Journal of Additive and Subtractive Materials Manufacturing*, 1(1), 82.
- [81] Rivera, O. G., Allison, P. G., Jordon, J. B., Rodriguez, O. L., Brewer, L. N., McClelland, Z., Hardwick, N. (2017). Microstructures and mechanical behavior of Inconel 625 fabricated by solid-state additive manufacturing. *Materials Science and Engineering: A*, 694, 1–9.
- [82] Obikawa, T., Yoshino, M., & Shinozuka, J. (1999). Sheet steel lamination for rapid manufacturing. *Journal of Materials Processing Technology*, 89–90, 171–176.
- [83] White, D. (2003). Ultrasonic consolidation of aluminum tooling. *Advanced Materials and Processes*, 161, 64–65.
- [84] Zhang, Y., Wu, L., Guo, X., Kane, S., Deng, Y., Jung, Y. G., Zhang, J. (2018). Additive Manufacturing of Metallic Materials: A Review. *Journal of Materials Engineering and Performance*, 27(1).
- [85] Obielodan, J. O., Ram, G. D. J., Stucker, B. E., & Taggart, D. G. (2009). Minimizing Defects Between Adjacent Foils in Ultrasonically Consolidated Parts. *Journal of Engineering Materials and Technology*, 132(1).
- [86] Gussev, M. N., Sridharan, N., Thompson, Z., Terrani, K. A., & Babu, S. S. (2018). Influence of hot isostatic pressing on the performance of aluminum alloy fabricated by ultrasonic additive manufacturing. *Scripta Materialia*, 145, 33–36.
- [87] Foster, D. R., Dapino, M. J., & Babu, S. S. (2013). Elastic constants of Ultrasonic Additive Manufactured Al 3003-H18. *Ultrasonics*, 53(1), 211–218.
- [88] Sridharan, N., Gussev, M. N., Parish, C. M., Isheim, D., Seidman, D. N., Terrani, K. A., & Babu, S. S. (2018). Evaluation of microstructure stability at the interfaces of Al-6061 welds fabricated using ultrasonic additive manufacturing. *Materials Characterization*, 139, 249–258.
- [89] Sridharan, N., Wolcott, P., Dapino, M., & Babu, S. S. (2016). Microstructure and texture evolution in aluminum and commercially pure titanium dissimilar welds fabricated using ultrasonic additive manufacturing. *Scripta Materialia*, 117, 1–5.

- [90] Palanivel, S., Nelaturu, P., Glass, B., & Mishra, R. S. (2015). Friction stir additive manufacturing for high structural performance through microstructural control in an Mg based WE43 alloy. *Materials & Design* (1980-2015), 65, 934–952.
- [91] Lewis, J. A., Smay, J. E., Stuecker, J., & Cesarano, J. (2006). Direct ink writing of three-dimensional ceramic structures. *Journal of the American Ceramic Society*, 89(12), 3599–3609.
- [92] Ahn, B. Y., Duoss, E. B., Motala, M. J., Guo, X., Park, S. Il, Xiong, Y., Lewis, J. A. (2009). Omnidirectional printing of flexible, stretchable, and spanning silver microelectrodes. *Science*, 323(5921), 1590–1593.
- [93] Hirt, L., Reiser, A., Spolenak, R., & Zambelli, T. (2017). Additive Manufacturing of Metal Structures at the Micrometer Scale. *Advanced Materials*, 29(17), 1–30.
- [94] Sachs, E., Cima, M., Williams, P., Brancazio, D., & Cornie, J. (1992). Three dimensional printing: Rapid tooling and prototypes directly from a CAD model. *Journal of Manufacturing Science and Engineering, Transactions of the ASME*, 114(4), 481–488.
- [95] Zhao, X., Evans, J. R. G., Edirisinghe, M. J., & Song, J. H. (2002). Direct ink-jet printing of vertical walls. *Journal of the American Ceramic Society*, 85(8), 2113–2115.
- [96] Reis, N., Ainsley, C., & Derby, B. (2005). Viscosity and acoustic behavior of ceramic suspensions optimized for phase-change ink-jet printing. *Journal of the American Ceramic Society*, 88(4), 802–808.
- [97] Rangarajan, S., Qi, G., Venkataraman, N., Safari, A., & Danforth, S. C. (2004). Powder Processing, Rheology, and Mechanical Properties of Feedstock for Fused Deposition of Si<sub>3</sub>N<sub>4</sub> Ceramics. *Journal of the American Ceramic Society*, 83(7), 1663–1669.
- [98] Morissette, S. L., Lewis, J. A., Clem, P. G., Cesarano, J., & Dimos, D. B. (2001). Direct-Write Fabrication of Pb(Nb,Zr,Ti)O<sub>3</sub> Devices: Influence of Paste Rheology on Print Morphology and Component Properties. *Journal of the American Ceramic Society*, 84(11), 2462–2468.
- [99] Microfabrica. May 14, 2020, from <http://microfabrica.com/>
- [100] Swiss Biotech company | Cytosurge AG. May 14, 2020, from <https://www.cytosurge.com/>
- [101] Takai, T., Nakao, H., & Iwata, F. (2014). Three-dimensional microfabrication using local electrophoresis deposition and a laser trapping technique. *Optics Express*, 22(23), 28109.
- [102] Ashkin, A. (1981). Applications of Laser Radiation Pressure., 210(4474), 85–86.
- [103] Ashkin, A. (1970). Acceleration and Trapping of Particles by Radiation Pressure. *Physical Review Letters*, 24(4), 156–159.
- [104] Ashkin, A., Dziedzic, J. M., & Yamane, T. (1987). Optical trapping and manipulation of single cells using infrared laser beams. *Nature*, 330(6150), 769–771.

- [105] Svoboda, K., & Block, S. M. (1994). Optical trapping of metallic Rayleigh particles. *Opt. Lett.*, 19(13), 930–932.
- [106] Upadhyay, M., Sivarupan, T., & El Mansori, M. (2017). 3D printing for rapid sand casting—A review. *Journal of Manufacturing Processes*, 29, 211–220.
- [107] Kuznetsov, A. I., Kiyam, R., & Chichkov, B. N. (2010). Laser fabrication of 2D and 3D metal nanoparticle structures and arrays. *Optics Express*, 18(20), 21198–21203.
- [108] Zenou, M., Sa'ar, A., & Kotler, Z. (2015). Laser jetting of femto-liter metal droplets for high resolution 3D printed structures. *Scientific Reports*, 5, 1–10.
- [109] Zhao D., Guo W., Zhang B., Gao F., (2018). 3D Sand Mold Printing: A Review And A New Approach. *Rapid Prototyping Journal*.
- [110] Hawaldar, N., & Zhang, J. (2018). A comparative study of fabrication of sand casting mold using additive manufacturing and conventional process. *International Journal of Advanced Manufacturing Technology*, 97(1–4), 1037–1045.
- [111] Haggerty, S., Michael, J., Williams, P. A., & Lawrence, P. E. (1993). Three-Dimensional Printing Techniques, United States Patent (19), (19).
- [112] Mostafaei, A., Stevens, E. L., Ference, J. J., Schmidt, D. E., & Chmielus, M. (2018). Binder jetting of a complex-shaped metal partial denture framework. *Additive Manufacturing*, 21, 63–68.
- [113] Will, J., Melcher, R., Treul, C., Travitzky, N., Kneser, U., Polykandriotis, E., Greil, P. (2008). Porous ceramic bone scaffolds for vascularized bone tissue regeneration. *Journal of Materials Science: Materials in Medicine*, 19(8), 2781–2790.
- [114] Lam, C. X. F., Mo, X. M., Teoh, S. H., & Hutmacher, D. W. (2002). Scaffold development using 3D printing with a starch-based polymer. *Materials Science and Engineering C*, 20(1–2), 49–56.
- [115] Snelling, D., Li, Q., Meisel, N., Williams, C. B., Batra, R. C., & Druschitz, A. P. (2015). Lightweight Metal Cellular Structures Fabricated via 3D Printing of Sand Cast Molds. *Advanced Engineering Materials*, 17(7), 923–932.
- [116] Caputo, M. P., Berkowitz, A. E., Armstrong, A., Müllner, P., & Solomon, C. V. (2018). 4D printing of net shape parts made from Ni-Mn-Ga magnetic shape-memory alloys. *Additive Manufacturing*, 21(2010), 579–588.
- [117] Yu, D. G., Branford-White, C., Yang, Y. C., Zhu, L. M., Welbeck, E. W., & Yang, X. L. (2009). A novel fast disintegrating tablet fabricated by three-dimensional printing. *Drug Development and Industrial Pharmacy*, 35(12), 1530–1536.
- [118] 3D printing - Additive | Make. April 18, 2020, from <https://make.3dexperience.3ds.com/processes/3D-printing>
- [119] Bai, Y., & Williams, C. (2015). An exploration of binder jetting of copper. *Rapid Prototyping Journal*, 21, 177–185.
- [120] Zhang, D. Q., Liu, Z. H., & Chua, C. K. (2013). Investigation on forming process of copper alloys via Selective Laser Melting (pp. 285–289).

- [121] Bakhiya, N., & Appel, K. E. (2010). Toxicity and carcinogenicity of furan in human diet. *Archives of Toxicology*, 84(7), 563–578.
- [122] Walker, J., Harris, E., Lynagh, C., Beck, A., Lonardo, R., Vuksanovich, B., MacDonald, E. (2018). 3D Printed Smart Molds for Sand Casting. *International Journal of Metalcasting*, 12(4), 785–796.
- [123] Ramakrishnan, R., Griebel, B., Volk, W., Günther, D., & Günther, J. (2014). 3D printing of inorganic sand moulds for casting applications. *Advanced Materials Research*, 1018, 441–449.
- [124] Meibodi, M. A., Giesecke, R., & Dillenburger, B. (2019). 3D printing sand molds for casting bespoke metal connections. *Intelligent and Informed - Proceedings of the 24<sup>th</sup> International Conference on Computer-Aided Architectural Design Research in Asia, CAADRIA 2019*, 1, 133–142.
- [125] D. Zhao, W. Guo, B. Zhang, F. Gao. (2018). 3D sand mould printing: a review and a new approach, *Rapid Prototyping Journal*, 18 (February) 2018, 1-25.
- [126] Snelling, D. A., Williams, C. B., Suchicital, C. T. A., & Druschitz, A. P. (2017). Binder jetting advanced ceramics for metal-ceramic composite structures. *International Journal of Advanced Manufacturing Technology*, 92(1–4), 531–545.
- [127] Rodríguez-González, P., Fernández-Abia, A. I., Castro-Sastre, M. A., Robles, P. E., Barreiro, J., & Leo, P. (2019). Comparative Study of Aluminum Alloy Casting obtained by Sand Casting Method and Additive Manufacturing Technology. *Procedia Manufacturing*, 41, 682–689.
- [128] Le Néel, T. A., Mognol, P., & Hascoët, J. Y. (2018). Design for Additive Manufacturing: Multi Material Sand Mold.
- [129] Lee, J., Bae, J., Park, S., Choi, J., Lee, S., Lee, J., ... Kim, D. H. (2018). Experimental and computational study on mechanical analysis of mesh-type lightweight design for binder-jet 3D printing. *Proceedings of the International Conference on Progress in Additive Manufacturing*, 2018-May, 237–243.
- [130] Sama, S. R., Badamo, T., Lynch, P., & Manogharan, G. (2019). Novel sprue designs in metal casting via 3D sand-printing. *Additive Manufacturing*, 25(December 2018), 563–578.
- [131] Evans, A. G., Hutchinson, J. W., Fleck, N. A., Ashby, M. F., & Wadley, H. N. G. (2001). The topological design of multifunctional cellular metals. *Progress in Materials Science*, 46(3–4), 309–327.
- [132] Reinhart, G., & Teufelhart, S. (2011). Load-Adapted Design of Generative Manufactured Lattice Structures, 12, 385–392.
- [133] ProJet CJP 460Plus - Color 3D Printer | 3D Systems. May 5, 2020, from <https://www.3dsystems.com/3d-printers/projet-cjp-460plus>.

## CURRICULUM VITAE

**Name, Surname:** Ertuğrul VARLIK  
**Birthplace and Date:** Trabzon, 02/08/1992  
**Email:** ertugrulvarlik@gmail.com  
**Website:** ertugrulvarlik.com

### Education & Work Experiences

Country	University & Company	Faculty / Institute & Position	Program & Department	Graduation Grade	Graduation Year & Period
TR	Karabük University	Faculty of Engineering	Metallurgical and Materials Engineering	3.24 out of 4	2017
TR	Atatürk University	Open Education Faculty	Occupational Health and Safety	2.68 out of 4	2019
TR	Marmara University	Institute of Pure and Applied Sciences	Metallurgical and Materials Engineering	3.57 out of 4	2020
TR	KARABUK IRON STEEL INDUSTRY TRADE & CO. INC.	Internship	IRON STEEL PRODUCTION		7/2015 8/2015
CZ	University of Chemistry and Technology	Internship / Research	EXPLORATION OF CORROSION RESISTANCE OF ULTRA HIGH-PERFORMANCE CONCRETE		7/2016 9/2016
USA	FOUR SEASONS JACKSON HOLE RESORT AND RESIDENCE	HOUSEKEEPING			6/2017 10/2017